QC
807.5
.U6
A7
no.153

NOAA Technical Memorandum ERL-ARL-153

FLOW AND DISPERSION NEAR CLUSTERS OF BUILDINGS

R. P. Hosker, Jr.
W. R. Pendergrass

Atmospheric Turbulence and Diffusion Division
Oak Ridge, TN 37831

Air Resources Laboratory
Silver Spring, Maryland
June 1987

LIBRARY
OCT 5 1987
N.C.
U.S. Dept. of Commerce

noaa NATIONAL OCEANIC AND ATMOSPHERIC ADMINISTRATION / Environmental Research Laboratories

QC
807.5
.U6A7
no. 153

NOAA Technical Memorandum ERL-ARL-153

FLOW AND DISPERSION NEAR CLUSTERS OF BUILDINGS

R. P. Hosker, Jr.
W. R. Pendergrass

Atmospheric Turbulence and Diffusion Division
Oak Ridge, TN 37831

Air Resources Laboratory
Silver Spring, Maryland
June 1987

UNITED STATES
DEPARTMENT OF COMMERCE

Malcolm Baldrige,
Secretary

NATIONAL OCEANIC AND
ATMOSPHERIC ADMINISTRATION

Anthony J. Calio,
Administrator

Environmental Research
Laboratories

Vernon E. Derr,
Director

NOTICE

The information in this document has been funded in part by the United States Environmental Protection Agency under Interagency Agreement IAG-DW13930021 to the Atmospheric Turbulence and Diffusion Division of the National Oceanic and Atmospheric Administration. It has been subject to the Agency's peer and administrative review, and it has been approved for publication as an EPA document. Mention of a commercial company or product does not constitute an endorsement by NOAA/ERL. Use for publicity or advertising purposes, of information from this publication concerning proprietary products or the tests of such products, is not authorized.

ATDL Contribution File No. 84/34

CONTENTS

Page

LIST OF FIGURES v

LIST OF SYMBOLS ix

ABSTRACT 1

1. INTRODUCTION 1

2. FLOW NEAR BUILDING CLUSTERS 2

2.1 Flow Near Isolated Buildings 2
2.2 Flow Near Extensive Arrays of Buildings 9
2.3 Flow Near Simple Clusters of Buildings 14

2.3.1 Previous Work 14
2.3.2 Systematic Study of Simple Clusters of Buildings 29

2.3.2.1 Single buildings 29
2.3.2.2 Two cubical buildings 36
2.3.2.3 Two rectangular buildings 42
2.3.2.4 Two-building summary 52
2.3.2.5 Four-building rectangular array 52
2.3.2.6 Three-building triangular array 58
2.3.2.7 Five-building cruciform array 61

3. CONCENTRATION CALCULATIONS 64

3.1 Concentrations Within and Very Close to a Building Complex 64

3.1.1 Concentrations Near a Dominant Building 65
3.1.2 Concentrations in a Street Canyon 66

3.2 Concentrations in the Intermediate and Far Wakes of a Building Complex 70

3.2.1 Available Models 70
3.2.2 Agreement With Data 74

4. SUMMARY AND RECOMMENDATIONS 77

4.1 Caveats 77
4.2 Flow Field Estimation 78
4.3 Concentration Estimation Procedures 80

ACKNOWLEDGEMENTS 83

REFERENCES 84

APPENDIX A 90

FIGURES

Page

Figure 1.--Recent model of flow near a sharp-edged building normal to a deep boundary layer wind (based on Woo, Peterka, and Cermak, 1977, and Hunt et al., 1978). 3

Figure 2.--Flow patterns near buildings of different L/H normal to boundary layer wind. (a) Nomenclature. (b) L/H small enough that roof and side reattachment do not occur. (c) L/H large, so that reattachment does occur. 5

Figure 3.--Critical length to height ratio $(L/H)_*$ for roof flow reattachment (from Equation 2-1) as a function of width to height ratio W/H, with zone of intermittency as suggested by Robins and Fackrell (1983). 6

Figure 4.--Zones of isolated roughness flow, wake interference flow, and skimming flow as functions of W/H. The critical separations s_* and s_{**} are defined by Equations (2-3) and (2-5) for a face-to-face spacing s of obstacles in a uniform grid. 12

Figure 5.--Surface scouring patterns (after Beranek, 1979) induced by an isolated model building (top row across), and by the same building surrounded by much lower buildings (bottom row). (a) Wind speed ratio $\gamma = 6/U = 1.6$. (b) $\gamma = 1.2$. 17

Figure 6.--Surface scouring patterns (after Beranek, 1979) produced by wind approaching the gap between two buildings. (a) Wind toward "mouth" of array. (b) Wind toward "apex" of array. Numerical values correspond to a kind of local wind speed amplification factor γ, described in the text. 18

Figure 7.--Surface scouring patterns (after Beranek, 1979) for three simple buildings aligned along the normal to the wide building face. (a) Incident wind parallel to alignment axis. (b) Wind at 45° to alignment axis. (c) Wind at 90° to alignment axis. The local wind speed amplification factor γ (numerical values) is described in the text. 19

Figure 8.--Surface scouring and flow patterns (after Beranek, 1979) for three simple buildings offset by one building width from alignment. (a) Incident wind normal to wide building face. (b) Same as (a), but showing surface flow patterns, rather than scouring patterns. (c) Wind at 45° to the long axis of the building. The local wind speed amplification factor γ (numerical values) is described in the text. 20

Page

Figure 9.--Beranek's (1979, 1984) "circles of influence" for (a) a tall, narrow building, (b) a tall, wide building, and (c) a very wide building. For the wide building, the zone of influence is rather elliptical in shape; it is approximated by two semicircles centered about 1.5 H inboard of the building sides, joined by straight lines across the gap. 22

Figure 10.--Beranek's (1979, 1984) empirical relations (Equations 2-8a, b) for the circle of influence parameters R/H and e/H as functions of the frontal aspect ratio W/H. 24

Figure 11.--Relationship between the circle of influence and building flow parameters, x_F, x_R. 25

Figure 12.--Calculated R/H versus W/H, for various L/H, using Fackrell and Pearce's (1981) expression for x_R/H and Fackrell's (1982) estimate for x_F/H, compared to Beranek's (1979, 1984) expression. 26

Figure 13.--Transition to flow interference regime. (a) Geometry. (b) s_*/H calculated, (assuming identical buildings), using Beranek's (1979, 1984) expressions for the circle of influence, compared to an empirical expression for s_*/H based on data of Hussain and Lee (1980). 28

Figure 14.--Sketches of flow patterns near typical building clusters (from Gandemer, 1976). (a) Wind normally incident to a gap between two wide structures. (b) Wind striking a wide obstacle at an angle. (c) Arrangement leading to a venturi effect. (d) Deflection and jetting of flow between two buildings. 30

Figure 15.--Surface flow patterns associated with three single building geometries normal to incident wind. (a) W/H = 1 = L/H. (b) W/H = 2, L/H = 1. (c) W/H = 3, L/H = 1. 31

Figure 16.--Surface flow patterns associated with a single building at an angle to the incident wind. (a) $\theta = 30°$. (b) $\theta = 45°$. 34

Figure 17.--Surface flow patterns associated with two buildings (W/H = 1 = L/H) normal to the incident wind, with crosswind separation s. (a) s = 2.67 H. (b) s = 2.33 H. (c) s = 2.0 H. (d) s = 1.33 H. (e) s = 1.0 H. (f) s = 0.67 H. (g) s= 0.67 H, seen from behind the buildings. (h) s = 0.67 H, closeup of the flow patterns between the buildings. (i) s = 0.33 H. 37

Page

Figure 18.--Surface flow patterns associated with two buildings (W/H = 1 = L/H) normal to the incident wind, with face-to-face alongwind separation s. (a) s = 3.33 H. (b) s = 3.0 H. (c) s = 2.33 H. (d) s = 1.67 H. (e) s = 1.33 H. (f) s = 1.0 H. (g) s = 0.33 H. 43

Figure 19.--Surface flow patterns associated with two buildings (W/H = 2, L/H = 1) normal to the incident wind, with crosswind separation s. (a) s = 2.67 H. (b) s = 2.33 H. (c) s = 2.0 H. (d) s = 1.67 H. (e) s = 1.33 H. (f) s = 1.0 H. (g) s = 0.67 H. (h) s = 0.33 H. 47

Figure 20.--Surface flow patterns associated with four buildings (W/H = 1, L/H = 1) in a rectangular grid, with an inter-building spacing s. (a) s = 3.33 H. (b) s = 3.0 H. (c) s = 2.67 H. (d) s = 2.33 H. (e) s = 2.0 H. (f) s = 1.67 H. (g) s = 1.33 H. (h) s = 1.0 H. (i) s = 0.67 H. 53

Figure 21.--Surface flow patterns for three buildings (W/H = 1 = L/H) in a triangular array, with inter-building alongwind spacing s_x and crosswind spacing s_y. (a) s_x = 2.0 H, s_y = 5.0 H. (b) s_x = 1.0 H, s_y = 2.67 H. (c) s_x = 0.67 H, s_y = 1.33 H. 59

Figure 22.--Surface flow patterns for five buildings (W/H = 1, L/H = 1) in a cruciform array, with inter-building alongwind spacing s_x and crosswind spacing s_y. (a) s_x = 1.0 H = s_y. (b) s_x = 0.67 H = s_y. (c) s_x = 0.33 H = s_y. 62

Figure 23.--Street canyon flow (after Hoydysh, Griffiths, and Ogawa, 1974). (a) Very long street canyon, with wind aloft normal to the canyon axis. (b) Street canyon flow near an intersection. 67

Figure 24.--Street canyon circulation model of Johnson et al. (1973), for flow within about ±60° of the normal to the canyon axis. 69

Figure A.1.-NOAA/ATDD meteorological wind tunnel. The two front test sections are used to develop a simulated atmospheric boundary layer, and model tests are performed in the last test section. 91

Figure A.2.-Schematic of ATDD boundary layer generating system, similar to that suggested by Counihan (1969). The trip fence has a sharp metal top edge; the vortex generators are formed from thin plastic sheets glued in place over wooden frames, and the surface roughness consists of approximately 1 cm gravel glued to special inserts for the tunnel floor. 92

Page

Figure A.3.-Normalized mean velocity profile in the simulated atmospheric boundary layer, measured 6 m downwind of the trip fence, with a reference wind speed of 4.15 m/s. 93

Figure A.4.-Vertical profiles of longitudinal and vertical turbulence intensities in the simulated atmospheric boundary layer, measured 6 m downwind of the trip fence, with a reference wind speed of 4.15 m/s. 94

LIST OF SYMBOLS

Symbols are listed below and are also defined in the text as needed. An attempt has been made to force consistency of nomenclature throughout; hence, readers who refer to the original papers can expect changes in notation. Units (length, time, mass, temperature) are indicated in square brackets after each symbol.

a	a constant, in empirical expression for $f(\theta)$.
A	characteristic area of an obstacle. $[L^2]$
A_p	projected frontal area of an obstacle. $[L^2]$
c	a constant, in Gifford's model for wake-enhanced dispersion.
d	boundary layer displacement height, usually appearing in log-law expression for the mean velocity profile. [L]
e	downwind displacement of the center of a building's "circle of influence" from the building's upwind face. [L]
$f(\theta)$	empirical expression to adjust concentration estimates for the angle of the incident wind.
h_e	effective release height for an effluent plume. [L]
H	height of a building. [L]
$\bar{H}$	mean height of the buildings in an array. [L]
K	nondimensional concentration coefficient.
L	alongwind dimension (length) of a building. [L]
$(L/H)_*$	critical value dividing building geometries that experience roof flow reattachment from those that do not; a function of W/H.
n	exponent in power-law form of velocity profile.
p	exponent in a power law.
Q	effluent source strength. [M/t]
R	"radius of influence" of a building. [L]
s	face-to-face spacing of adjacent roughness elements or buildings. [L]
s_x	alongwind face-to-face spacing of buildings.
s_y	crosswind face-to-face spacing of buildings.

s_* critical face-to-face building spacing for transition between "isolated roughness" flow regime and the "wake interference" flow regime. [L]

s_{**} critical face-to-face building spacing for transition between "wake interference" flow regime and the "skimming flow" regime. [L]

S center-to-center spacing of adjacent roughness elements or buildings. [L]

$\bar{S}$ mean center-to-center spacing of adjacent roughness elements or buildings in a random array [L]

U wind speed at a defined height or location. [L/t]

U_{ref} reference velocity at a specified height. [L/t]

u_* friction velocity determined from slope of log-law fit to a boundary layer flow. [L/t]

u'_{rms}, v'_{rms}, w'_{rms} root-mean-square values of turbulent velocity fluctuations in the along-wind, cross-wind, and vertical directions, respectively. [L/t]

W crosswind dimension (width) of a building. [L]

x,y,z alongwind, crosswind, and vertical Cartesian coordinates. [L]

x_F length of frontal separation zone, measured from upwind building face. [L]

x_R length of recirculating wake zone, measured from downwind building face. [L]

x_V, y_V, d_V distance of center of lee-edge vortices from lee face of building and centerline, and diameter of those vortices respectively.

x_{yo}, x_{zo} virtual source locations upwind of an effluent source, based on the crosswind and vertical plume size behind an obstacle or building. [L]

y_{HV} maximum crosswind distance of the horseshoe vortex system from the flow centerline.

z_o aerodynamic roughness length associated with log-law form of a boundary layer flow. [L]

γ Beranek's (1979) velocity ratio $U_{ref}/U = 6\ ms^{-1}/U$.

δ boundary layer depth. [L]

λ_p $H^2/(H^2 - s^2)$, a measure of building density in a region.

π	3.14159...
σ_y, σ_z	plume dispersion parameters in crosswind and vertical directions. [L]
σ'_y, σ'_z	wake-enhanced plume dispersion parameters. [L]
Σ_y, Σ_z	wake-enhanced plume dispersion parameters. [L]
θ	angle between incident wind direction and the normal to the most exposed building face. [radians]
χ	effluent concentration in air. [M/L^3]
χ_{CL}	ground level centerline concentration. [M/L^3]

FLOW AND DISPERSION NEAR CLUSTERS OF BUILDINGS

R. P. Hosker, Jr. and W. R. Pendergrass

ABSTRACT. This report is intended as an information summary and, to a limited extent, as an interim and rather qualitative guide for those who must routinely face the complex air quality problems associated with atmospheric flow and effluent dispersion near clusters of buildings. A brief summary of the flow patterns expected near isolated simple buildings serves as an introduction. Flow patterns associated with varying densities of uniformly sized buildings in an extensive array are then discussed. Previous work on flow near simple, isolated building clusters is reviewed, along with the concept (Beranek, 1979, 1984) of a "region of influence". A systematic study of near-ground-level flow patterns within simple building clusters is summarized. The suite of presently available models for estimating near-building and wake concentrations is briefly described. It appears to be possible to arrive at rough concentration estimates (or, at least, bounds) close to buildings only in cases where one building of a cluster is dominant in size, or within an extensive array of similarly-sized structures. The recent literature (Fackrell, 1984) suggests that several models developed for single-building intermediate and far wake concentration estimates are also useful for building clusters; the appropriate model depends on whether the effluent source is in the near wake region at ground level, or is a roof-mounted vent, or is a roof-mounted stack of typically modest size. Problems associated with very wide buildings and with cases when the wind approaches at an angle to the buildings are described, and some possible remedial steps are suggested. Additional work is needed in several areas to improve present understanding and to provide better guidance to the practitioner; research recommendations are therefore included.

1. INTRODUCTION

The behavior of effluent plumes near buildings and groups of buildings is of common concern. Buildings strongly perturb local wind fields, and thereby influence the transport and dispersion of air pollutants. Consequences for the building inhabitants can range from the nuisance level (e.g., occasional infiltration of objectionable odors) through the serious (violations of exposure standards) to the dangerous (exposure to toxic levels of chemical or radiological materials). Adequate predictive capability is generally not available, and recourse to wind tunnel and/or field studies has often been necessary. The problem is especially troublesome in the nuclear industry, where the trajectories, concentrations, and effects of radioactive plumes must be assessed for both routine and emergency releases. The consequences of on- or off-site releases of non-radiological toxic materials may also be important with regard to nuclear reactor control room habitability and general site safety.

Field and laboratory research over the last two decades has provided some limited guidance for estimating flow and dispersion near isolated buildings, near some building clusters, and in certain urban configurations. Recent reports (e.g., Hosker, 1980, 1982, 1984; Meroney, 1982; Wilson and Britter, 1982) have dealt with individual buildings; presently available information and calculation procedures for wake flow and effluent dispersion near simple, isolated structures have been summarized in those publications. This report reviews some of the information available for the much more complex problem of a building cluster, for both flow and dispersion prediction.

2. FLOW NEAR BUILDING CLUSTERS

2.1 Flow Near Isolated Buildings

Before dealing with the complicated flow patterns that may occur within and around clusters of buildings, one should have a good working understanding of the flow near single buildings. This flow can be very complex even if the geometry of the building is rather simple. Characteristics of the flow near a simple block-like building have been discussed in an earlier NRC report (Hosker, 1982), and will be briefly summarized here. Details and references may be found in the earlier work.

Consider a deep, turbulent, atmospheric boundary layer normally incident on a simple building of height H, along-wind length L, and width W. Many investigators have worked to develop the conceptual flow model shown in Figure 1. The main features of the flow are as follows: upwind of the obstacle, there is a "displacement zone", where the incident fluid is first influenced by the presence of the building. Within this zone, both wind speed and direction are affected as the flow attempts to travel around and over the body. The exposed front surfaces of the obstacle will experience a pressure higher than ambient as the approaching air decelerates. Because the incident wind speed diminishes with decreasing height, a downward-directed pressure gradient will be established as the flow decelerates near the upwind face. This gradient drives a downward-directed flow along the front surface; at the ground, this flow moves out from the building, causing the approach flow to separate from the ground some distance upwind. The result is a standing eddy in front of the lower portion of the building. The exact upwind separation location depends on the building width to height ratio, the upstream surface roughness, and the approach flow characteristics relative to the building. For a very wide (quasi-two-dimensional) structure, the displacement zone may extend as much as 5 to 10 H upwind of the obstacle, although some laboratory workers have found flow perturbations to only 4 H upwind. Actual flow separation from the ground ahead of a two-dimensional obstacle will generally be about 2 H upwind of the structure, with flow reattachment to the windward face occurring above the frontal vortex at a height of roughly 0.6 H (± 25%). If the building is not very wide, the inherent three-dimensional character of the flow field results in a smaller displacement zone, with flow separation upwind of the frontal vortex less than 2 H ahead of the windward face (see Fackrell, 1982, for an empirical

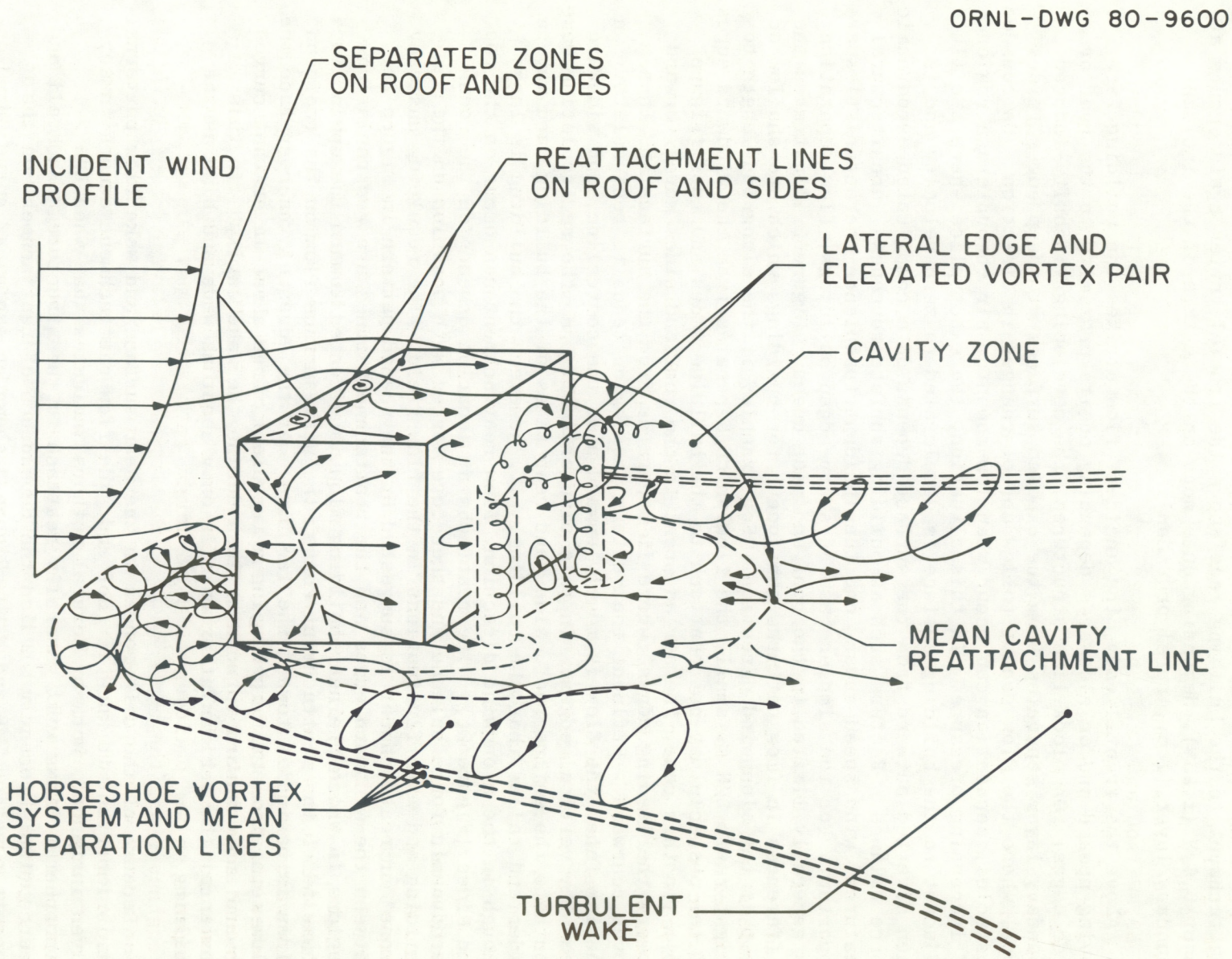

Figure 1. Recent model of flow near a sharp-edged building normal to a deep boundary layer wind (based on Woo, Peterka, and Cermak, 1977, and Hunt et al., 1978).

expression for the maximum upwind extent of the frontal vortex). Flow reattachment to the building face above the frontal vortex again occurs at about 0.6 H (± 25%), depending once more on the nature of the incident boundary layer (i.e., rural or urban).

Above the frontal eddy, the incident flow strikes the building face, moving upward and/or sidewards depending on its proximity to the roof or side edges. On block-like structures, the developing viscosity-induced boundary layer separates from the exposed surfaces at sharp edges (sides, roof) where the flow cannot follow abrupt changes in direction. On rounded obstacles, separation can occur when low-momentum air encounters a region of increasing pressure. In this situation, the exact place where the fluid adjacent to the building surface is decelerated to zero velocity and is then diverted outward from the surface depends on a complicated aerodynamic force balance. Factors such as building surface roughness, architectural features, wind speed shear, and the incident turbulence characteristics are important. For the simpler case of sharp-edged buildings, flow separation is generally limited to the roof and side edges. Figure 2 illustrates the differences in flow patterns that occur for buildings which are shallow or deep in the alongwind direction. For example, if the alongwind length to height ratio L/H is small, the flow which separates from the windward edges of the obstacle may not reattach to the building sides and roof (Figure 2b). In this case, the air adjacent to the roof and sides moves forward toward the leading edges, where it separates from the surface and then moves rearward. Effluent that enters the region tends to recirculate. On the lee face, the flow is mostly upward near the centerline, and sideward near the vertical edges. In this case of small L/H, the recirculating wake contacts the entire roof, side, and rear faces of the building, and may be wider and taller than the building. If, however, the building is large enough in the alongwind direction, flow reattachment can occur on the roof and sides (Figure 2c). The reattachment location depends on the local aerodynamic force balance and therefore varies with position on the building and with fluctuations in the flow field. The resulting unsteady "zone" of reattachment is suggested by the shaded pattern in Figure 2c. Between the windward edges and the reattachment zones are recirculation regions in which the near-building flow is directed toward the upwind face. Downwind of the reattachment zones, the near-surface flow on the roof and sides is basically toward the lee face. At the edges of the rear face the flow separates again, producing a turbulent, free shear layer that curves inward and downward to more or less define the wake cavity. In this instance, the recirculating wake is only about as wide and high as the building.

Because of the differences in the near-surface and wake flow patterns, it is important to know if roof and side flow reattachment occurs in any given instance. Work by several authors indicates that when L/H > 1, atmospheric flows will generally reattach to the structure. Fackrell and Pearce (1981) recently studied the dependence of reattachment on the geometric ratios L/H and W/H. Figure 3 shows an empirical curve based on their recommendation; the line is generated by the expression

$$(L/H)_* \cong \frac{0.72\ (W/H)}{1 + 0.51\ (W/H)} \quad . \qquad (1)$$

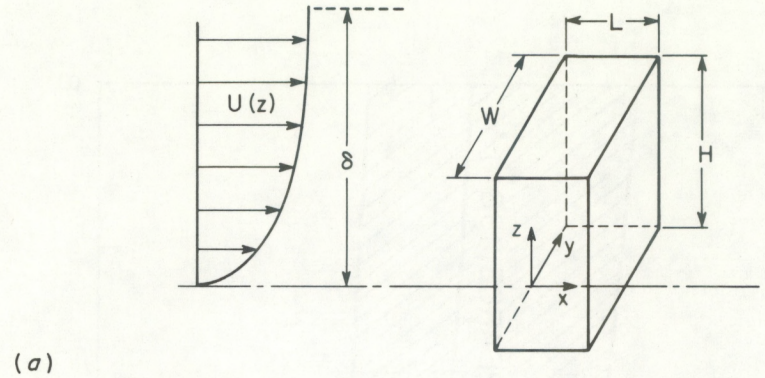

(a)

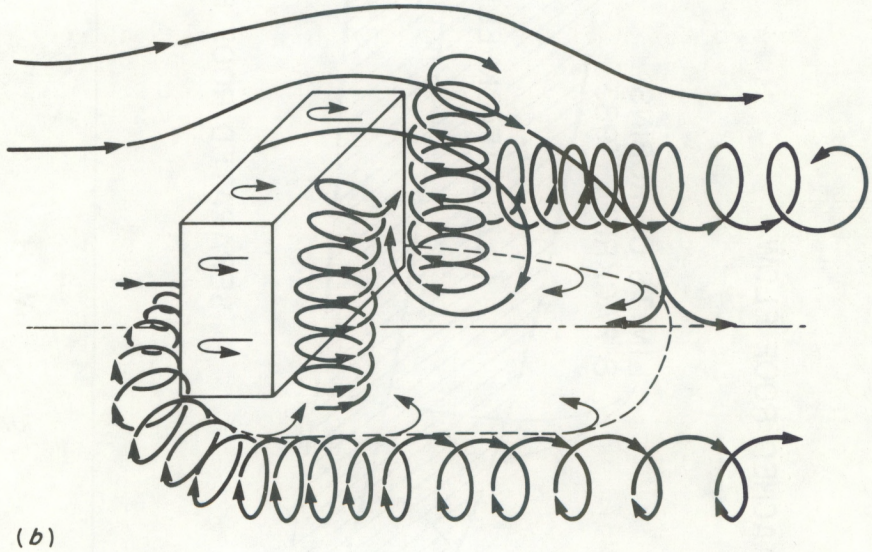

(b)

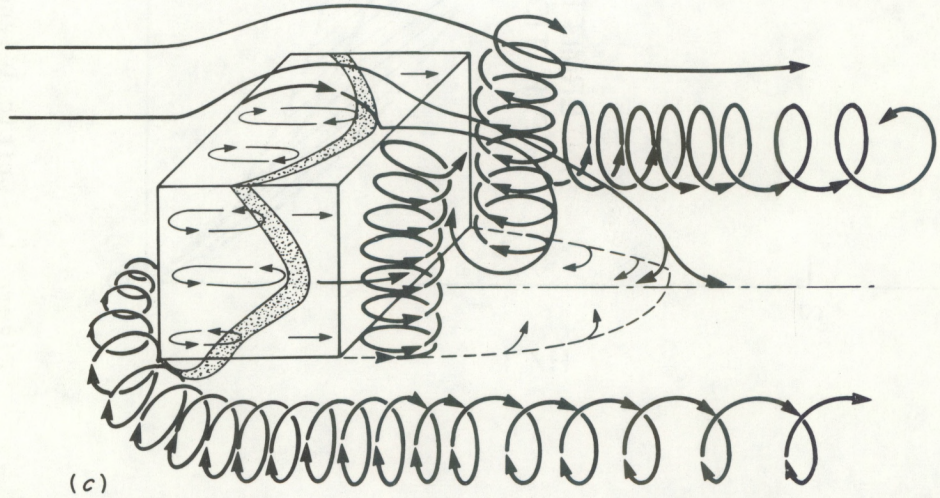

(c)

Figure 2. Flow patterns near buildings of different L/H normal to boundary layer wind. (a) Nomenclature. (b) L/H small enough that roof and side reattachment do not occur. (c) L/H large, so that reattachment does occur.

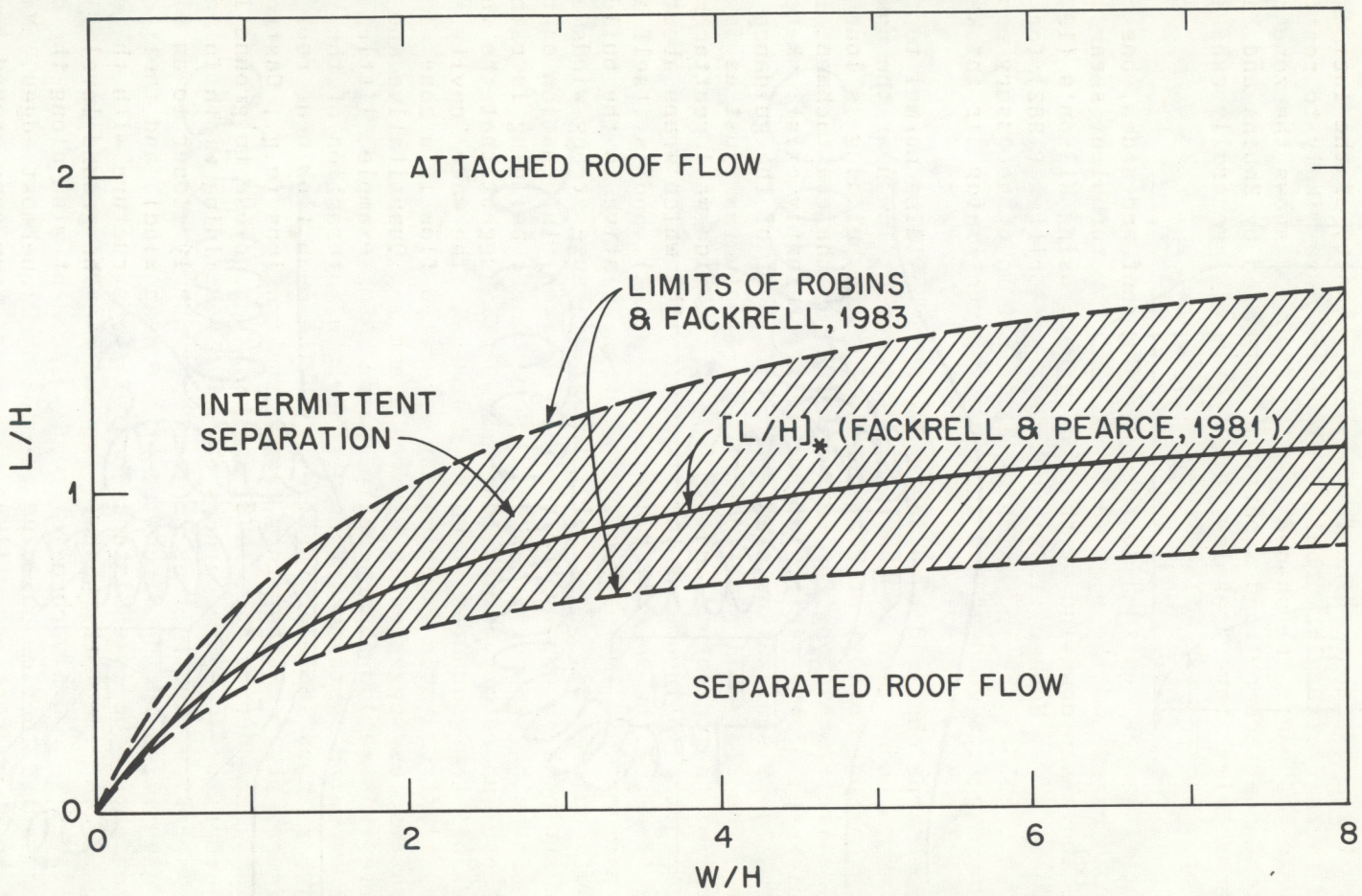

Figure 3. Critical length to height ratio $(L/H)_*$ for roof flow reattachment (from Equation 2-1) as a function of width to height ratio W/H, with zone of intermittency as suggested by Robins and Fackrell (1983).

When $L/H > (L/H)_*$ for a given W/H, the flow will usually reattach to the building; when $L/H < (L/H)_*$, the flow will usually remain separated from the building roof and sides. This is not a rigorous division, however; buildings with geometries close to the critical value can exhibit intermittent reattachment. The turbulence intensity of the incident flow is also a factor; strongly turbulent flows are more likely to reattach for a given value of L/H. The shaded area in Figure 3 shows the zone of intermittent reattachment and separation suggested by Robins and Fackrell (1983); geometries above or below this region will generally exhibit steady attached or separated roof flow, respectively.

If the flow does reattach to the building roof and sides, one can estimate the extent of the roof cavity and of the turbulent shear layer and roof wake above and downwind of the roof cavity using Wilson's (1979 a,b) methods; see, e.g., Hosker (1982) or Wilson and Britter (1982) for details. The technique allows the approximate determination of necessary roof stack heights and suggests good or bad locations of ventilator air intakes.

The phenomena observed near the sides of a building normal to the wind are similar to those seen on the roof: separated flow near the upwind edge, with the possibility of reattachment if the building is long enough. No quantitative expressions for features such as the reattachment length or the thickness of the recirculating cavity presently exist; sketches and laboratory flow visualization studies provide most of the guidance available. The side-wall reattachment zone fluctuates, just as in the roof case. Some of the curvature and breadth of the side wall reattachment zone may be due to the influence of the frontal vortex which wraps about the structure (forming the so-called horseshoe vortex), and is itself a highly variable phenomenon. The path of this vortex relative to the building sides is of considerable practical interest, because strong winds and intense turbulence accompany the vortex. However, information on the behavior of the horseshoe vortex even close to the building is rather sparse. Both laboratory and field measurements suggest that the vortex wake rises off the ground as it moves downwind. The wake "cavity" found behind any bluff obstacle experiencing separated flow is a zone of very complex motion, as suggested in Figures 1 and 2. Quantitative and even qualitative information is generally sparse. For example, little is known about the elevated vortex pair produced by the interaction of the vertically-oriented lee-edge vortices with the mean flow near roof level (e.g. Figures 2b,c). Laboratory flow visualizations (e.g., Castro and Robins, 1977; Hatcher et al., 1978) suggest that, close to ground level, these lee-edge vortices are perhaps 30% of the building width in "diameter" (strictly speaking, their cross-section is probably closer to an ellipse, with the elongation in the direction of the mean wind), and their centers are located about the same distance behind the structure with the outer edges roughly in line with the building sides. The ground-level flow in these vortices is roughly parallel to the incident wind along the outer edges, and toward the lee building face on the innermost edges. Material which enters these vortices will spiral upward from near ground level to travel off downwind within the elevated vortex pair; there is evidence that these vortices are shed periodically, leading to an intermittent flushing of the entire wake cavity region.

The along-wind extent of the cavity zone can be estimated from the building geometry within ± 50% or better from a number of empirical expressions (Hosker, 1979; Fackrell and Pearce, 1981; Wilson and Britter, 1982). Fackrell and Pearce postulate a weak dependence on the building length to height ratio even when the flow has reattached to the building roof and sides; however, they limit the range of L/H between 0.3 (with this result applying to all shorter structures) and 3.0 (with this result applying to all longer buildings). The agreement of their estimate with laboratory data is quite good.

Quantitative data on other cavity dimensions are still sparse. If reattachment to the building roof and sides does not occur, the maximum height of the cavity can be somewhere between 1.5 H and 2.5 H above ground (see the summary by Hosker, 1984); the value will be strongly affected by roof slope. Empirical expressions for the maximum cavity width in the non-reattached case have been proposed by Fackrell (1982) and by Hosker (1982); the formulations, though quite different, appear to fit the limited data equally well. If flow reattachment does take place, the situation is simpler: the maximum cavity height and width are closely approximated by the building height and width, respectively.

The turbulent far wake of a very wide (two-dimensional) obstacle behaves somewhat like a developing turbulent boundary layer. Downwind of the cavity, a turbulent layer develops just above the ground; within this layer, the mean velocity depends in the usual logarithmic manner on height and local surface roughness, and the turbulence is similarly dependent on the underlying surface characteristics. The flow in the "mixing" layer above this region is "self-preserving" in the sense of many wake and boundary-layer flows (e.g., Schlichting, 1960). Within this mixing layer, the mean velocity "defect" (the difference between the velocities observed at a given location with and without the obstacle in place) and the perturbations to the turbulent shear stresses both die out for this two-dimensional body approximately as $(x/H)^{-1}$. The decay of the mean velocity defect and stress perturbations is more rapid than this in the wall layer close to the ground. The overall wake height increases roughly as $(x/H)^{1/2}$. A more detailed summary of the relevant theoretical and experimental literature can be found in Hosker (1984). The far wake of a truly three-dimensional obstacle, such as a building, can be considerably more complex because of the presence of potentially persistent longitudinally-oriented vortices. These are important from the dispersion point of view because elevated pollutant plumes can be swept from above the wake down to near ground level by the action of such trailing vortices. However, these may not be a significant problem in many cases of interest. For example, with a block-like building at right angles to the wind in a well-mixed atmosphere, the horseshoe and lee-edge vortices apparently dissipate rather quickly under the action of strong ambient turbulence. The wake is then essentially a pure "momentum" wake of the type commonly studied in aerodynamics. For such a building wake, the mean velocity defect is found to decay roughly as $(x/H)^{-1.5}$ or $(x/H)^{-1.6}$, while the mean square turbulence intensity excess (i.e., the increase over what would be observed at the same location if the building were absent) dies off as $(x/H)^{-2}$. The crosswind profile of the mean velocity defect is approximately bell-shaped, with the maximum defect occurring along the wake centerline. Generally this type of wake will be indistinguishable from the

background (ambient) turbulence within 10 to 20 H of the building, although this distance probably depends on the building aspect ratio W/H, as well as on the ambient turbulence characteristics. However, when organized vorticity becomes important in the wake, as may occur for rounded obstacles such as hemispheres, or for block buildings at an angle to the wind, or for block buildings normal to the wind in a stable atmosphere, the far wake can be dramatically changed in character and persistence. For example, the vortices may advect the relatively high-momentum air aloft down toward the ground level wake centerline, producing a mean velocity excess instead of the usual deficit. Mean velocity defects here appear outboard of the vortices, well off the centerline. Similarly, a wake centerline pollutant excess can be generated if the vortices interact with an otherwise elevated effluent plume, and a wake centerline temperature excess can appear if the incident atmospheric flow is stable. The persistence of these features seems to vary with the characteristics of the obstacle and the ambient flow, at least in laboratory studies. The laboratory work generally suggests that a detectable wake of some sort may extend 50 to 100 H downwind of an obstacle when vortices are important, depending on ambient turbulence level, atmospheric stability, and building shape. A more detailed summary may be found in Hosker (1984). It may be somewhat difficult to detect wake vortices in the field because of their probable meander in the ambient turbulence, and because the vortices may also rise upward and spread outward from the centerline with increasing downwind distance.

2.2 Flow Near Extensive Arrays of Buildings

At the other extreme of the building flow problem is the flow in an extensive building array. One can visualize the physical situation between the isolated structure and array cases as follows (see, e.g., Counihan, 1971, and Hussain and Lee, 1980, among others). When obstacles to an incident flow field are placed well apart -- a few tens of obstacle heights or more -- there will be relatively little interaction among their individual flow fields. The flow near each obstacle will be similar to that around isolated obstacles. Up- and down-wind separation and recirculation zones will be generated by each obstacle, as well as a turbulent wake. A frontal horseshoe vortex may be present if the obstacle is aerodynamically bluff. Great spatial nonuniformity of the near-surface flow will therefore be encountered. As the obstacles are placed progressively closer together, their individual flow fields begin to interact. The individual wakes are disturbed, and the up- and down-wind recirculation zones will deviate from their "normal" size and shape. Secondary flows may begin to appear between the elements. As the roughness element density is further increased, individual wake flows are no longer possible; instead, stable secondary flows -- vortices -- are produced in the gaps between elements, and the main flow no longer enters these spaces, but skims over the top of the dense obstacle array.

Hussain and Lee (1980) defined three distinct flow regimes on the basis of changes in near-obstacle aerodynamics with increasing obstacle density: the "isolated roughness" regime, the "wake interference" regime, and the "skimming flow" regime. They suggested that the transition from the isolated roughness case to the wake interference regime would occur when

the separation and recirculation zones up- and down-wind of an individual element were disrupted by the flows around neighboring elements*. The transition from the wake interference regime to skimming flow occurs when a stable vortex pattern is first established in the crosswind gaps between elements. The specific transition densities therefore depend upon the geometry of the individual elements, as well as on the pattern of the array and its density.

For example, Hussain and Lee's (1980) wind tunnel experiments indicated that the isolated roughness regime occurs for cubical elements (dimension H) in a regular, grid-like array when the element face-to-face spacing s is greater than $s_* \cong 2.4$ H, corresponding to a plan area ratio $H^2/(H+s)^2 \equiv \lambda_p$ (a measure of element density) less than about 8.5%, where s_* denotes the interference flow transition spacing. If the array is staggered rather than rectilinear, then $s_*/H \cong 1.4$ and the transition density is about twice as large, 17%. The change from the wake interference regime to skimming flow occurs when $s/H = s_{**}/H \cong 1.4$ for a grid-like array of cubes, corresponding to an area ratio of about 17%; a staggered array can tolerate even tighter spacing, with $s_{**}/H \cong 0.7$ and $\lambda_p \cong 34\%$, where s_{**} denotes the skimming flow transition spacing.

These transition values for element spacing seem to agree with the observations of others, as Hussain and Lee pointed out. For example, suppose that the isolated roughness to wake interference transition in a grid-like array occurs when the face-to-face spacing is less than or equal to the sum of the lengths of the upwind obstacle's recirculating wake and the downwind obstacle's frontal separation zone:

$$s_* \cong x_R + x_F \ . \qquad (2)$$

For a cube, $x_R \cong 1.5$ H (assuming a turbulent incident flow, such that the flow which initially separates at the upwind "roof" edge reattaches to the roof -- see e.g., the reviews by Hosker, 1980, 1982, 1984), and x_F is about 1 H (same references). Hence s_* is estimated to be about 2.5 H, which agrees well with Hussain and Lee's result of 2.4 H. The transition between the wake interference regime and skimming flow is also reasonable in the light of work by Roshko (1955), Tani, Iuchi, and Komoda (1961), and Fox (1964), who found that a stable vortex was first established in a two-dimensional crosswind gap (a "notch") when the gap width to height ratio was 1.15, 1.4, or 1.25, respectively, with the differences probably being attributable to the varying experimental conditions. Hussain and Lee (1980) observed transition to skimming flow for a cube face-to-face spacing s_{**} of about 1.4 H, at least partially confirming the notion that this transition occurs when stable vortices are established in the crosswind gaps between elements.

Hussain and Lee (1980) also observed that the transitions between flow regimes also depended on the shape of the roughness elements as well as their spacing. Their data on the isolated roughness to wake interference transition can be fitted very well in the range $0.5 \leq W/H \leq 4$ by the expression

* See also the discussion of Beranek's (1979; 1984) "influence area", below.

$$s_*/H \cong 1.0 + 1.4\ (W/H)^{0.25} \qquad (3)$$

where W is the crosswind width of the obstacles. Notice that a comparison of Equation (3) with Equation (2) suggests that if x_F/H is about unity over the modest range of aspect ratios in the experiments, then the wake recirculation zone length of each element in the array at the time of the transition must be roughly

$$x_R/H \cong 1.4\ (W/H)^{0.25} \qquad (4)$$

However, this is a much weaker dependence of x_R/H on W/H than that postulated by Hosker (1979), Fackrell and Pearce (1981), or by Wilson and Britter (1982) for isolated obstacles, suggesting that the wake recirculation zone of an element in an array has already been somewhat modified by the presence of other wakes and obstacles by the time the element density is large enough to trigger transition to the wake interference regime. In other words, the simple picture suggested by Hussain and Lee (1980) of an abrupt change from no interaction to wake interference is probably not strictly correct. This is unfortunate, even if not surprising, because it limits the direct use of relations developed for isolated obstacles in predicting flow transition points for arrays of obstacles.

Hussain and Lee's (1980) data on face-to-face obstacle spacing for the transition from the wake interference regime to skimming flow can be fitted by the expression

$$s_{**}/H \cong 1.25 + 0.15\ (W/H) \qquad (5a)$$

for $W/H \leq 2$, and

$$s_{**}/H \cong 1.55 \qquad (5b)$$

for $W/H \geq 2$. That is, the frontal aspect ratio of the flow obstacles in an array is important in the transition to skimming flow only for $W/H \leq 2$; for wide obstacles, formation of a stable secondary flow in the crosswind gaps of the array depends primarily on the interelement spacing, and not on the exact shape.

Equations (3) and (5) are plotted in Figure 4, to show the different flow regimes as functions of crosswind aspect ratio W/H. In view of the limited data base, this division should be regarded as tentative. Face-to-face spacing-to-height ratios s/H that are close to the boundary line could fall in either class. Furthermore, the division applies only for blocklike obstacles in a regular rectangular grid; different arrangements would give different results.

Dependence of the flow regimes on the obstacles' alongwind length to height ratio L/H is rather weak, probably because the turbulent flow reattaches to the "roof" of each obstacle that is longer than some critical

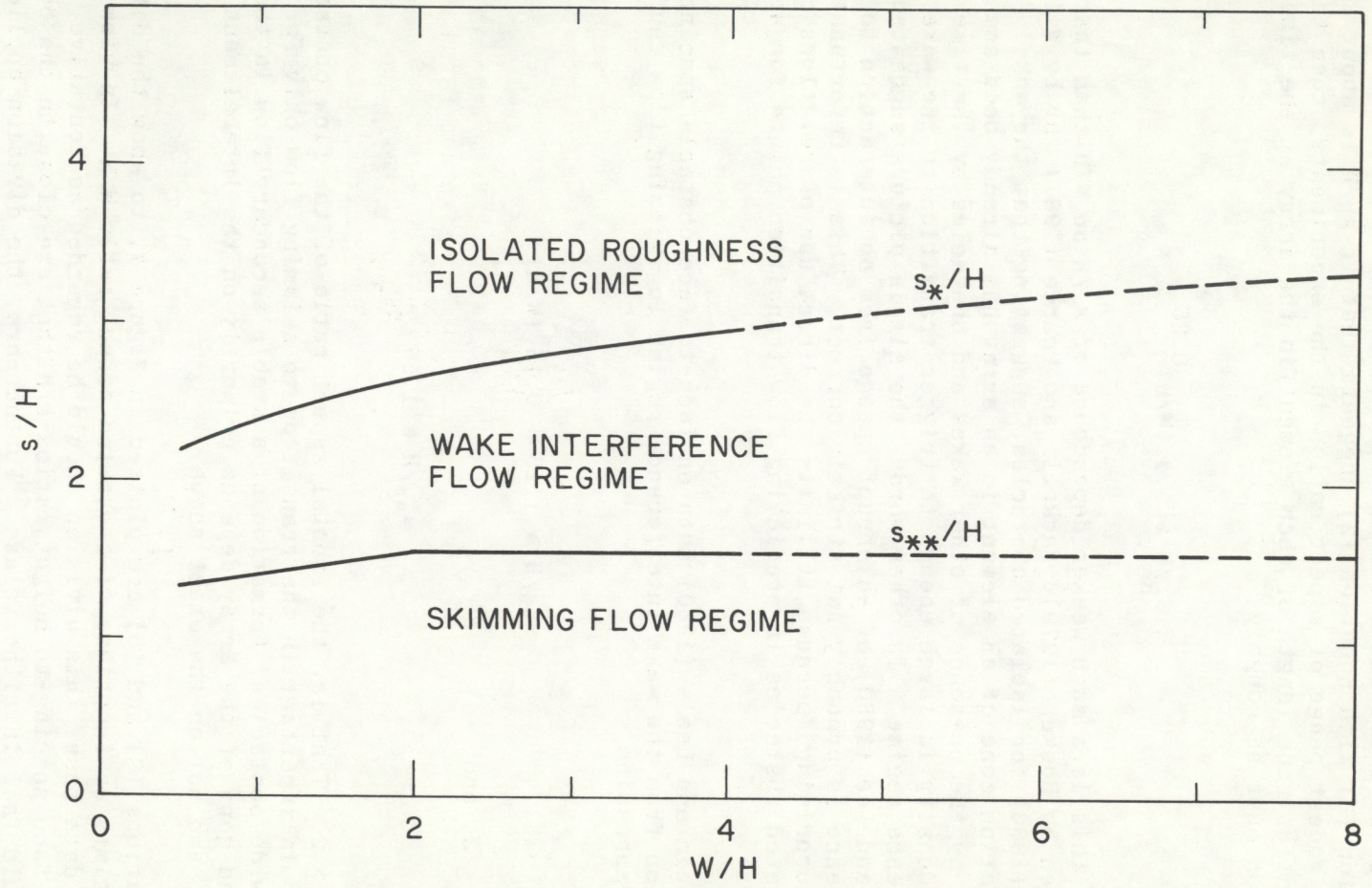

Figure 4. Zones of isolated roughness flow, wake interference flow, and skimming flow as functions of W/H. The critical separations s_* and s_{**} are defined by Equations (2-3) and (2-5) for a face-to-face spacing s of obstacles in a uniform grid.

value close to unity (e.g., Hosker, 1980, 1982). When L/H = 0.5, Hussain and Lee (1980) found that the face-to-face spacing s_* for transition between the isolated roughness and wake interference regimes is about 2.1 H, while for L/H = 1.0, 1.5, and 2.0, s_*/H = 2.4, 2.5, and 2.6, respectively. Evidently the flow pattern within the array is relatively invariant with L/H for L/H $\geq$ 1. The face-to-face spacing s_{**} for the wake interference to skimming flow transition is almost completely independent of L/H; s_{**}/H = 1.3 for L/H = 0.5, and s_{**}/H = 1.4 for all other values of L/H tested by Hussain and Lee.

In densely packed regions with even moderately tall buildings, face-to-face building spacing to height ratios s/H will often be $\leq$ 1.5. Under these circumstances, the flow would be expected to be in the "skimming" regime, with well-developed secondary flows in the gaps between the buildings, and the mean flow passing over the rooftops with little penetration into the "street canyons". Clearly this has important implications for local transport and dispersion of pollutants released below the rooftops. Quantitative estimates of the rate of transfer of recirculating pollutants from the below-rooftop flow to the above-building flow are not yet possible, because the exact nature of the secondary flow patterns (especially at intersections and for varying wind directions) must depend somewhat on the geometry of the particular building array. The presence of taller structures within the grid can also be expected to perturb local flows significantly. Additional work is needed to clarify the below-rooftop flows for a variety of conditions, and to assess pollutant transfer to and from these flows.

Above the rooftops, there is a region of turbulent, spatially nonhomogeneous flow in which the influence of individual roughness elements may still be detected. This is significant for pollutant concentration monitoring and for meteorological measurements, because roof or tower-mounted sensors may still be within this region of strong variability. It would be useful to know the height above which crosswind horizontal nonhomogeneity becomes negligible. Mulhearn and Finnigan's (1978) laboratory study of a random roughness surface suggested that the spacing of the elements was a controlling parameter. They found that the mean wind profile was well-described by the usual log-law expression for heights z > S, where S was the mean center-to-center spacing of their roughness elements. They cited other studies conducted both in the laboratory and the field which reached similar conclusions. They also noted that the Reynolds shear stress continued to show horizontal nonuniformities until z > 2 S. Raupach, Thom, and Edwards (1980) studied the height of the roughness sublayer over uniform arrays of simple obstacles of center-to-center spacing S. They found that the flow became horizontally uniform in the crosswind direction for z $\geq$ H + S. However, they observed a layer of greater than ambient diffusivity, attributed to wake diffusion, above the obstacles, such that the usual log-law velocity profile was not followed until z $\geq$ H + 1.5 S. Their simple wake diffusion model was able to successfully predict horizontally-averaged mean velocity profiles. They suggested that a "safe" height for measurements over a rough surface should be

$$z \geq H + 1.5\ S \qquad (6)$$

Further experiments in the laboratory and in the field are needed to confirm this estimate, which is reminiscent of the well-known "good engineering practice" (GEP) rule for placing stack effluent above the region of influence of isolated buildings.

2.3 Flow Near Simple Clusters of Buildings

2.3.1 Previous Work

The least understood portion of the near-building air pollutant transport and dispersion problem deals with relatively short distances -- a few hundred metres or so -- in flow fields dominated by the aerodynamics of many buildings. In many (perhaps most) instances the shapes, relative sizes, and distribution of the buildings will be so individual as to preclude any generalized description of the likely flow and dispersion patterns. Recourse to highly specific experimental or numerical studies will be necessary.

The situation is not entirely hopeless, however. A good deal of experimental effort has been directed toward particular buildings and groups of buildings, often for architectural purposes such as wind loading, pedestrian comfort, or stack and air vent design for smoke and odor control. Careful examination of these case studies can provide some insights into the more general situation. When one or two buildings are sized so as to dominate their neighbors, one can sometimes appeal to the work conducted on isolated buildings, because the surrounding smaller structures tend to serve in this instance as mere roughness elements.

Relatively little theoretical work has been done on the general aerodynamic problem of flow near clusters of obstacles, except for very simple examples such as an array of rods (e.g., Goldstein, 1965). Laboratory studies of idealized systems such as pairs of two-dimensional cylinders and plates suggest some interesting properties. For edge-to-edge spacings s between 0.1 and 1 W, where W is the crosswind width of each obstacle, the near wake region is both unsteady and asymmetric, with one body having a larger cavity region than the other at a given instant. The phenomenon is bistable; the wake does not favor either body, but switches back and forth. The jet-like flow through the gap between the bodies may be the cause of this asymmetry -- the jet seems to behave as a kind of fluidic oscillator. The review by Hosker (1984) describes the relevant literature. The effects of finite building height, wind speed shear, and incident turbulence on this phenomenon have not been adequately studied. The consequences for pollutant dispersion of the between-building jet and asymmetric bistable wake must depend upon the location of the source (e.g., an upwind source's emissions may be transported through the inter-building gap, while effluent emitted directly into the wake of one of the structures may experience an intermittently greater dilution), but are largely unknown.

A number of experimental studies of simple building clusters have been reported. Unfortunately, most have been conducted on laboratory scales with techniques and instrumentation which may have influenced the results.

Quantitative conclusions must be drawn with considerable caution, although some interesting qualitative results are available.

For example, several authors have studied in the laboratory the common two-body problem of a high-rise building downwind of a lower structure (Isyumov and Davenport, 1975; Penwarden and Wise, 1975; Beranek, 1984; among others). There is some conflict in the descriptions -- for example, Isyumov and Davenport (1975) reported highly turbulent, intermittent flow in the gap between the buildings, whereas Penwarden and Wise (1975) observed (at least in a time-averaged sense) an organized vortex in this region. The incident boundary layer flow used by Isyumov and Davenport was probably a more realistic approximation of the atmosphere, and may be responsible for the discrepancy. However, Britter and Hunt (1979) suggested that the quantitative results of both earlier studies should be regarded with caution because the heated-sensor anemometers used in both investigations cannot produce accurate data in highly turbulent reversing flows. In particular, such instruments inherently combine data on the mean and turbulent components of the flow, and do not provide information on the local flow direction.

Although the results may not be quantitatively precise, however, they may be qualitatively rather useful. In any case, the exact results depend strongly on variables such as the relative building heights, the separation of the buildings, and the aspect ratios of both buildings. Winds approaching at an angle to the two buildings must introduce considerable complexity in the form of vortex-containing wakes, although the present authors are aware of no reports describing this situation.

Britter and Hunt (1979) conducted their own investigation into the flow patterns produced by a low upwind building and a tall downwind structure using a pulsed hot-wire anemometer, which is not subject to the limitations described above. They observed a vortex structure between the two buildings which they attributed to the rollup of the turbulent shear layer shed from the lee roof edge of the upwind building; this shear layer would normally serve as the outer boundary of the recirculating wake region behind the upwind structure if the high-rise building were not in the way. Britter and Hunt's simple theoretical model predicts the maximum wind velocity between the buildings fairly well, for buildings that are not too far apart and when the downwind building is more than 2.5 times taller than the upwind one. But the physical picture (and hence the applicable model) is different for other geometries. For example, the upwind building may have a well-defined recirculation zone when the buildings are widely spaced, so that the shear layer does not strike the tall building, or the shear layer may pass right over the downwind building if the latter is not very tall. Other models must be postulated for such cases.

Britter and Hunt (1979) recommend that the aerodynamic interactions between buildings be classified as being either <u>weak</u> or <u>strong</u>. If one obstacle influences the flow about another, but is not itself affected by the presence of the second building, the interaction is weak; one might model the flow in terms of perturbations to the pressure field, drawing on knowledge of the flow about isolated obstacles. On the other hand, if the flow around the downwind body does affect that around the upwind obstacle, the interaction is strong; the modeling may involve vortex generation and

stretching, for example, to deduce the velocity fields. This distinction might be a useful way to consider building cluster problems, since weak interaction cases might be approached as perturbations of isolated obstacle flows for each of the structures involved. Strong interactions are inherently coupled and demand special treatment.

Beranek (1979; 1984) reported flow visualization tests on a number of rectangular buildings, both singly and in arrays. Figure 5 is an interesting comparison of the near-surface scouring patterns he observed for isolated large buildings (Figure 5a) and for the same buildings surrounded by smaller structures (Figure 5b). As suggested above, when there is a great disparity in building heights, the flow fields around the large buildings will generally be similar to those observed in isolated building tests. Beranek suggested that strong interactions among the flow fields of buildings of similar size can be expected when the regions of aerodynamic influence (i.e., the up- and down-wind zones of recirculations and strong flow modification) of the various buildings begin to overlap. He gave some rules of thumb for estimating the extent of these regions of influence for single buildings of various shapes; these are discussed below. Baranek also showed surface scouring patterns (some of which are reproduced in Figures 6, 7, and 8) obtained by photographic superposition of the patterns generated on a sand-covered surface during a carefully timed sequence of stepwise wind speed increases. The darkest areas shown are therefore the regions subject to strong scouring over the whole range of incident wind speeds, whereas the lightest areas are those scoured only during the strongest winds. The regions can be distinguished (approximately) by a wind speed "amplification factor" $\gamma = 6/U$; U is the value of the incident wind speed in m/s, and 6 m/s is the local wind speed needed to move the sand in Beranek's facility. Thus a scoured region that first appears at a fairly low incident wind speed -- 3 m/s, say -- means that the surface level winds in that area have reached 6 m/s, corresponding in this case to $\gamma = 2.0$; i.e., the local winds in the scoured area are roughly twice as strong as the incident wind. The amplification factor must be regarded as approximate, because it includes both mean and turbulent winds, and because other factors can affect sand movement. Nevertheless, Beranek's technique is especially useful for determining regions of strong vorticity and/or jetting. For example, Figure 6 shows a V-shaped simple array with the wind blowing directly toward the gap from different sides. A combination of jetting and vortex generation produces high winds and strong local surface scouring just downwind of the gap in each instance; vortices generated at the outboard building edges produce locally strong winds there as well. The wind is decelerated as it approaches the building array, before it accelerates to enter the gap. Figure 7 shows a complex of three simple buildings aligned along the normal to the wide building face as the wind shifts from flow parallel to the alignment axis to flow normal to the axis. The effects of the upwind vortices and recirculating wake cavity are evident in Figures 7a and 7b; the patterns are quite different, probably reflecting flow channeling, lee-edge separation, and perhaps vortex generation for the case of 45° wind incidence, shown in Figure 7b. Figure 8 shows the same three buildings offset from each other. Figures 8a and 8b show the wind at normal incidence; Figure 8a indicates the zones of local speed amplification, while Figure 8b shows the near-surface flow field. The wind is diverted around the cluster as a whole, but there seems to be significant jetting of

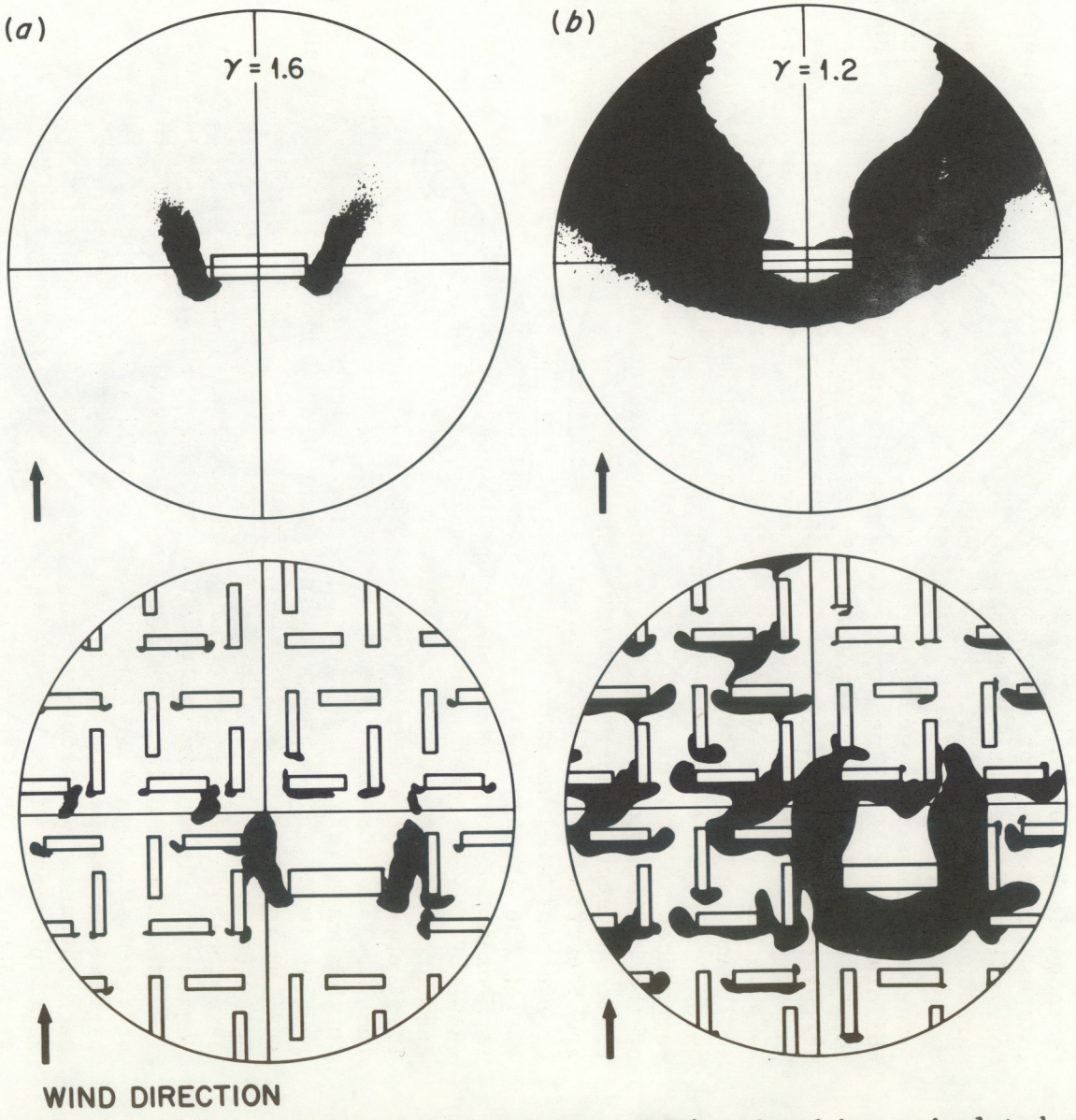

Figure 5. Surface scouring patterns (after Beranek, 1979) induced by an isolated model building (top row across), and by the same building surrounded by much lower buildings (bottom row). (a) Wind speed ratio $\gamma = 6/U = 1.6$. (b) $\gamma = 1.2$.

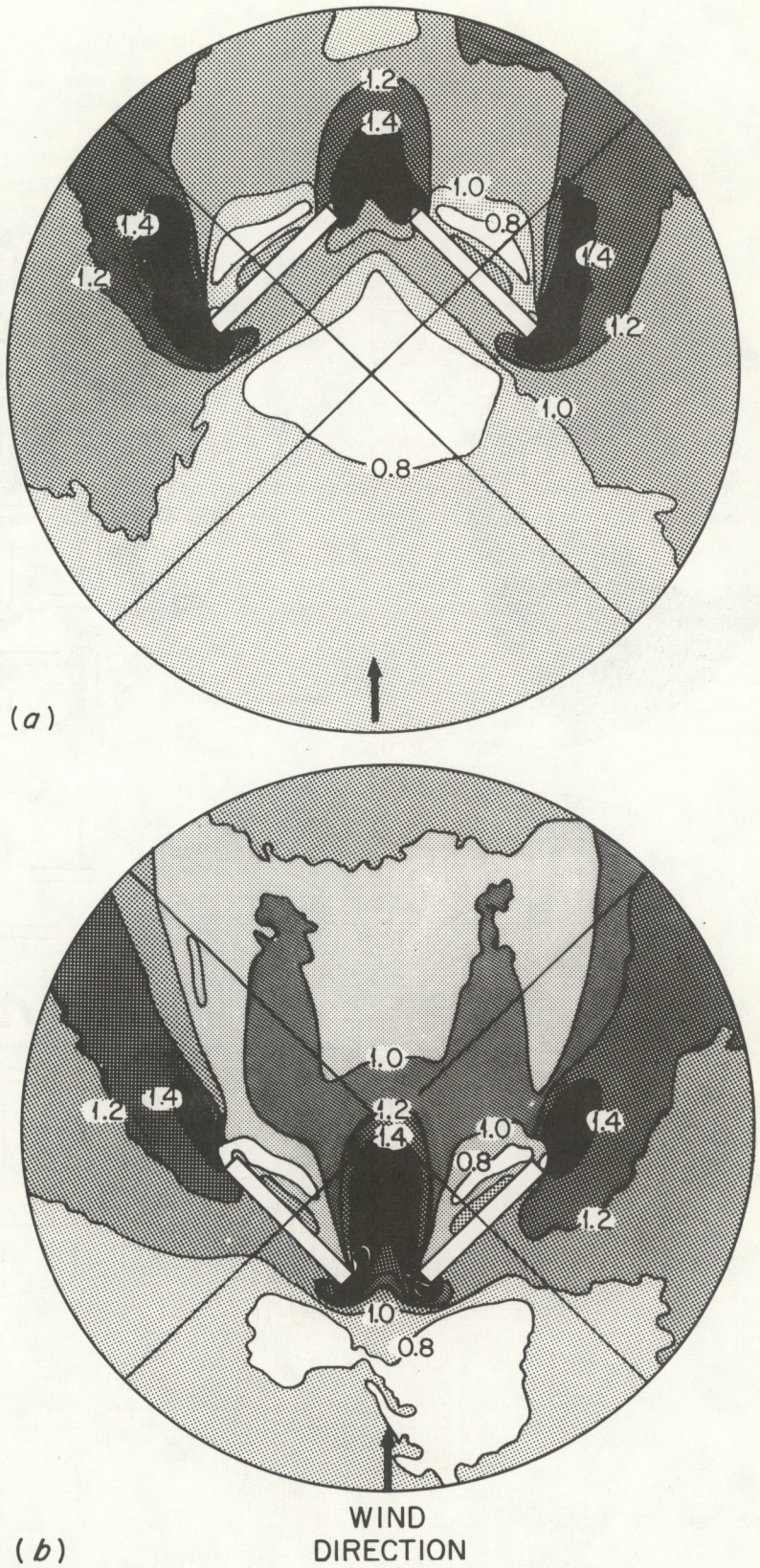

Figure 6. Surface scouring patterns (after Beranek, 1979) produced by wind approaching the gap between two buildings. (a) Wind toward "mouth" of array. (b) Wind toward "apex" of array. Numerical values correspond to a kind of local wind speed amplification factor γ, described in the text.

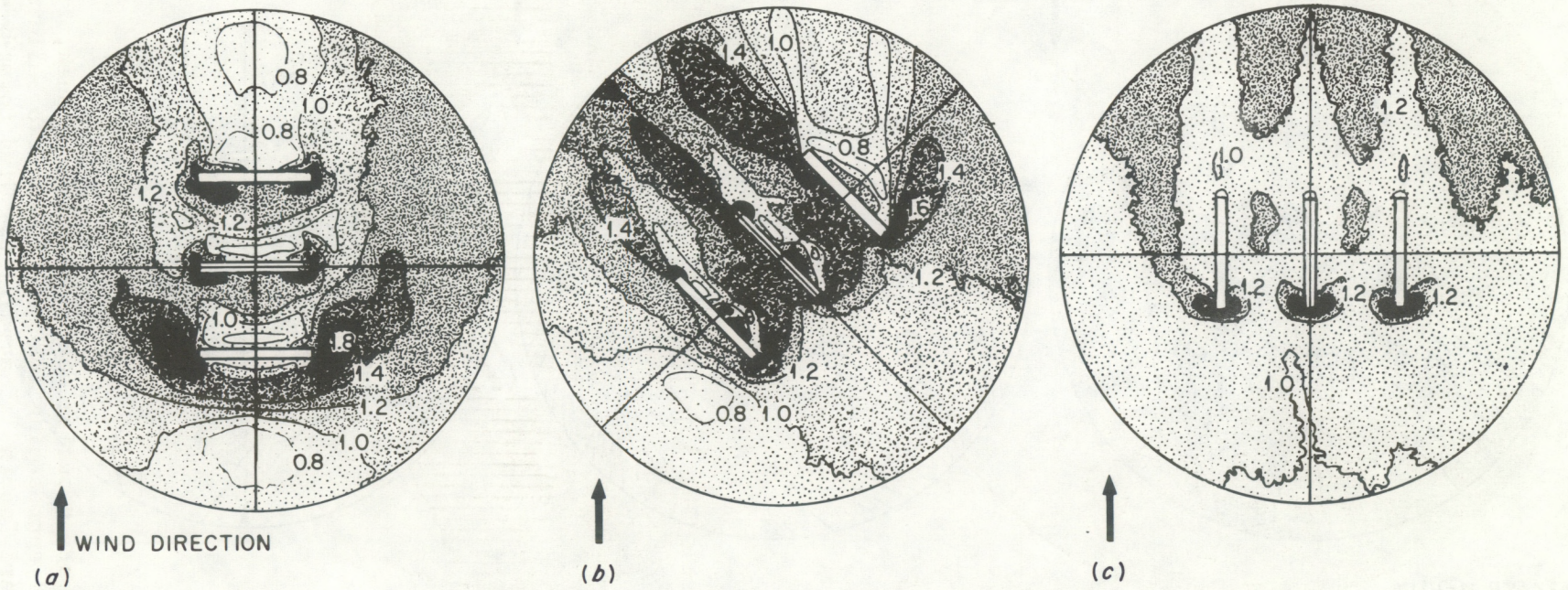

Figure 7. Surface scouring patterns (after Beranek, 1979) for three simple buildings aligned along the normal to the wide building face. (a) Incident wind parallel to alignment axis. (b) Wind at 45° to alignment axis. (c) Wind at 90° to alignment axis. The local wind speed amplification factor γ (numerical values) is described in the text.

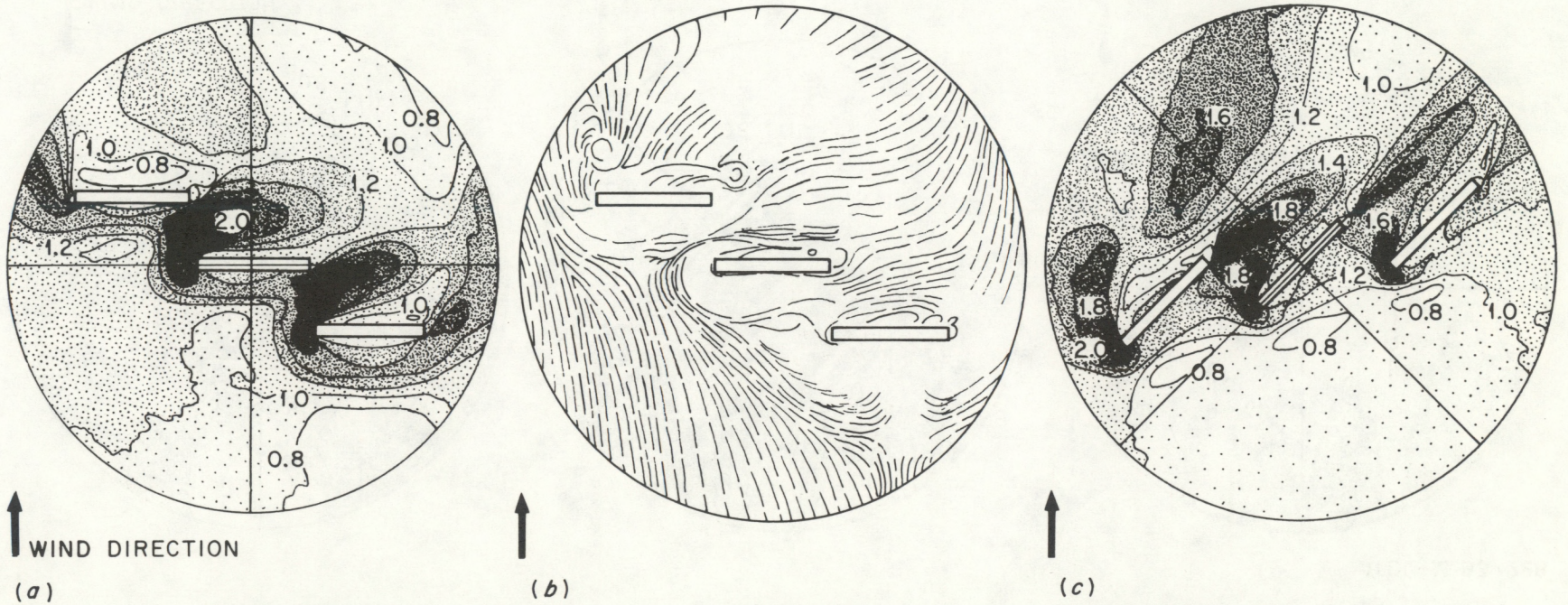

Figure 8. Surface scouring and flow patterns (after Beranek, 1979) for three simple buildings offset by one building width from alignment. (a) Incident wind normal to wide building face. (b) Same as (a), but showing surface flow patterns, rather than scouring patterns. (c) Wind at 45° to the long axis of the building. The local wind speed amplification factor γ (numerical values) is described in the text.

the flow from the stagnation zones just ahead of each structure through the gaps, so that the recirculating cavity regions normally expected behind the two upwind buildings are nearly obliterated. The wake of the leemost building, on the other hand, resembles the expected wake for an isolated bluff obstacle, except that the lee-edge vortex and the portion of the wake closest to the centerline are displaced toward the centerline by the somewhat angled crossflow. Figure 8c shows the local speed amplification factor for wind incident at 45° to the plane of the buildings; the influences of jetting and corner vortices are evident.

Beranek (1979, 1984) has suggested a simple and potentially useful scheme for estimating the "influence area" of an isolated building and, by extending the method, for estimating when adjacent buildings will have mutually interfering flow fields. Consider Figure 1. The building strongly perturbs the incident flow in the region between the frontal vortex system and the mean cavity reattachment line. This zone of strong disturbance can be roughly approximated at ground level, for many buildings, by a circle that passes through the flow separation point upwind of the building, and the wake cavity reattachment point on the lee centerline. If the building is very wide or very long, the perturbation boundary is more elliptical in shape; it can be approximated by two half-circles surrounding each end of the structure, joined by straight lines. Figure 9 illustrates Beranek's concept; R is the radius of the circle of influence, and e is the downwind displacement of the circle's center from the windward building face.

Beranek suggests that for proportionately tall buildings (Figure 9a), where $W/H < 0.8$, only the portion of the structure below a height $h' \cong 1.25$ W affects the extent of the influence area, and so R must be independent of the actual building height:

$$R \cong 1.6 \sqrt{Wh'} \cong 1.8\ W \qquad (7a)$$

For these tall buildings, the location of the center of the circle of influence is likewise independent of H:

$$e \cong 0.5\ W \qquad (7b)$$

For buildings of intermediate frontal aspect ratio (Figure 9b), where $0.8 < W/H < 3$, the circle of influence depends on both frontal dimensions:

$$R/H \cong 1.6 \sqrt{W/H} \qquad (8a)$$

The circle is centered a distance

$$e/H \cong 0.9 \sqrt{W/H} \qquad (8b)$$

behind the upwind building face.

For proportionately wide structures (Figure 9c), where $W/H > 3$, the region of influence is approximated by two connected semicircles whose radius is independent of the building width:

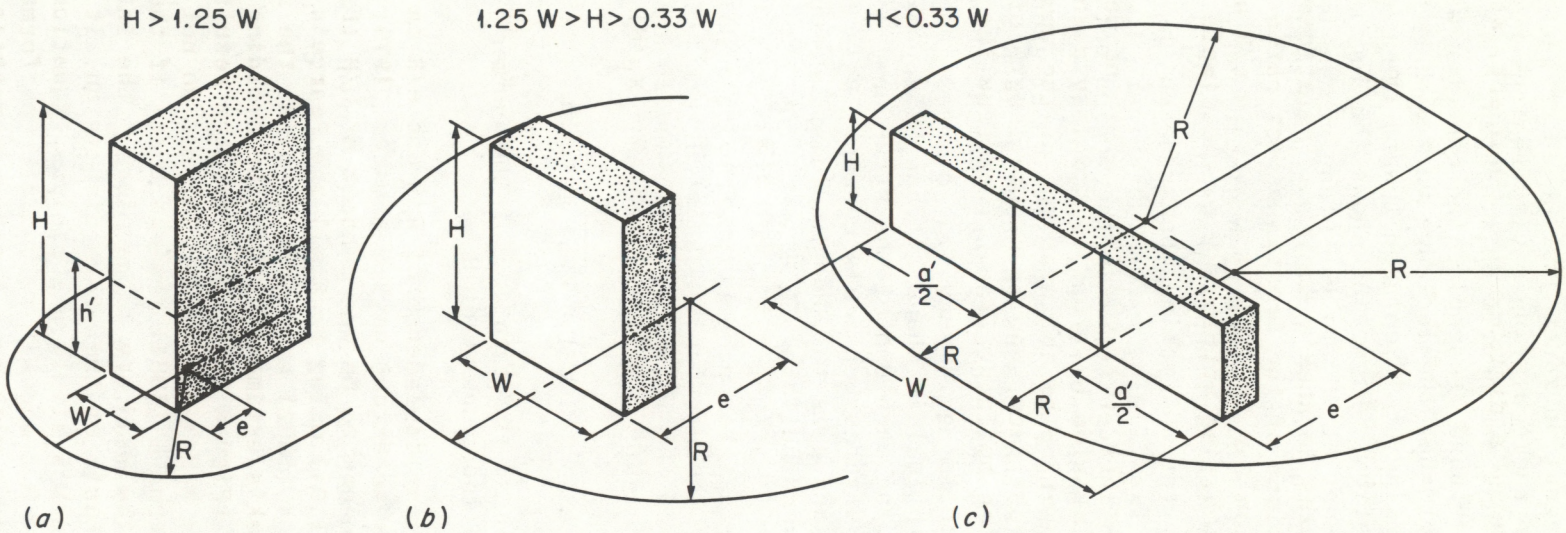

(a) $R \cong 1.6\sqrt{Wh'} \cong 1.8W$; $e \cong 0.5\ W$; $(h' \cong 1.25\ W)$

(b) $R \cong 1.6\sqrt{WH}$; $e \cong 0.9\sqrt{WH}$

(c) $R \cong 1.6\sqrt{a'H} \cong 2.8H$; $e \cong 0.9\sqrt{a'H} \cong 1.6\ H$; $(a' \cong 3\ H)$

Figure 9. Beranek's (1979, 1984) "circles of influence" for (a) a tall, narrow building, (b) a tall, wide building, and (c) a very wide building. For the wide building, the zone of influence is rather elliptical in shape; it is approximated by two semi-circles centered about 1.5 H inboard of the building sides, joined by straight lines across the gap.

$$R/H \cong 2.8 \qquad (9a)$$

These circles are centered a distance W - 3 H apart, at a distance

$$e/H \cong 1.6 \qquad (9b)$$

downwind of the front building face.

Figure 10 illustrates Beranek's empirical relations; the ratios R/H and e/H are shown as functions of the frontal aspect ratio W/H. There is no apparent physical reason for the discontinuity in e/H at W/H = 0.8; the abrupt change can probably be attributed to the simple functions Beranek fitted to the data.

Note that Equations (7), (8), and (9) exhibit no dependence on the along-wind building dimension L. This is probably a shortcoming of Beranek's procedure. Let x_F be the distance of the upwind separation point from the building's front face, and x_R be the length of the recirculation zone relative to the lee building face. Then from the geometry of Figure 11,

$$x_F + L + x_R = 2\ R$$

and

$$x_F + e + R = 2\ R$$

Hence

$$R/H = 0.5\ (L/H + x_R/H + x_F/H) \qquad (10a)$$

and

$$e/H = 0.5\ (L/H + x_R/H - x_F/H) \qquad (10b)$$

Aside from the linear dependence of R/H and e/H on L/H, it is known that x_R/H depends to some extent on L/H (Hosker, 1979; Fackrell and Pearce, 1981), although x_F/H seems to be independent of L/H (Fackrell, 1982). If we evaluate Equation (10a) using Fackrell and Pearce's (1981) expression for x_R/H and Fackrell's (1982) equation for x_F/H, the results for R/H are fairly close to Beranek's estimate within the building geometry ranges of $W/H < 3$ and $L/H \leq 0.5$ (Figure 12). However, the results do not agree with Beranek's estimate for $W/H > 3$ for any L/H, and do not agree, even for $W/H < 3$, if $L/H \geq 0.5$. Beranek (1984) remarks that, if the dimensions of the building parallel to the wind are rather large, the influence area has to be modified. On the basis of the above discussion, it would seem best to limit the use of Beranek's simple expressions (Equations 7, 8, 9) to geometries where $L/H \leq 0.5$ and $W/H < 3$; different formulations are apparently needed to cope with more extreme geometries.

Regardless of the exact form of the expression for R/H as a function of W/H and L/H, the concept of a radius of influence remains useful, particularly when it is applied to adjacent buildings. Consider Figure

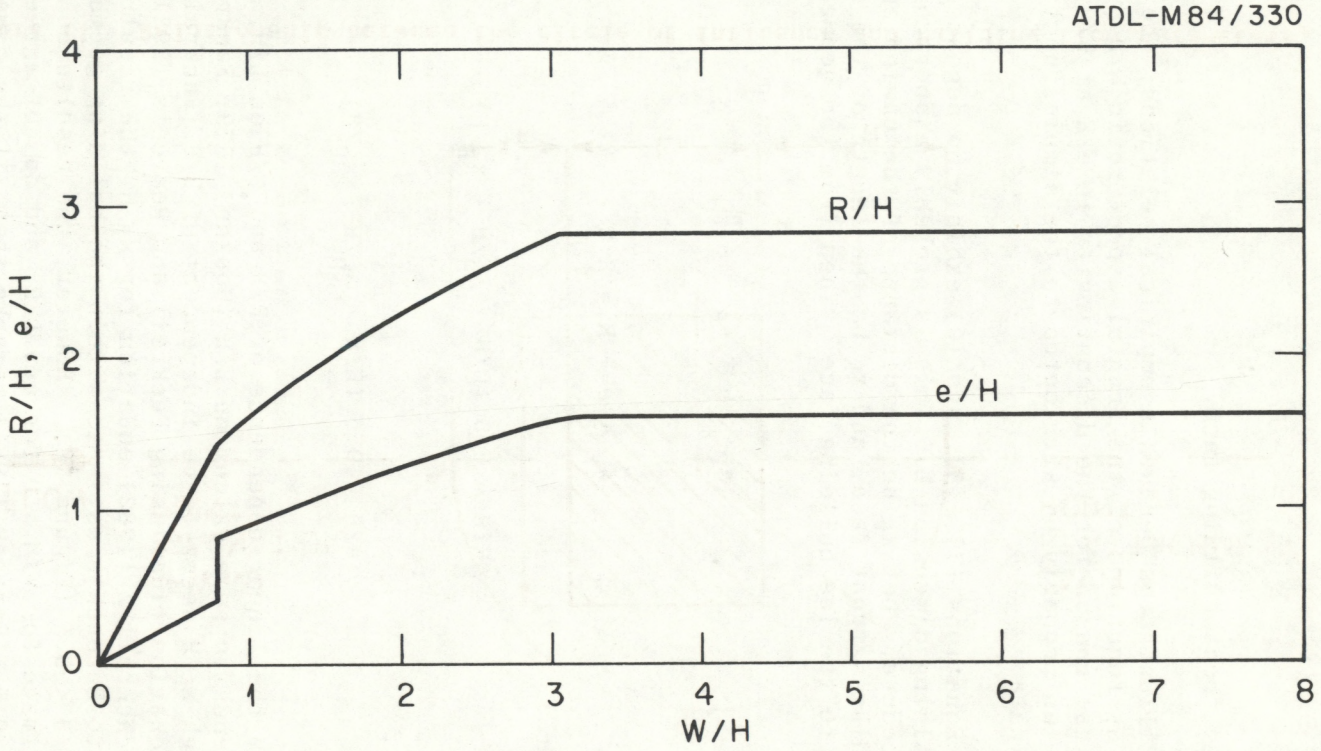

Figure 10. Beranek's (1979, 1984) empirical relations (Equations 2-8a, b) for the circle of influence parameters R/H and e/H as functions of the frontal aspect ratio W/H.

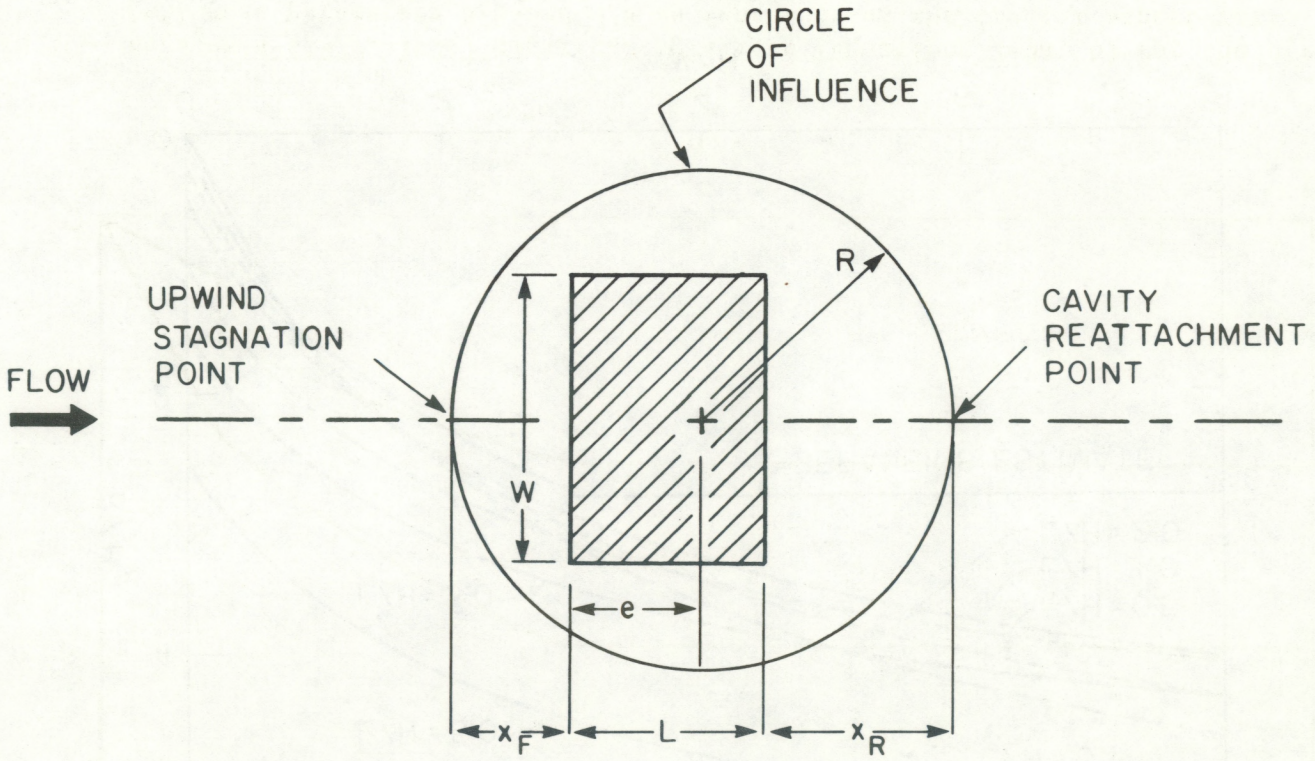

Figure 11. Relationship between the circle of influence and building flow parameters, x_F, x_R.

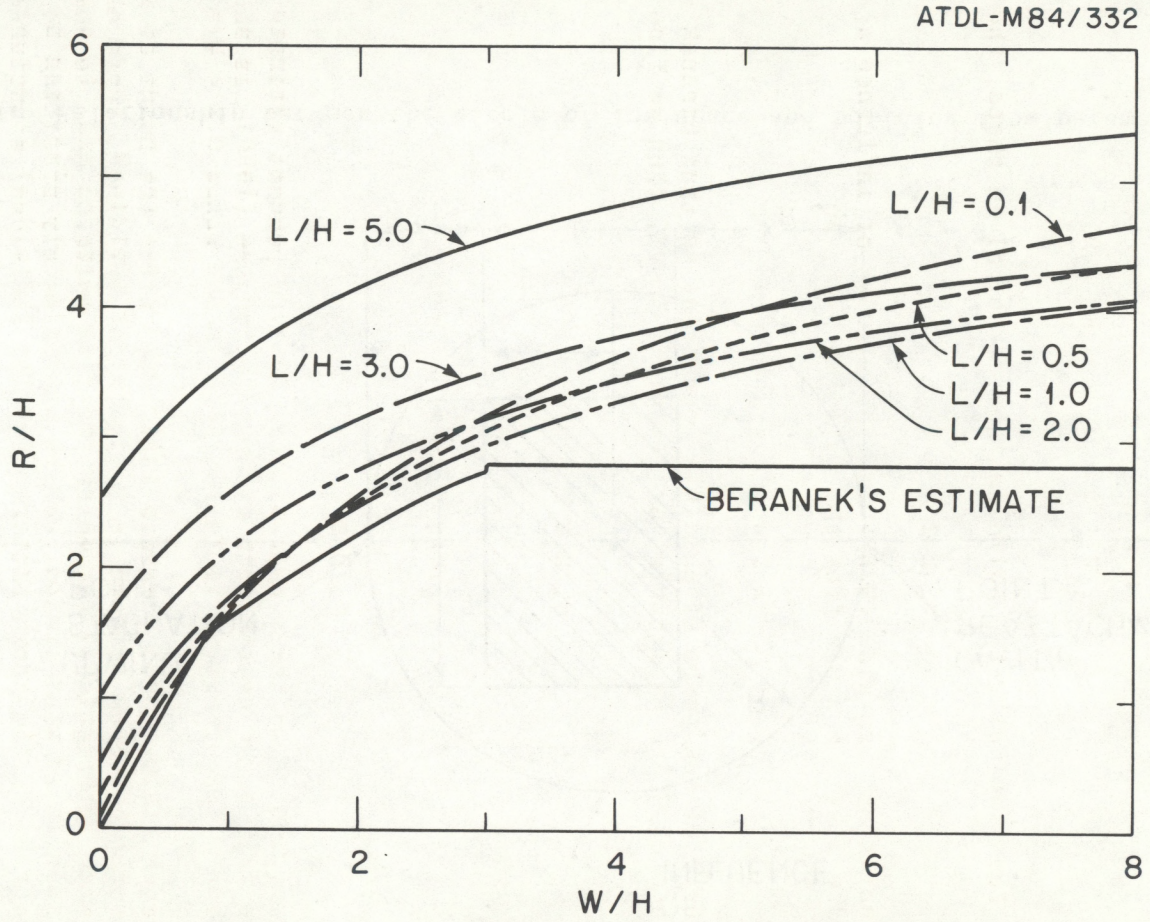

Figure 12. Calculated R/H versus W/H, for various L/H, using Fackrell and Pearce's (1981) expression for x_R/H and Fackrell's (1982) estimate for x_F/H, compared to Beranek's (1979, 1984) expression.

13a, which shows two buildings of crosswind widths W_1 and W_2, separated by a face-to-face spacing s. If the circles of influence of these buildings overlap, then the flow field near each structure is subject to interference from the other. We expect to see a transition from "isolated roughness" flow to the "wake interference" regime when the circles of influence first touch: that is, $s = s_*$ when

$$W_1/2 + s + W_2/2 \cong R_1 + R_2$$

Suppose for simplicity the buildings are identical in shape; then

$$s_* \cong 2\ R - W \qquad (11a)$$

If the buildings are wide (W/H > 3), the circles of influence are centered a distance 3 H/2 from the building side, so

$$s_* = 2\ R - 3\ H \qquad (11b)$$

If we restrict the range of possible geometries so that Beranek's simple relations for R are applicable, as discussed above, then we find for W/H < 0.8,

$$s_*/H \cong 2.6\ W/H; \qquad (12a)$$

for 0.8 < W/H < 3,

$$s_*/H \cong 3.2\ \sqrt{W/H} - W/H \qquad (12b)$$

and for W/H > 3

$$s_*/H \cong 2.6 \qquad (12c)$$

Figure 13b shows these expressions; the independent estimate given by Equation (3), based on the data of Hussain and Lee (1980), is shown for comparison. The agreement is fairly good in the range 0.8 < W/H < 3.

Beranek (1979, 1984) suggests that, even after the point of mutual flow interference has been reached in a cluster of buildings, there are some cases (weak interactions) for which the flow patterns and, to some extent, the maximum local wind speeds, can be approximately predicted by a kind of superposition of the known patterns for the individual structures. In other cases (strong interactions), between-building jetting, vortex formation, and other effects preclude any simple estimates of the wind patterns and speeds; wind tunnel or field tests will be needed for these configurations. It should be borne in mind by the air pollution specialist that Beranek's work, while very instructive, was performed primarily from the point of view of pedestrian discomfort in built-up regions. His results are thus somewhat qualitative in nature, although some quantitative estimates of maximum local wind speeds can be made. In any case, a careful reading of the original publications (especially Beranek, 1984) is recommended.

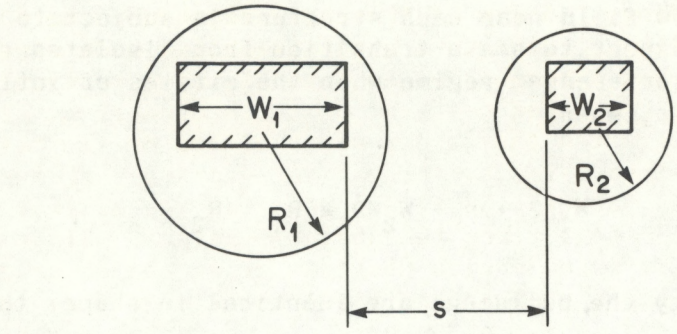

(a)

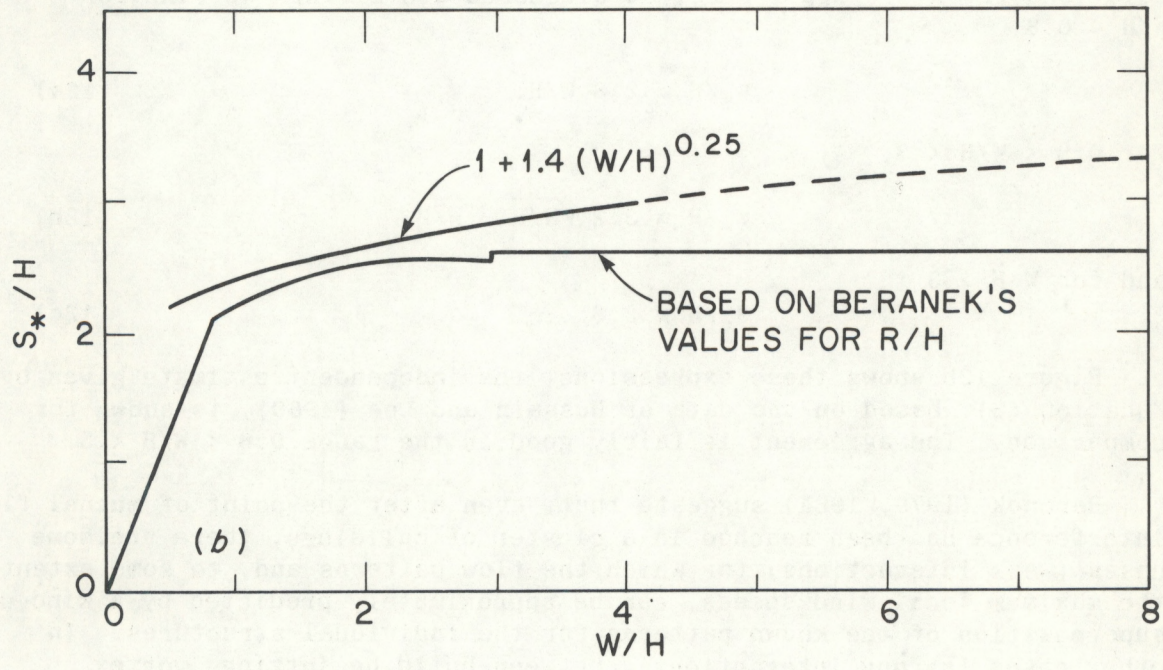

Figure 13. Transition to flow interference regime. (a) Geometry. (b) s_*/H calculated, (assuming identical buildings), using Beranek's (1979, 1984) expressions for the circle of influence, compared to an empirical expression for s_*/H based on data of Hussain and Lee (1980).

Gandemer (1976) published an interesting series of sketches and photographs of the flow patterns characteristic of some other common arrangements of buildings. A few of these are reproduced here. Figure 14a shows the wind normally incident to a gap between two wide structures. The flow accelerates to pass through the gap, and standing vertically-oriented lee-edge vortices are generated near the obstacle corners on either side of the gap. Gandemer suggested that a gap width of one or two building heights gives the maximum velocity through the gap; this agrees well with the study of Logan and Barber (1980), who reported the maximum speed was reached for gaps of 1.5 to 2 times the obstacle height. Figure 14b illustrates the wind striking a wide obstacle at an angle, producing a wake vortex. The jetting and vortex production effects near a gap or end must be quite complex in this case, but details are unavailable. Figure 14c is another common arrangement leading to a venturi effect; if the buildings are somewhat curved, the passageway between them is an excellent approximation to a true nozzle, and very high wind speeds can be reached at the "throat". The maximum speed in the gap will be found when the opening is two or three times wider than the average building height. Figure 14d shows the jetting that can be induced between zones of locally high (semi-stagnation region) and low (wake) pressure; quite high speeds can be reached, and the local flow direction can be quite different than the incident one. If the buildings are tall towers, the strongest winds through the gap will be reached when the spacing is about one-fourth the width of the buildings.

2.3.2 Systematic Study of Simple Clusters of Buildings

To elucidate the complex flow patterns which occur within even very simple clusters of buildings, a systematic laboratory study was undertaken of identical cubical buildings placed at various distances from one another. Between one and five buildings were used in any given test; more than 75 cases were examined. Emphasis was placed on the time-averaged flow patterns near ground level, as revealed by flow visualization techniques. The work was conducted in a boundary-layer wind tunnel. Details of the experimental program are given in Appendix 1. A brief summary of the findings is given here; a more complete description of the study will be published separately. Study of complete sequences of such photos can provide considerable insight at low cost into flow patterns near ground level. Additional visualization work (smoke, helium bubbles, etc.) and direct measurements are still needed to determine the flow patterns aloft. Recent techniques such as video digitization can simplify and quantify the analyses.

2.3.2.1 Single buildings

Figure 15 shows photographs of the surface flow patterns (pigment in oil film) associated with three different single building geometries, all placed normal to the incident wind. These patterns are representative of the time-averaged ground level flows generally observed near all simple buildings (see Figures 1 and 2). The frontal separation zone, the horseshoe vortex system, the lee-edge vortex pair, and the wake cavity reattachment line can all be discerned in the photos. Measurements from

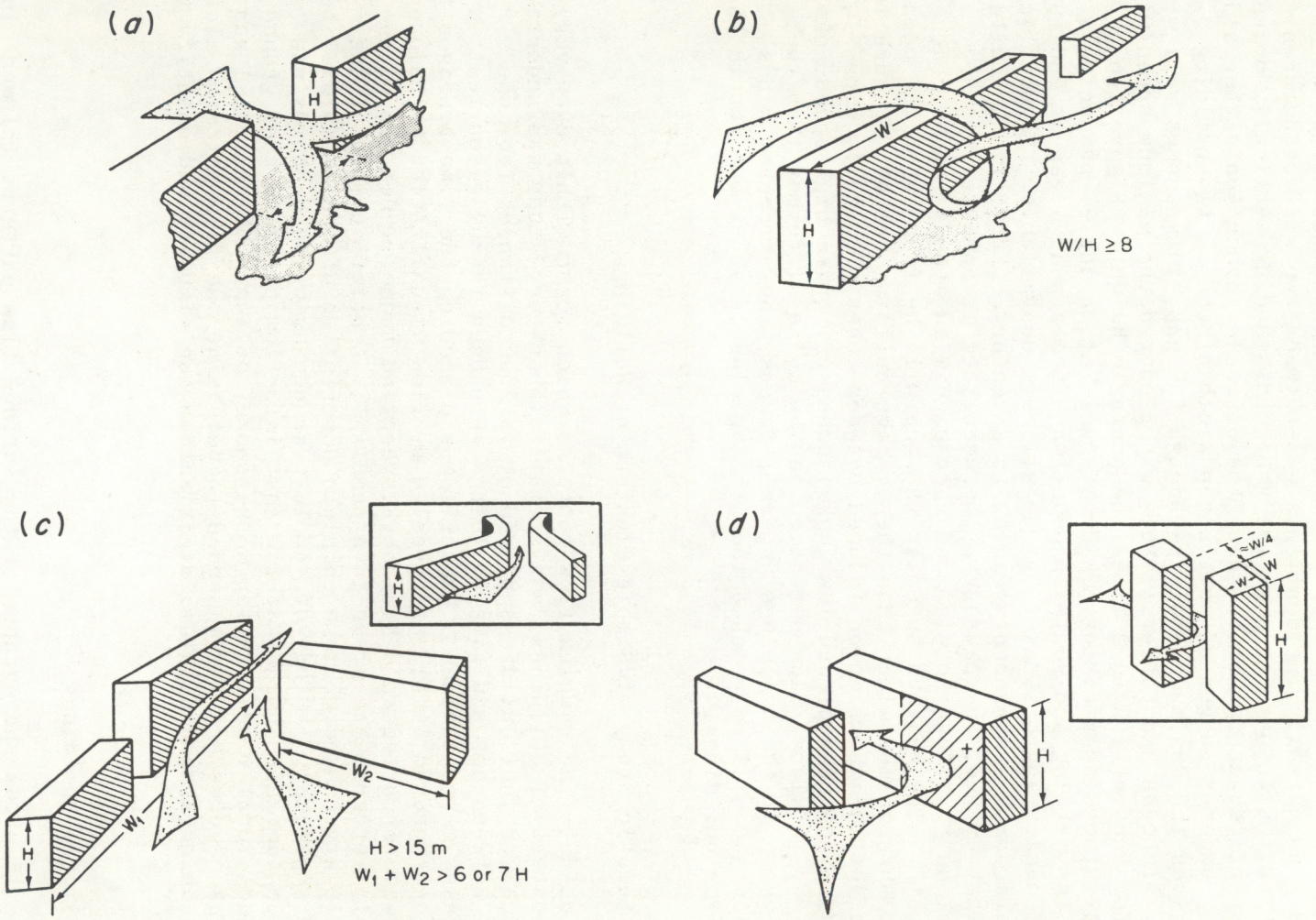

Figure 14. Sketches of flow patterns near typical building clusters (from Gandemer, 1976). (a) Wind normally incident to a gap between two wide structures. (b) Wind striking a wide obstacle at an angle. (c) Arrangement leading to a venturi effect. (d) Deflection and jetting of flow between two buildings.

(a) W/H = 1 = L/H

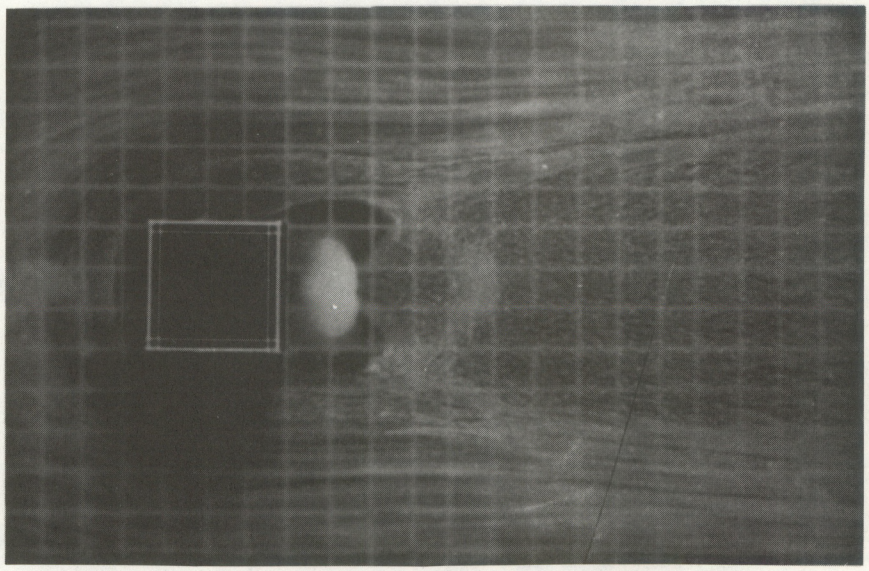

Figure 15. Surface flow patterns associated with three single building geometries normal to incident wind. (a) W/H = 1 = L/H. (b) W/H = 2, L/H = 1. (c) W/H = 3, L/H = 1.

(b) W/H = 2, L/H = 1.

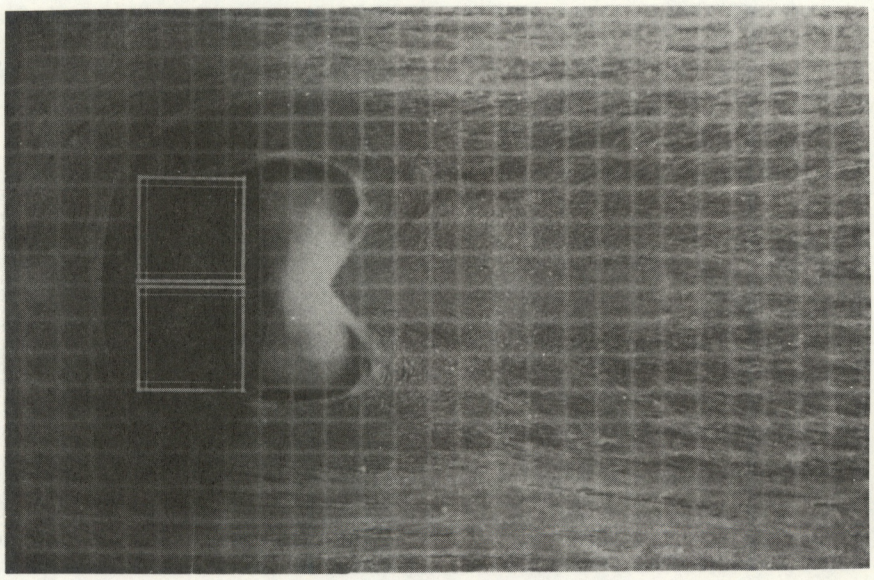

(c) W/H = 3, L/H = 1.

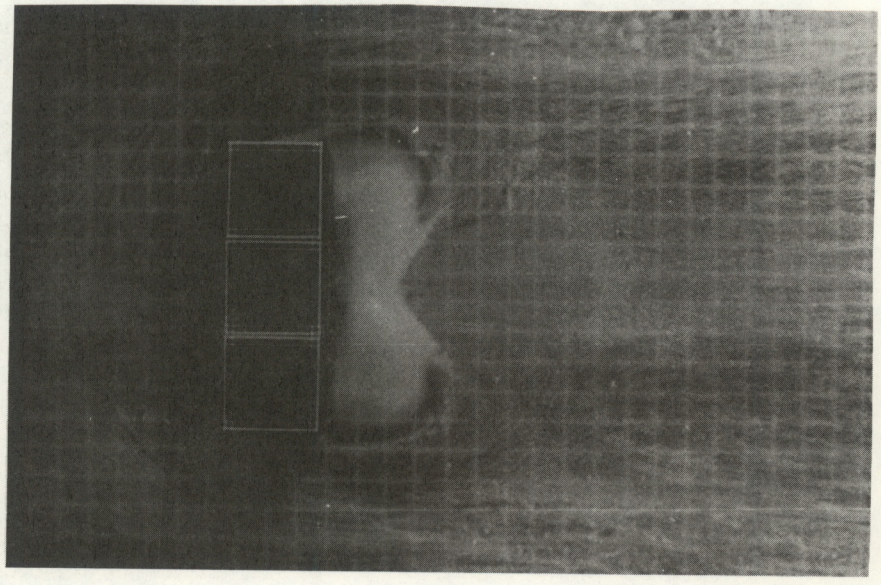

Figure 15 (continued)

the photographs of features such as lines of demarcation between flow zones are quite feasible, although necessarily somewhat subjective. For example, the frontal separation point upwind of the cubical building (Figure 15a, W/H = 1 = L/H) is $x_F \cong 0.4$ H. However, the frontal separation point for the widest building shown (Figure 15c, W/H = 3, L/H = 1) is more difficult to determine, but an estimate of $x_F \cong 1$ H seems quite reasonable. Table 1 shows the various perturbed flow parameters evaluated from Figure 15.

Table 1. Measurements of flow phenomena associated with winds normally incident on isolated simple buildings with L/H = 1.

			lee-edge vortex pair			
W/H	x_F/H	y_{HV}/H	x_V/H	y_V/H	d_V/H	x_R/H
1	0.4	1.0	0.3	0.3	0.3	0.66
2	0.6	1.3	0.5	0.3	0.5	1.9
3	1.0	1.6	0.66	0.3	0.6	3.0

Notes:

x_F and x_R are the lengths of the frontal separation zone and the recirculating cavity zone, relative to the windward or lee building faces, respectively.

y_{HV} is the maximum crosswind distance of the horseshoe vortex system from the centerline.

x_V, y_V, and d_V specify the distance of the center of the lee-edge vortices from the lee building face and the centerline, and the approximate diameter of those vortices, respectively.

Two other simulations were performed using single buildings; the cubical structure (W/H = 1 = L/H) was rotated so that its most exposed windward face was, successively, 30° and 45° from the crosswind direction. Figure 16a shows the result for the 30° inclination. The flow pattern is greatly distorted from the normal incidence case. The frontal separation occurs only about 0.3 H upwind of the building in this more "streamlined" configuration, and the horseshoe vortex system is skewed to the right (i.e., along the more exposed face). A side recirculation zone is present only behind the right corner. The lee edge vortices are elongated along the direction of the approach flow; while these vortices are offset relative to each other, they both are centered about 0.66 H downstream of their respective building corners. The even more stream-lined 45° configuration is shown in Figure 16b. Here the flow is diverted along the exposed sides of the building, and no upwind separation occurs. The flow appears to be separating about two-thirds of the way along each exposed face, contributing to very elongated lee-edge vortices centered about 1 H downstream of the building corners. These results are consistent with those of other observers (e.g., Castro and Robins, 1977).

(a) $\theta = 30°$.

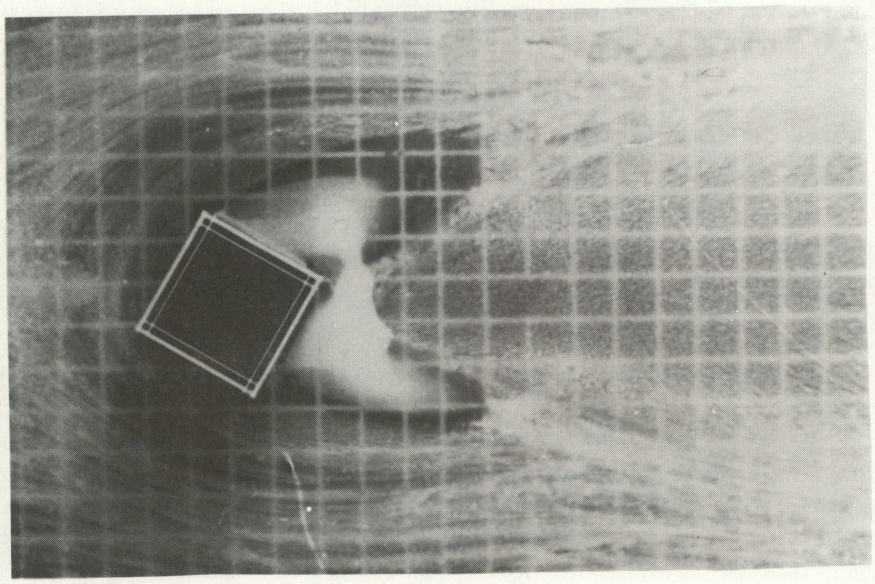

Figure 16. Surface flow patterns associated with a single building at an angle to the incident wind. (a) $\theta = 30°$. (b) $\theta = 45°$.

(b) $\theta = 45°$.

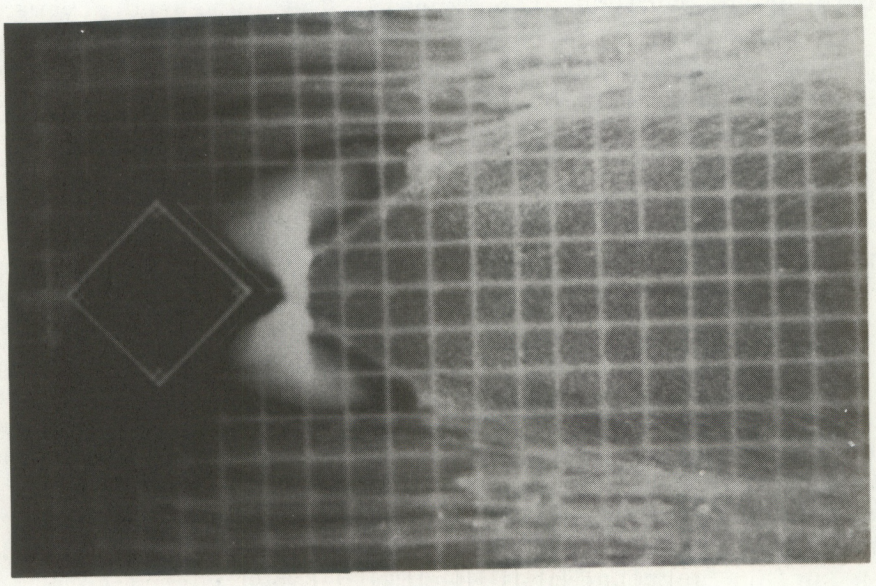

Figure 16 (continued)

2.3.2.2 Two cubical buildings

The simplest possible building complex consists of only two structures. A large number of array geometries are possible even in this case: the buildings can be in a crosswind or alongwind line, or staggered, or rotated so that the sides are not parallel, or combinations of these. Figure 17 illustrates the results of a progressive decrease in separation distance for a cross-wind array of two cubical buildings (W/H = 1 = L/H). Figure 17a shows a face-to-face separation s = 2.67 H. Each building shows a distinct frontal separation region and horseshoe vortex pattern. The flow fields do not appear to interact significantly near the buildings; only for distances more than about 4 H downwind of the buildings are noticable wake interactions present. When the separation s is reduced to 2.33 H (Figure 17b), the near-building patterns are unchanged, but the point of wake interaction moves to about 1.67 H downstream of the buildings. However, for a further reduction of s to 2.0 H (Figure 17c), there is a significant change in the shape of the horseshoe vortex patterns in the region between the buildings. The horseshoe vortices between the structures apparently form a persistent central "tail" in the wake region, separating the recirculation zones. The increased movement of pigment in the oil film along this "tail" indicates increases in the local flow speed and surface shear stress. At s = 1.33 H (Figure 17d), the flow interactions are quite obvious. The dark area between the two buildings has been swept clear of pigment, illustrating the higher local wind speed in this region as a kind of jet is formed. It is interesting that the combined horseshoe vortices between the buildings do not appear to be quite as persistent as was the case at s = 2.0 H. The flow patterns associated with the outboard edges of each building are essentially unaffected by the decreasing separation distance. The lee-edge vortices are still present and unmoved from their original positions at much wider separations, but the inboard vortices seem to be slightly altered in shape. At a separation s = 1.0 H (Figure 17e), the decreased persistence of the central horseshoe vortex "tail" is evident, and the central region immediately between the structures is nearly clear of pigment, indicating strong local winds in the between-building jet. The lee-edge vortices show enough change that the flow pattern directly behind the buildings is larger on the outboard sides, although the inboard vortices appear to be quite strong, judging by the clean surface surrounding a sharply defined vortex core. At a separation s = 0.67 H (Figure 17f), the central "tail" in the wake has nearly disappeared. The lee-edge vortices are asymmetric enough that a non-symmetric accumulation of pigment is evident in the near wake of each building; the inboard lee-edge vortices are elongated, as shown more clearly in the view from behind the buildings, Figure 17g. A close-up view of the inter-building flow pattern is shown in Figure 17h. The acceleration of the flow between the buildings is reflected in the smooth pattern and effective scouring of pigment in the oil film in this region. With a further decrease in spacing to s = 0.33 H (Figure 17i), the frontal separation zone and horseshoe vortices begin to assume the characteristics associated with a single building of W/H = 2, although there is still a strong flow through the opening between the buildings. The inboard lee-edge vortices are significantly larger than the outboard ones, and very strong, judging by the well-scoured area around the central core. The limiting case in this sequence of gradual decreases in separation is the single building case, shown previously in Figure 15b.

(a) s = 2.67 H.

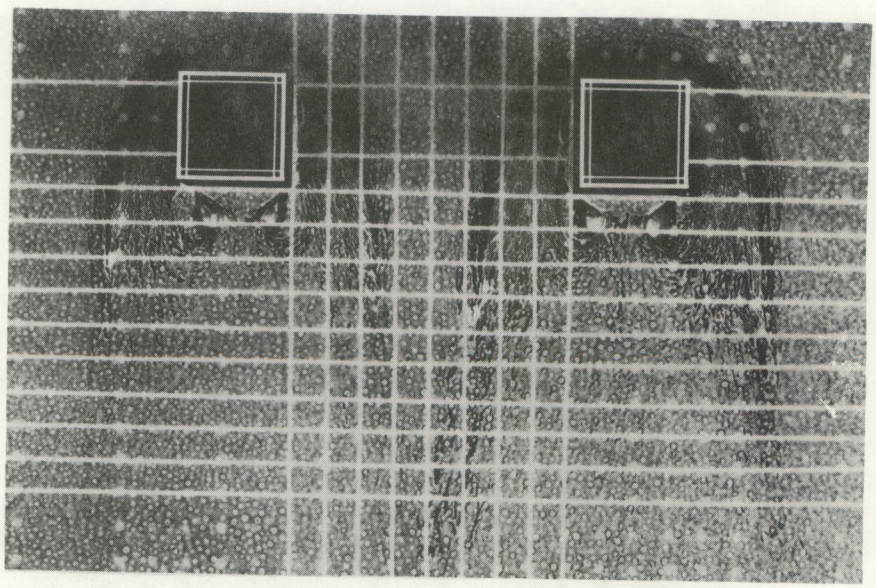

Figure 17. Surface flow patterns associated with two buildings (W/H = 1 = L/H) normal to the incident wind, with cross-wind separation s. (a) s = 2.67 H. (b) s = 2.33 H. (c) s = 2.0 H. (d) s = 1.33 H. (e) s = 1.0 H. (f) s = 0.67 H. (g) s= 0.67 H, seen from behind the buildings. (h) s = 0.67 H, closeup of the flow patterns between the buildings. (i) s = 0.33 H.

(b) s = 2.33 H

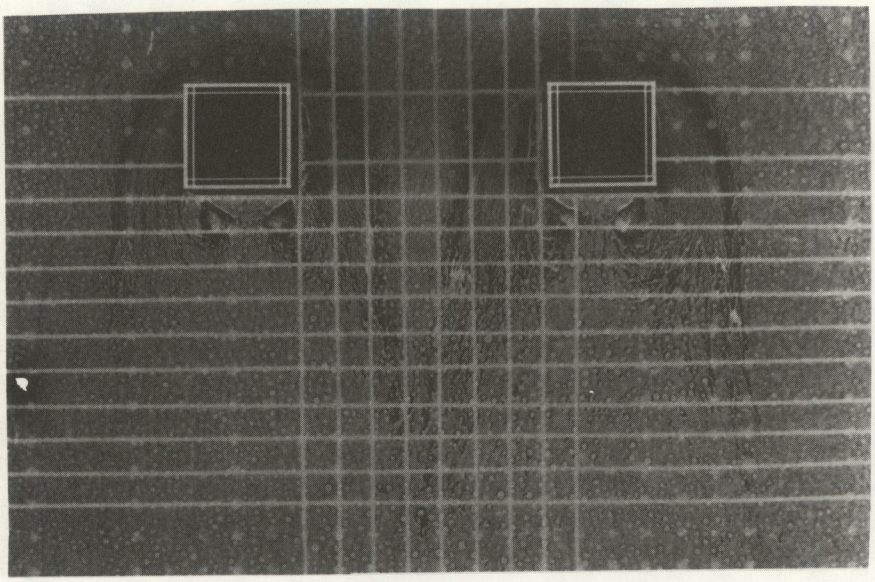

(c) s = 2.0 H

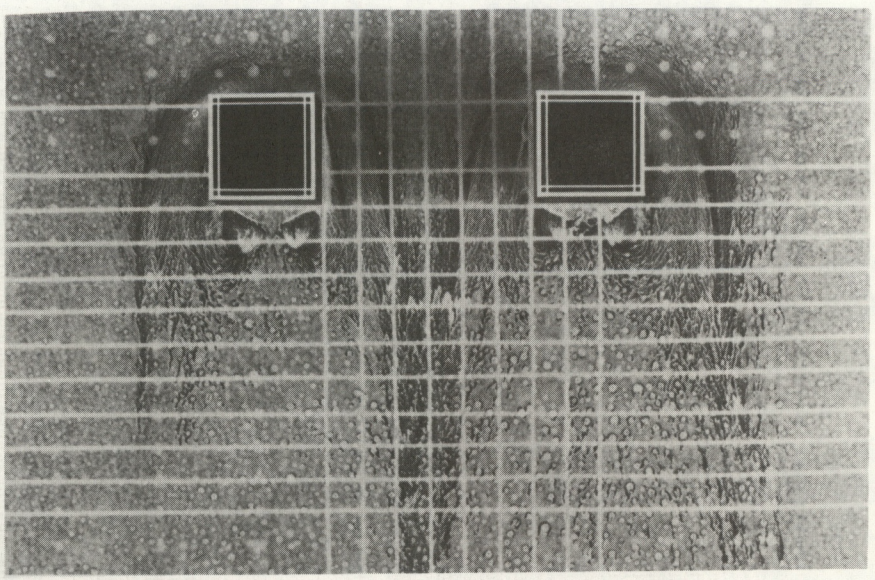

Figure 17 (continued)

(d) s = 1.33 H.

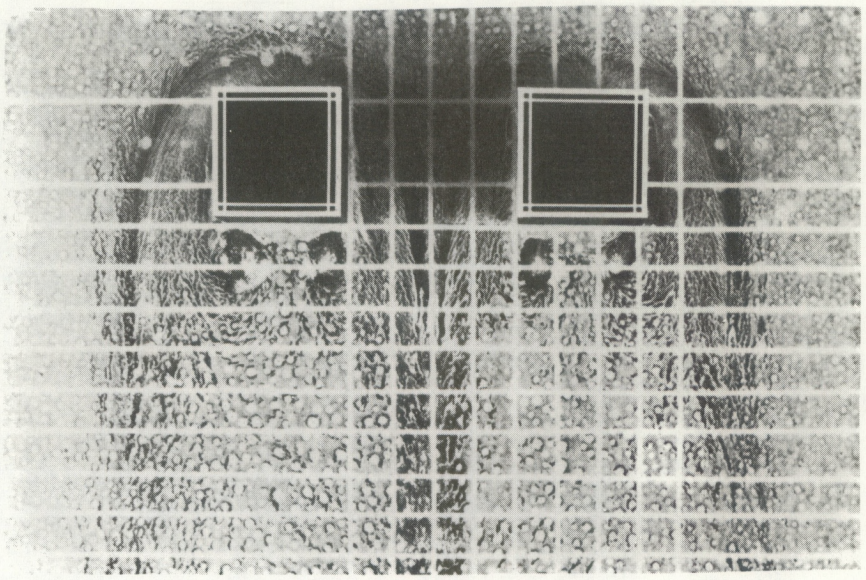

(e) s = 1.0 H.

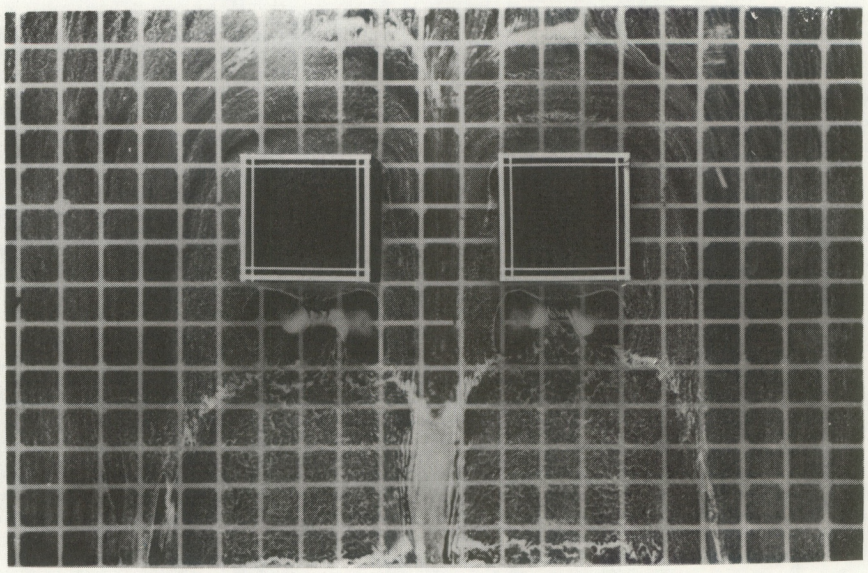

Figure 17 (continued)

(f) s = 0.67 H.

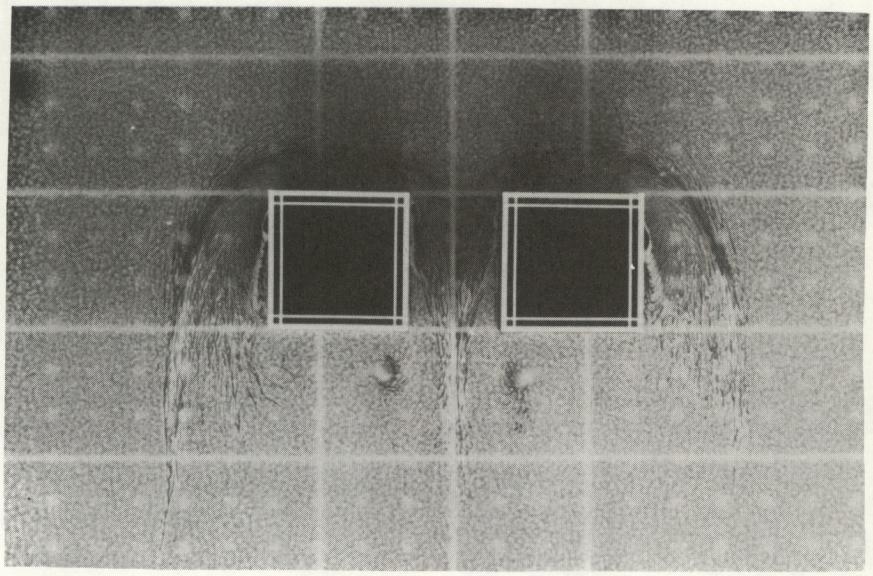

(g) s= 0.67 H, seen from behind.

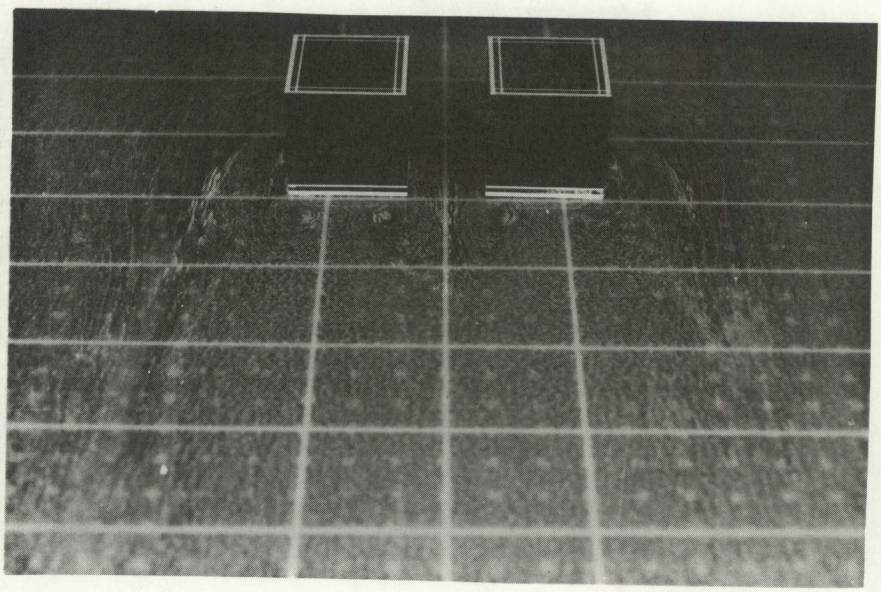

Figure 17 (continued)

(h) s = 0.67 H, closeup of flow patterns.

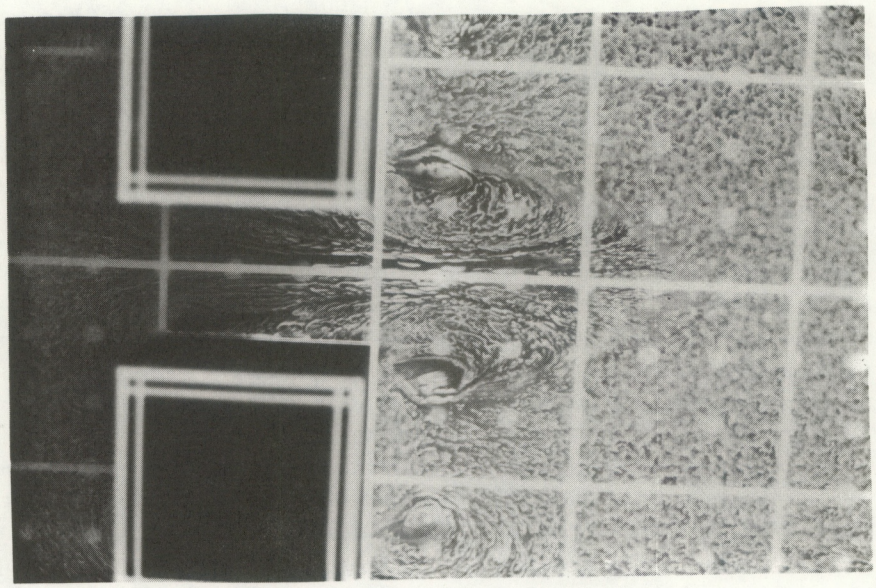

(i) s = 0.33 H.

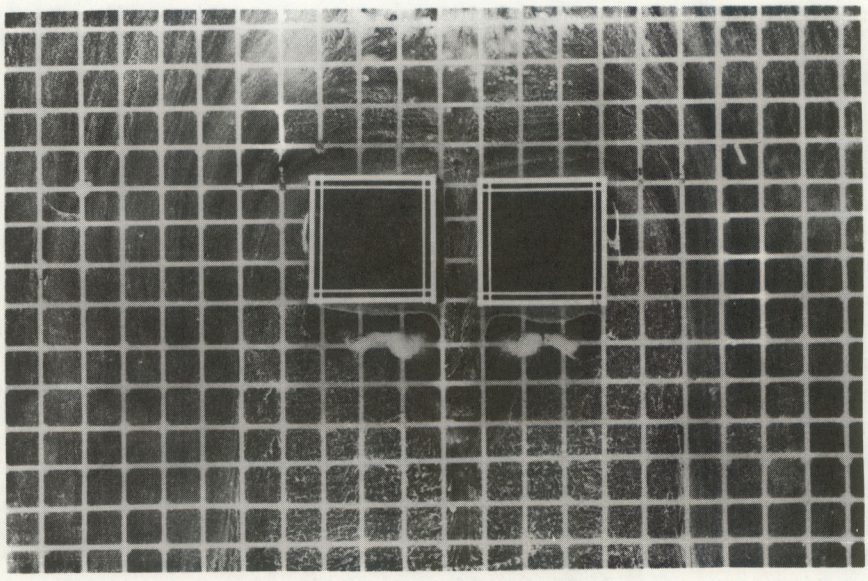

Figure 17 (continued)

A similar sequence of decreasing separation is shown in Figure 18, again for cubical buildings (W/H = 1 = L/H), but now in an alongwind array. In Figure 18a, the face-to-face separation is 3.33 H. Although each building exhibits its own characteristic surface flow pattern that appears to be independent of the other's presence, there is nevertheless a slight outward broadening of the horseshoe vortex system associated with the upwind building. This broadening is more noticeable as the separation is decreased. For s = 3.0 H (Figure 18b), the picture is not much changed, but at s = 2.33 H (Figure 18c), flow interactions become more obvious. The separation zone ahead of the downwind building is more diffuse, and there is some evidence of interaction with the wake of the leading building, especially along the centerline. The lee-edge vortices are somewhat weakened. At s = 1.67 H (Figure 18d), the wake of the upwind structure has weakened or perhaps even eliminated the horse-shoe vortex ahead of the lee building. The lee-edge vortices behind the upwind building are displaced outward from the centerline, and those behind the downstream building seem to be quite weak. When s = 1.33 H (Figure 18e), the upwind separation zone and horseshoe vortex system of the downwind building have vanished, and the lee-edge vortices of the upwind building have moved further out from the wake centerline. At a separation of 1.0 H, (Figure 18f), the organization of these lee-edge vortices appears to be somewhat disrupted. For s = 0.33 H (Figure 18g), the flow between the two buildings is nearly stagnant, and the flow pattern is beginning to strongly resemble that around a single structure of L/H = 2.

2.3.2.3 Two rectangular buildings

To examine the influence of the building geometry on the flow patterns discussed above, tests were conducted for wider buildings (W/H = 2, L/H = 1) placed in a crosswind array. For a face-to-face separation of 2.67 H (Figure 19a), there is little obvious interaction, although the inboard sides of the horseshoe vortex pairs show slightly sharper curvature as they pass through the gap between the buildings, and the outboard lee-edge vortices are somewhat elongated relative to their inboard counterparts. These effects were not as noticeable for the buildings with W/H = 1 (Figure 17a). In Figure 19b (s = 2.33 H), the inboard horseshoe vortices create a "tail" in the center of the wake, as described above, and the outboard lee-edge vortices are larger than the inboard ones. However, the inboard vortices may be somewhat more intense, since the scouring of pigment is more obvious and the central core is sharply defined. For s = 2.0 H (Figure 19c), the vortex-induced "tail" in the center of the wake dissipates rapidly; it does not appear to persist as long as the outboard portions of the horseshoe vortices. The outboard lee-edge vortices are now considerably broader in extent than the inboard pair. These trends continue for s = 1.67 H (Figure 19d) and s = 1.33 H (Figure 19e). The higher speeds in the between-building jet are shown by the efficient removal of pigment right along the flow centerline, and the inboard lee-edge vortices are more sharply defined (but not as broad) as the outboard pair. By the time s has decreased to 1.0 H (Figure 19f), the frontal separation zones ahead of the two buildings have begun to merge, and the strongly scoured region in the between-building gap has decreased in length. When s = 0.67 H (Figure 19g), the flow through the gap is apparently weaker, judging by the extent of pigment scouring, although the

(a) s = 3.33 H.

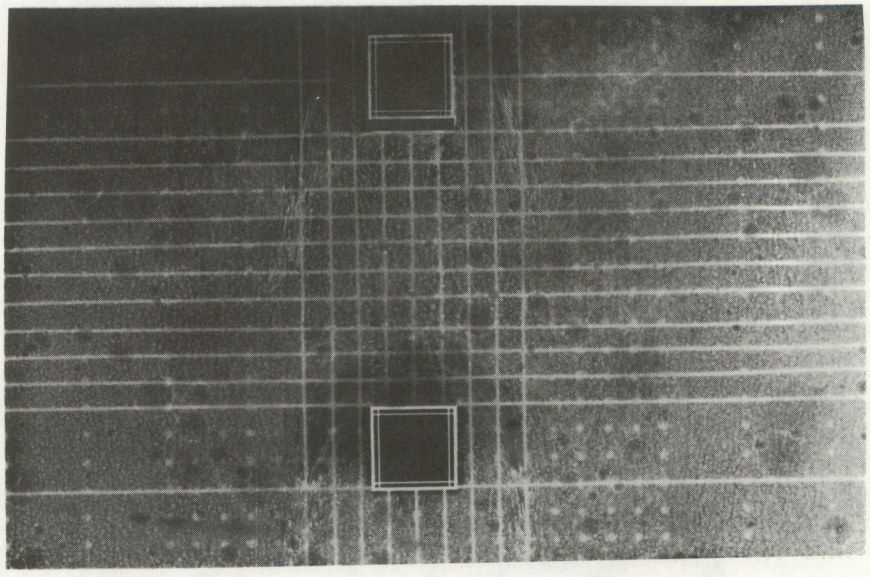

Figure 18. Surface flow patterns associated with two buildings (W/H = 1 = L/H) normal to the incident wind, with face-to-face along-wind separation s. (a) s = 3.33 H. (b) s = 3.0 H. (c) s = 2.33 H. (d) s = 1.67 H. (e) s = 1.33 H. (f) s = 1.0 H. (g) s = 0.33 H.

(b) s = 3.0 H

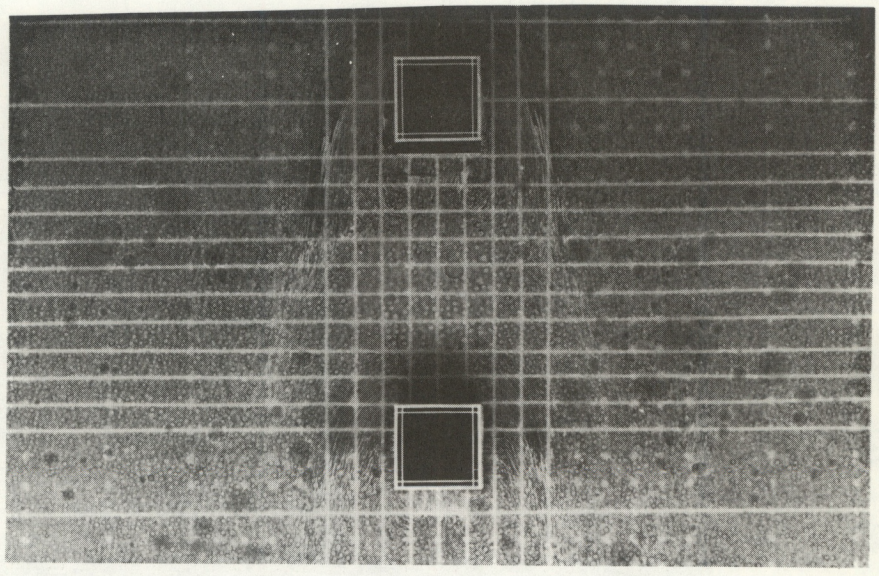

(c) s = 2.33 H.

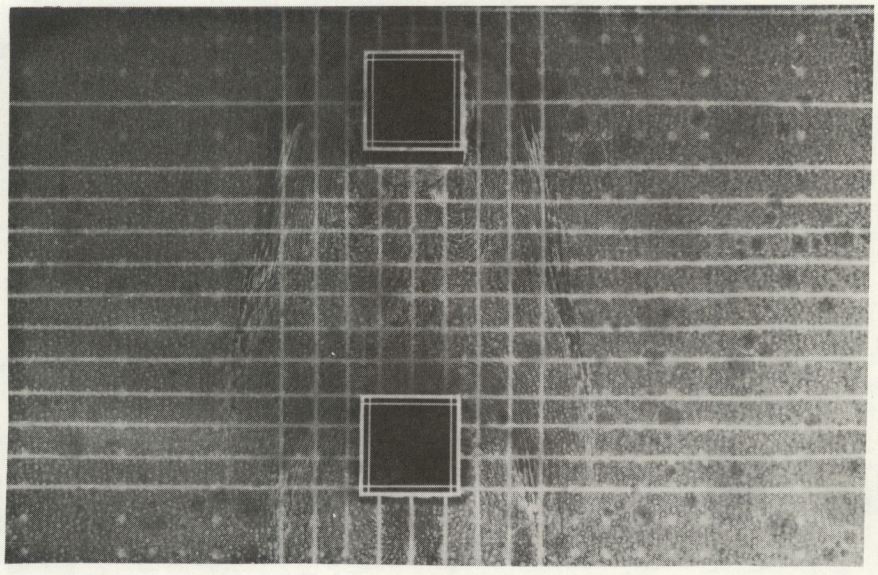

Figure 18 (continued)

(d) s = 1.67 H.

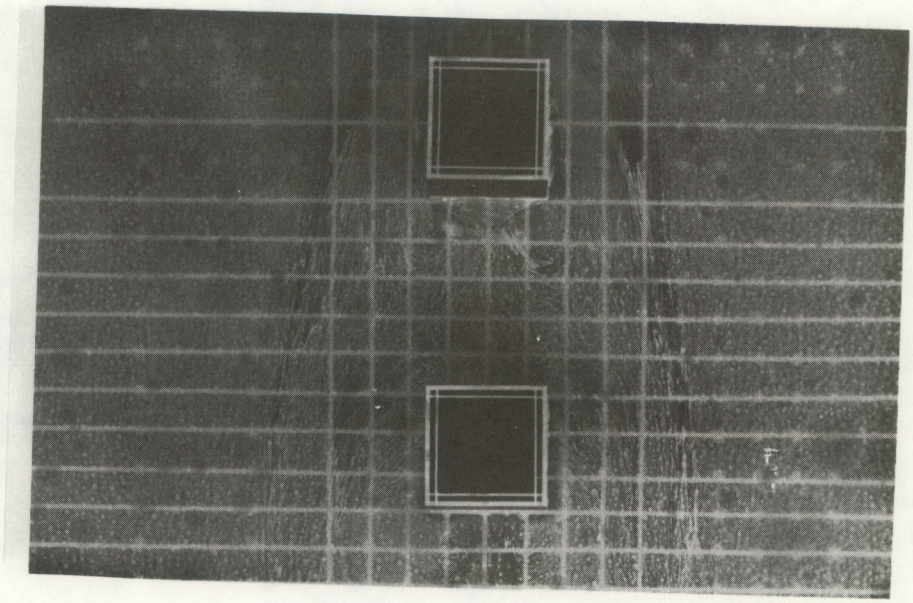

(e) s = 1.33 H.

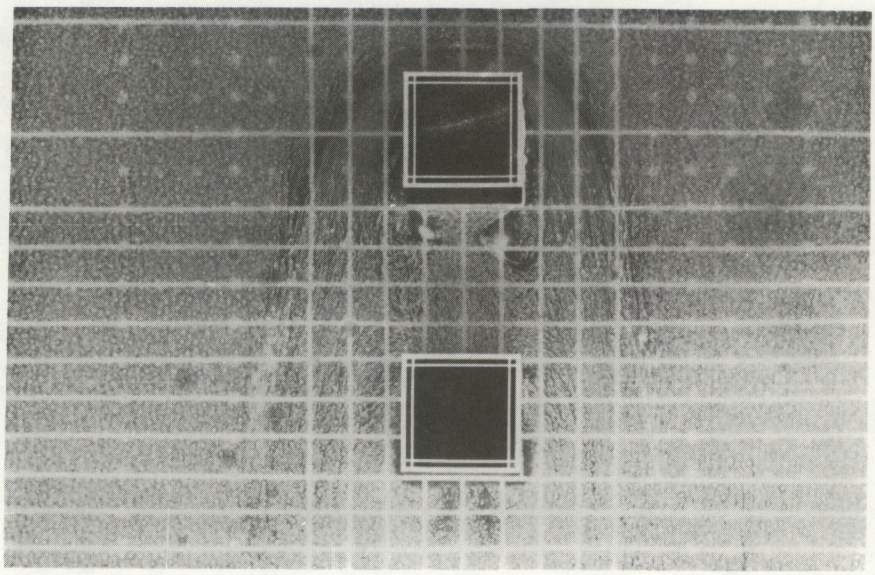

Figure 18 (continued)

(f) s = 1.0 H

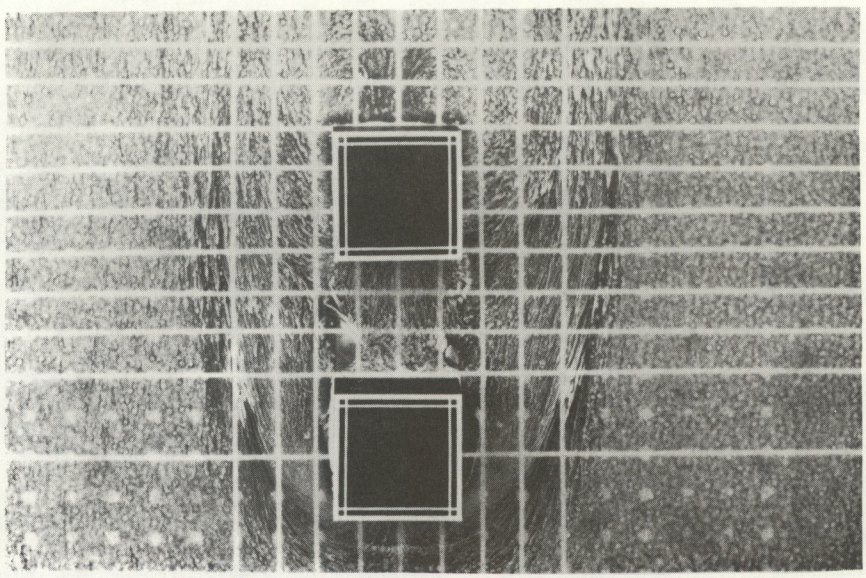

(g) s = 0.33 H

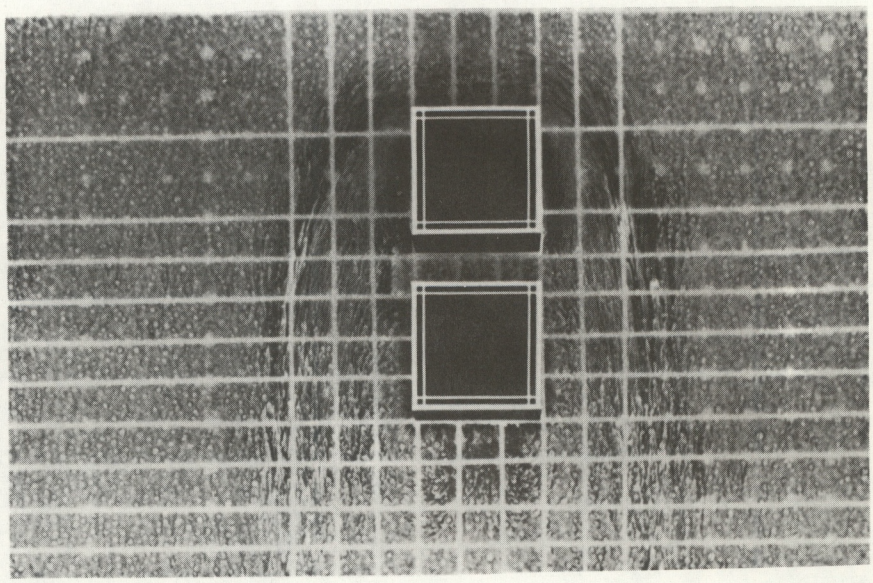

Figure 18 (continued)

(a) s = 2.67 H.

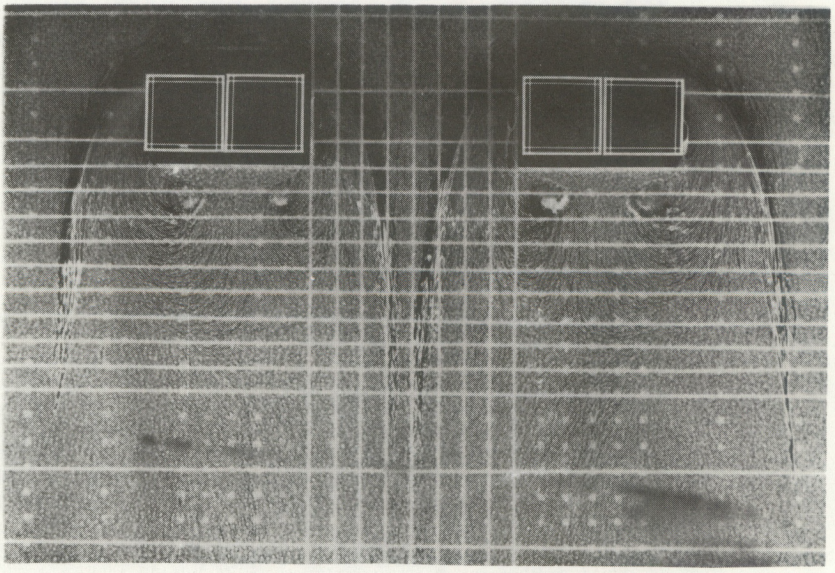

Figure 19. Surface flow patterns associated with two buildings (W/H = 2, L/H = 1) normal to the incident wind, with cross-wind separation s. (a) s = 2.67 H. (b) s = 2.33 H. (c) s = 2.0 H. (d) s = 1.67 H. (e) s = 1.33 H. (f) s = 1.0 H. (g) s = 0.67 H. (h) s = 0.33 H.

(b) s = 2.33 H.

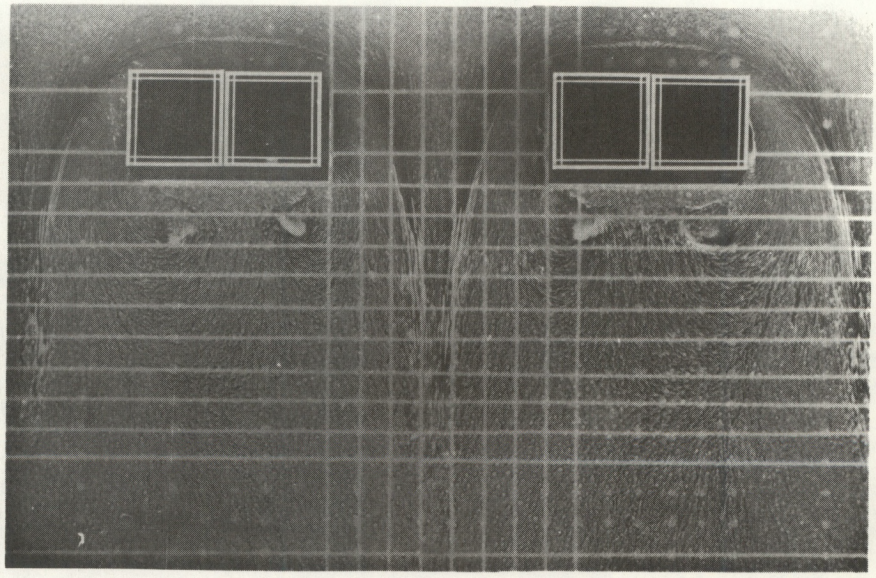

(c) s = 2.0 H.

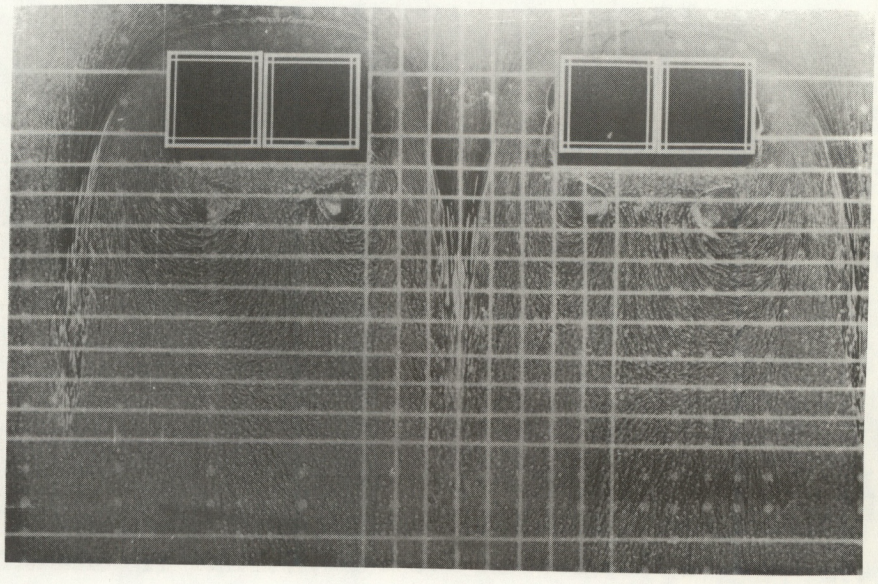

Figure 19 (continued)

(d) s = 1.67 H.

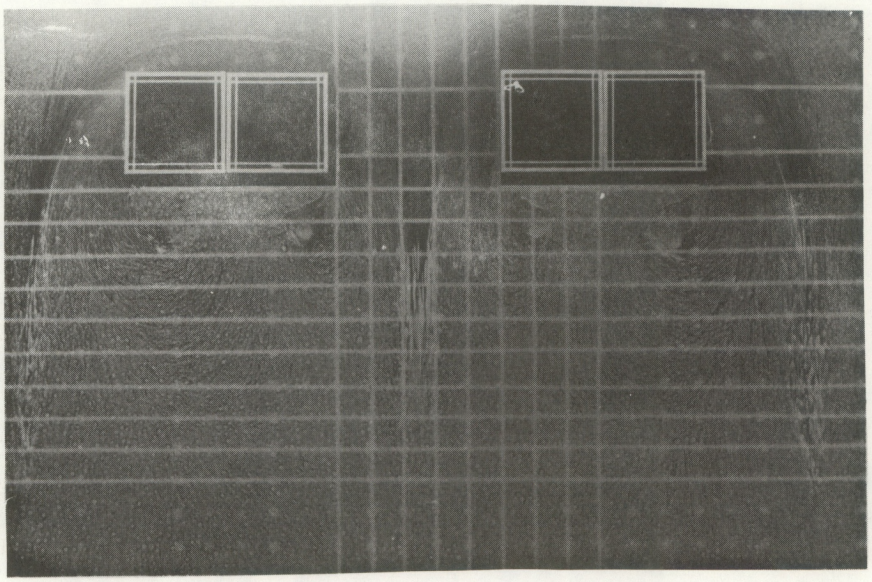

(e) s = 1.33 H.

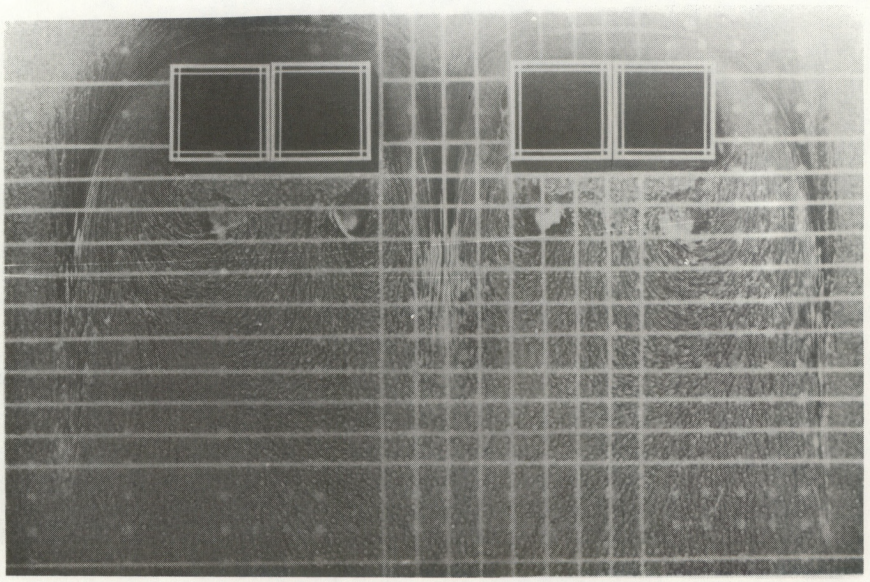

Figure 19 (continued)

(f) s = 1.0 H.

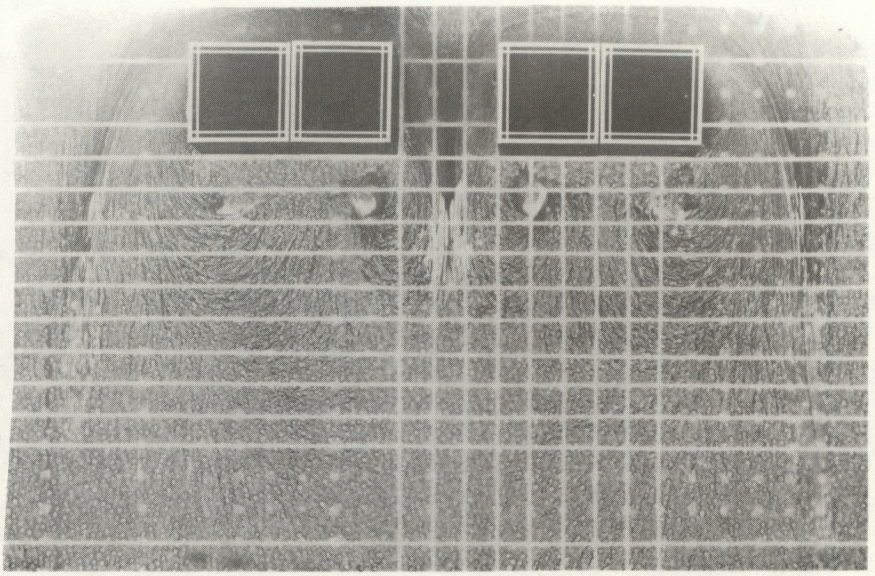

(g) s = 0.67 H.

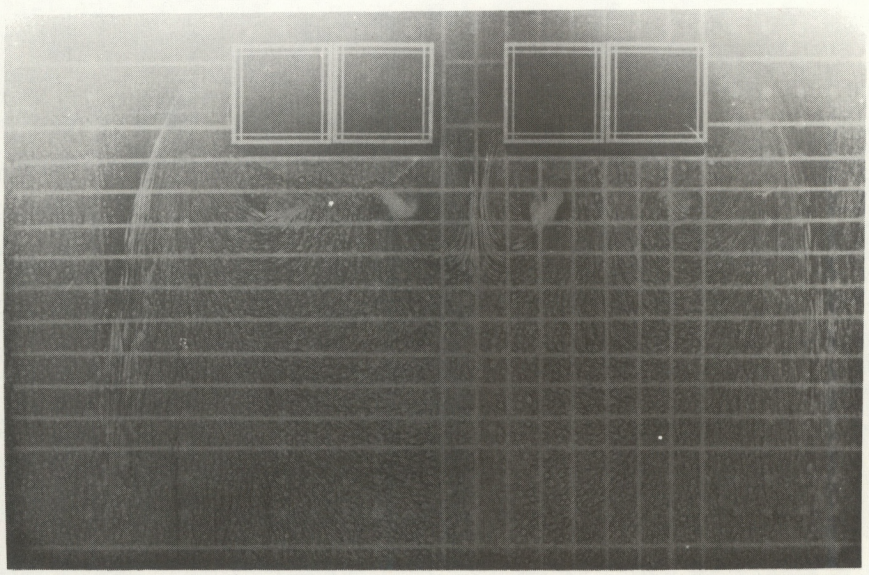

Figure 19 (continued)

(h) s = 0.33 H.

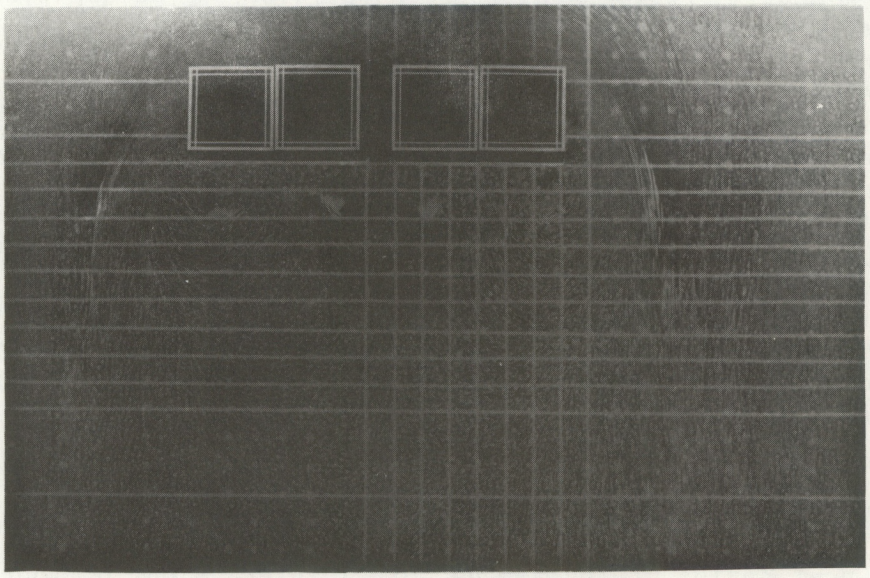

Figure 19 (continued)

inboard lee-edge vortex pair remains strong and sharply defined. For s = 0.33 H (Figure 19h), the far wakes have begun to merge into a pattern resembling that of a single, wide (W/H = 4) building. The inboard pair of lee-edge vortices are still well-defined, but have decreased in size.

2.3.2.4 Two-building summary

For buildings separated in the cross-wind direction, the building geometry was found to affect the results. Significant interactions* were observed for s/H ≅ 2.33 for a building cross-wind width to height ratio W/H = 1, and for s/H ≅ 2.67 for W/H = 2. These values agree quite well with the estimates of transition s_*/H shown in Figure 13b.

For the alongwind array with W/H = 1, small changes in the horseshoe vortex system generated by the upwind building were observed for separation distances as large as 3.3 H, although no change in the flow pattern about the downwind building was visible at this distance. It is not until s ≅ 2.33 H that the horseshoe vortex ahead of the downwind structure begins to show signs of interaction with the upwind building's wake. Again, this result agrees well with the transition estimates of Figure 13b. When s is decreased to 1.67 H, the horseshoe vortex system has been strongly modified; this is not too surprising, because a wake cavity length of about 1.5 H would be expected for the upwind building alone (e.g, Hosker, 1979; Fackrell and Pearce, 1981).

2.3.2.5 Four-building rectangular array

In the next series of tests, the mutual interactions of four cubical (W/H = 1 = L/H) buildings were examined. A simple rectangular grid arrangement was chosen. For simplicity, the edge-to-edge spacing s was kept the same in both the alongwind and crosswind directions. Figure 20a shows the patterns observed for s/H = 3.33. A cursory inspection would reveal no evidence of flow interaction; the individual patterns are very similar to those observed around isolated obstacles. However, close examination reveals some broadening of the outermost horseshoe vortex system patterns; the vortices from the upwind buildings are apparently deflected slightly away from the array centerline by the flow about the downwind buildings. Furthermore, the inboard horseshoe vortex pair generated by the upwind buildings produces an area of higher speed (increased pigment scouring) along the centerline in the area between the downwind buildings. These perturbations persist with little change as the separation distance is reduced to s/H = 3.0 (Figure 20b), 2.67 (Figure 20c), and 2.33 (Figure 20d). Somewhere between s = 2.33 H and s = 2.0 H (Figure 20e), stronger interactions become evident. This transition is once again in reasonable agreement with the values suggested in Figure 13b, and with the earlier observations for only two buildings. At s = 2.0 H, the wakes of the upwind buildings are beginning to perturb the horseshoe vortices and frontal separation zones of the downwind structures. A

*Noticeable changes in the flow patterns, speedup in the between-building gap, wake region perturbations, or other modifications.

(a) s = 3.33H.

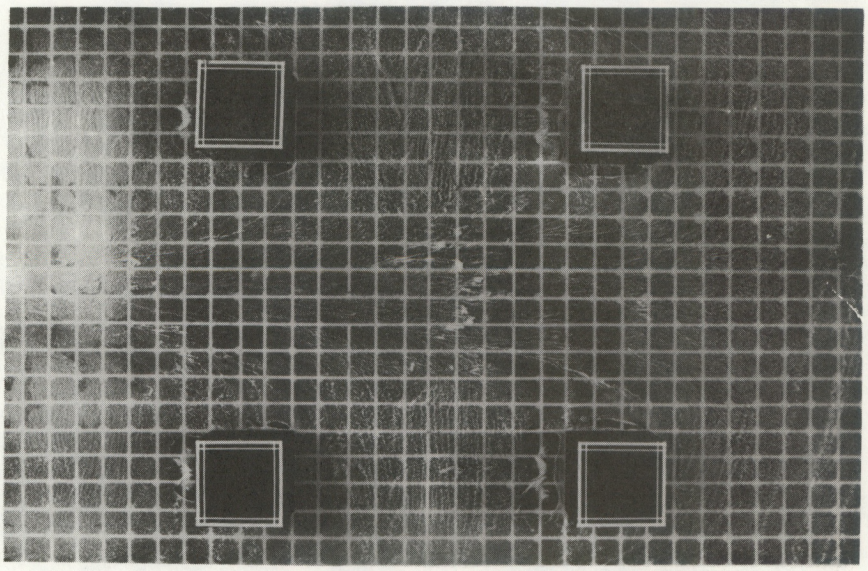

Figure 20. Surface flow patterns associated with four buildings (W/H = 1, L/H = 1) in a rectangular grid, with an inter-building spacing s. (a) s = 3.33 H. (b) s = 3.0 H. (c) s = 2.67 H. (d) s = 2.33 H. (e) s = 2.0 H. (f) s = 1.67 H. (g) s = 1.33 H. (h) s = 1.0 H. (i) s = 0.67 H.

(b) s = 3.0 H.

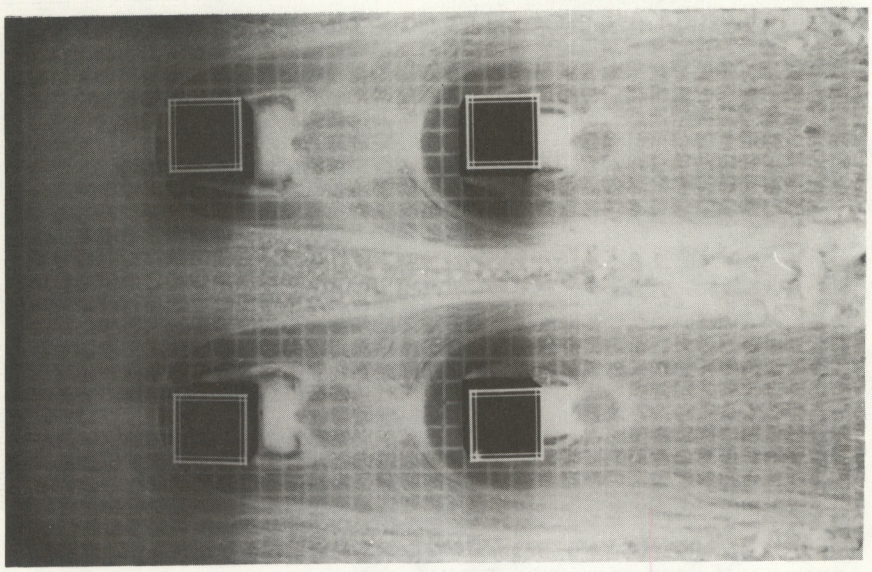

(c) s = 2.67.

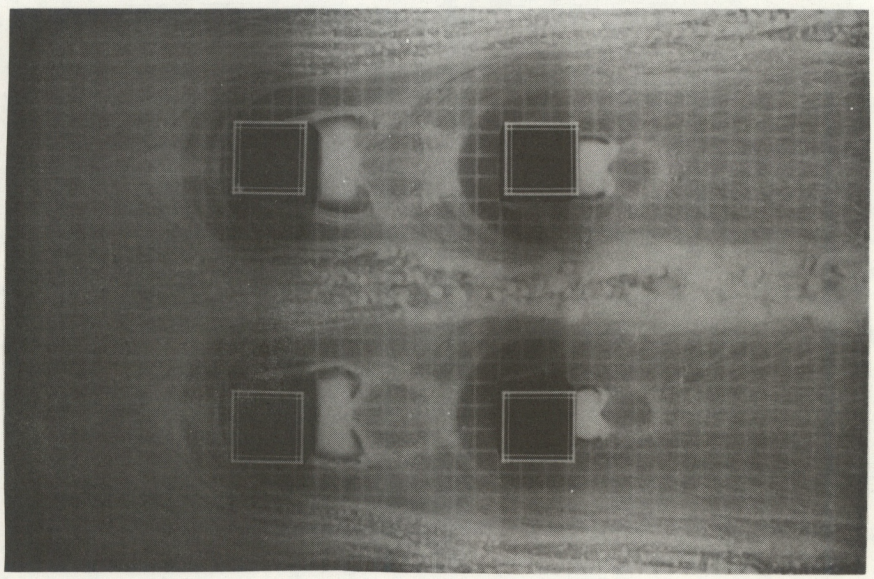

Figure 20 (continued)

(d) s = 2.33 H.

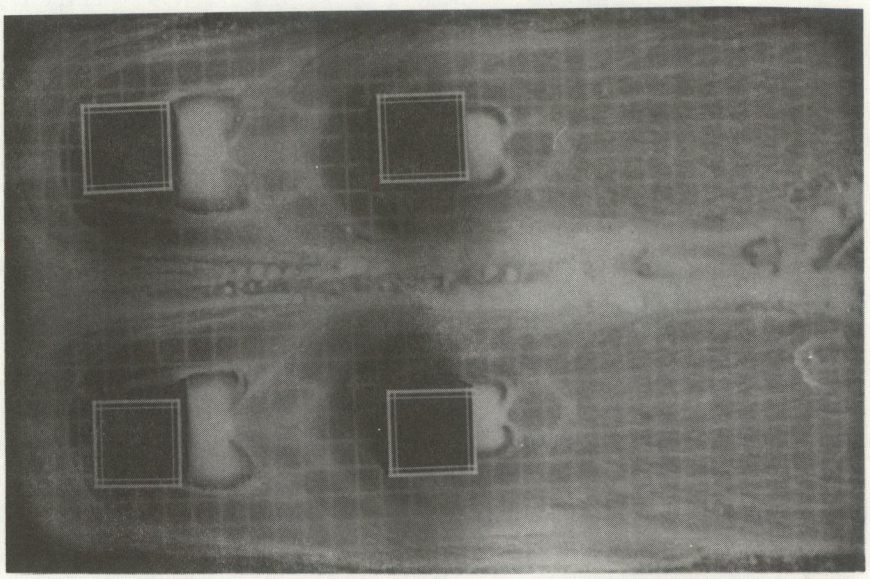

(e) s = 2.04 H.

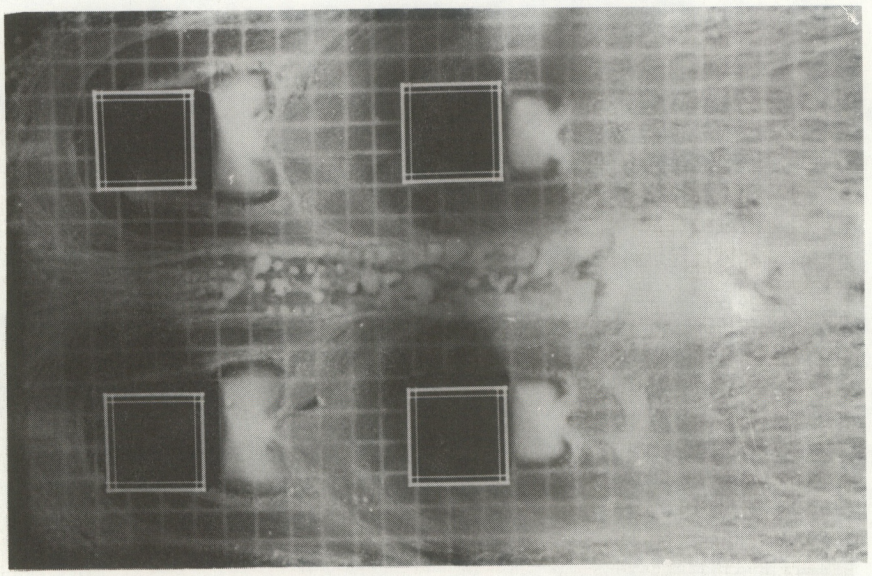

Figure 20 (continued)

(f) s = 1.67 H.

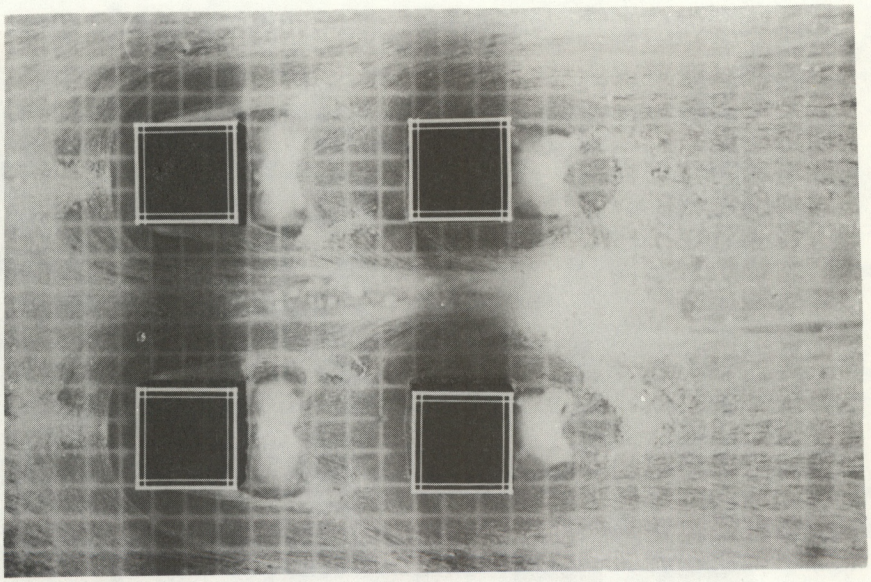

(g) s = 1.33 H.

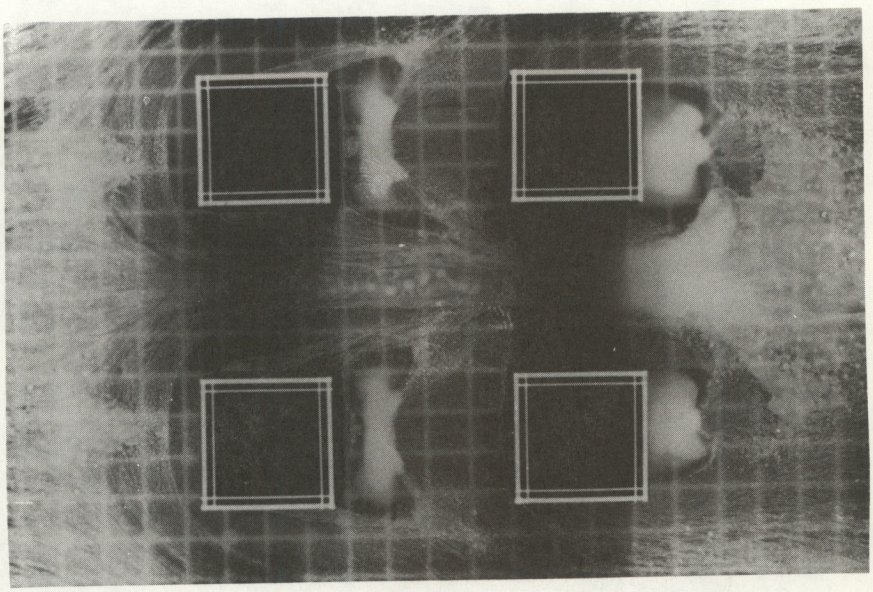

Figure 20 (continued)

(h) s = 1.0 H.

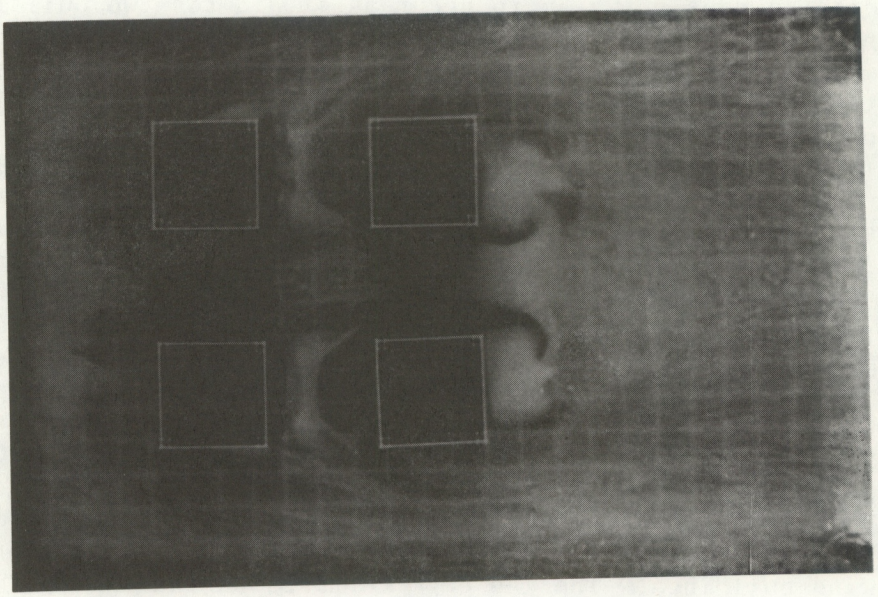

(i) s = 0.67 H.

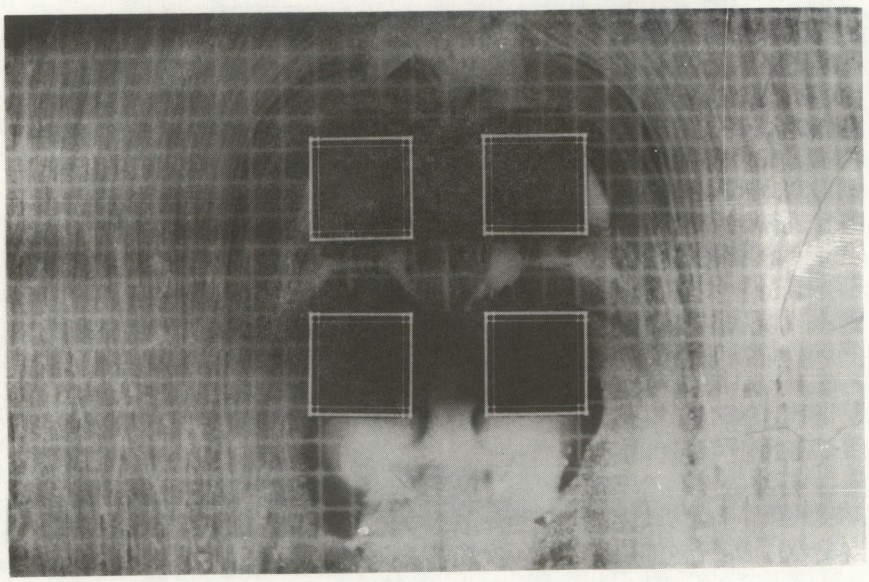

Figure 20 (continued)

further reduction in s to 1.67 H (Figure 20f) produces noticeable pigment scouring along the centerline between the rear buildings, but only over a short distance; in particular, an extended "tail" due to the interaction of horseshoe vortices does not seem to occur as it did for two buildings in a crosswind array. The outboard lee-edge vortices behind the rear buildings are displaced toward the wake centerline, compared to the upwind set, and the vortices do not seem to be as well defined. There is a hint of asymmetry in these vortices, with the outboard ones covering more area. At s/H = 1.33 (Figure 20g), the flow speeds within the building complex appear to be smaller: pigment scouring along the centerline near the downwind buildings is greatly reduced, the frontal separation zones of these buildings have virtually merged with the wakes of the upwind structures, and the lee-edge vortices are poorly defined, even for the upwind obstacles. Figure 20h (s = 1.0 H) shows strong flow in the gap between the windward buildings that persists down into the gap between the lee obstacles. The lee-edge vortices closest to the centerline appear to be stronger and more sharply defined than their outboard counterparts, particularly for the downwind buildings. At s = 0.67 H (Figure 20i), the outer flow pattern is beginning to resemble that of a single structure with W/H = 2 = L/H. The frontal separation zones have nearly merged, and large lee-edge vortices are beginning to appear behind the outboard rear corners of the downwind buildings. The lee-edge vortices behind the upwind buildings have disappeared. The flow in the crosswind gap of the array, in fact, seems to be rather stagnant, and no obvious pigment patterns can be seen. However, a strong jet persists down the centerline gap, judging by the scouring of pigment in the oil film.

2.3.2.6 Three-building triangular array

The previously discussed tests of rectangular arrays suggested that the flow patterns, at least for fairly large s, could be viewed as the merger of the patterns produced by "single-column" alongwind building arrays. Tests of other array configurations were then performed; the first used three cubical (W/H = 1 = L/H) buildings in a "triangle" array. Figure 21a shows an example; the alongwind face-to-face spacing s_x = 2.0 H and the crosswind spacing s_y = 5.0 H in this photo. The main flow interaction at this spacing appears to be the deflection toward the centerline of the horseshoe vortex system generated by the upwind building as the system nears the downwind pair of structures. With these spacings approximately halved (s_x = 1.0 H, s_y = 2.67 H; Figure 21b), the interactions are much more obvious. The entire wake of the leading building is strongly deflected into the centerline region by the presence of the two downwind obstacles. The combination of the upwind building's wake system and the horseshoe vortex system of the trailing buildings produces a zone of fairly high speed on either side of the centerline between the downwind building pair. However, the patterns about the downwind pair seem to be relatively unchanged from the isolated obstacle case, with the exception of the separation/ reattachment zone on the inboard side walls; this zone is much more elongated and apparently stronger than its counterpart on the outboard side walls. A further reduction in spacing (s_x = 0.67 H, s_y = 1.33 H; Figure 21c) apparently produces high wind speeds directed through the gaps between the upwind and downwind buildings. There is an accumulation of pigment on either side of the leading building, suggesting that material

(a) s_x = 2.0 H = s_y = 5.0 H.

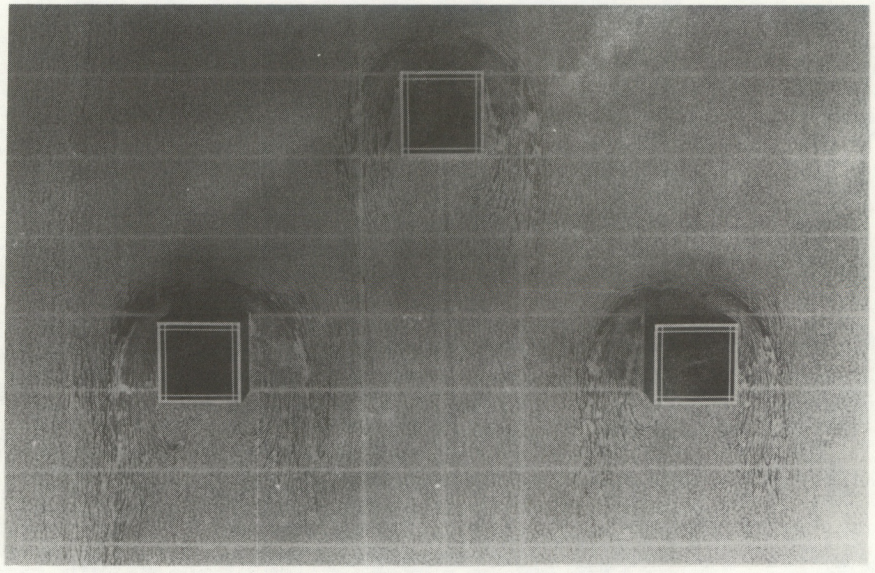

Figure 21. Surface flow patterns for three buildings (W/H = 1 = L/H) in a triangular array, with inter-building along-wind spacing 33 H = s_y. s_x and cross-wind spacing s_y. (a) s_x = 2.0 H, s_y = 5.0 H. (b) s_x = 1.0 H, s_y = 2.67 H. (c) s_x = 0.67 H, s_y = 1.33 H.

(b) s_x = 1.0H, s_y = s.67 H.

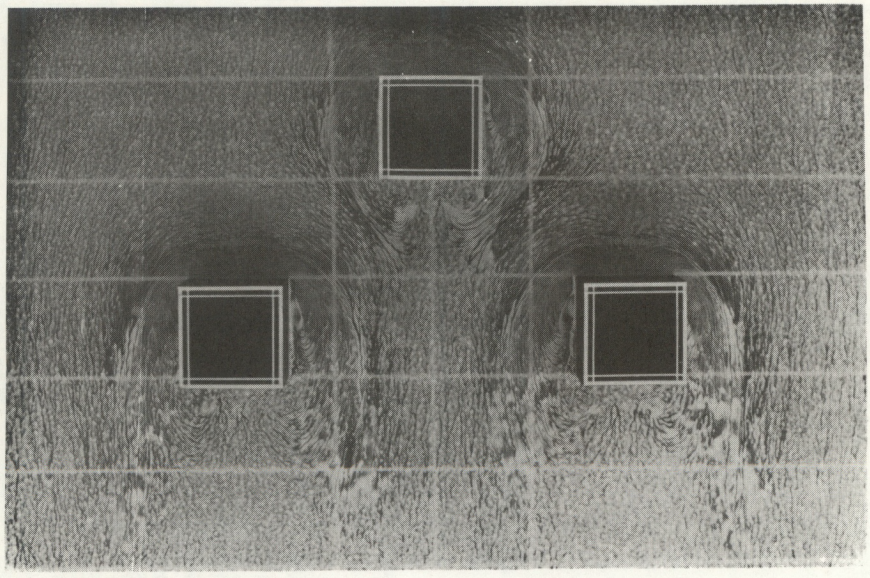

(c) s_x = 0.67 H, s_y = 1.33 H.

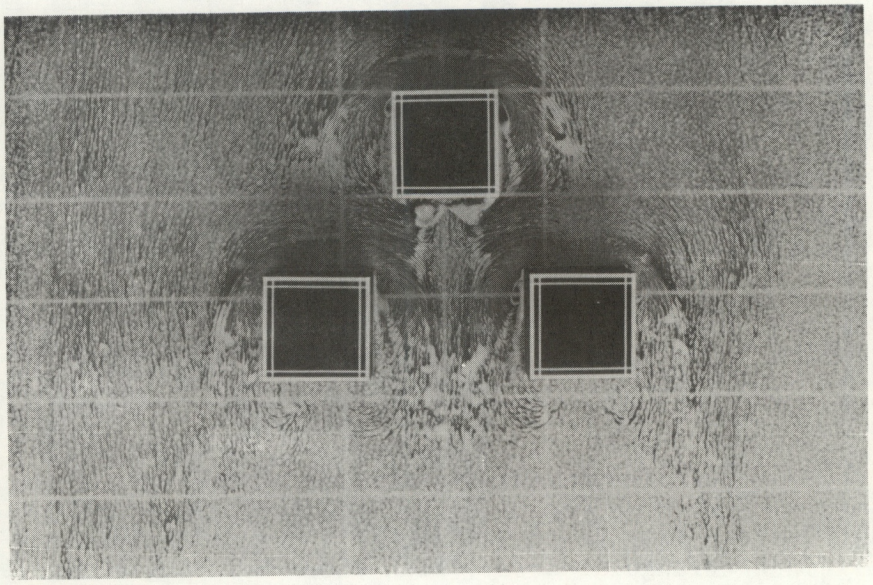

Figure 21 (continued)

transported by the horseshoe vortex system of that building winds up in a near-stagnation region ahead of the systems associated with the downwind buildings. The lee-edge vortices behind the upwind building are small but well-defined, and there is a sort of stagnation zone along the wake centerline just behind the vortices. The region on both sides of the centerline between the downwind buildings is fairly well scoured, suggesting locally high speeds. The inboard pair of lee-edge vortices for these buildings are a bit larger and better defined than the outboard pair In a test not shown here, it was found that a spacing s = 0.33 H was small enough that the leading building's horse-shoe vortex pattern spread and merged with those of the downwind obstacles to encircle the building cluster; flow through the inter-building gaps was still evident, however.

2.3.2.7 Five-building cruciform array

Two cubical (W/H = 1 = L/H) buildings were added to the previously discussed triangle array to produce a cruciform building cluster. Figure 22a (s_x = 1.0 H = s_y) illustrates flow patterns showing rather strong interaction and sheltering effects. The external patterns around the upwind and left and right buildings are quite similar to those around the three buildings of Figure 21b with similar overall spacing -- the horseshoe vortex system of the upwind building is deflected toward the centerline and somewhat dissipated as the system "legs" approach the left and right buildings. The systems around the left and right buildings still superficially resemble those around isolated obstacles. However, the presence of additional buildings along the centerline deflects the flow patterns away from the centerline, compressing the horseshoe vortex system slightly against the inboard sides of the left and right buildings. The inboard side wall separation/reattachment zones of these buildings are very clearly defined; in particular, there is a strongly scoured zone close to the inboard windward corners. The central building seems to have a rather weak influence on the flow approaching it, and the downwind building is even more sheltered.

A modest reduction in spacing (s_x = 0.67 H = s_y; Figure 22b) produces a further disruption of the horseshoe vortex system generated by the leading building. It is interesting that there is relatively little pigment scouring in the diagonal gaps between the leading building and the left and right ones. However, the flow patterns around the left and right obstacles are strongly asymmetric, and there seems to be quite strong flow through the centers of the gaps between those buildings and the central obstacle. The central building seems to interact very weakly with the flow, aside from its effect on the horseshoe vortices of the left and right buildings, and the downwind building is quite well sheltered.

An additional reduction in spacing (s_x = 0.33 H = s_y; Figure 22c) produces an outward spreading of the horseshoe vortex system of the upwind building. Evidently the gaps between the buildings are no longer large enough to conduct the mass flow necessary, and the flow must be deflected outward to (at least partially) pass around the complex as a whole. The deflected vortex system shows signs of merging with the systems still in evidence around the left and right buildings. Fairly well defined lee-edge vortices can be seen behind the upwind building. The inboard side wall

(a) $s_x = 1.0\ H = s_y$.

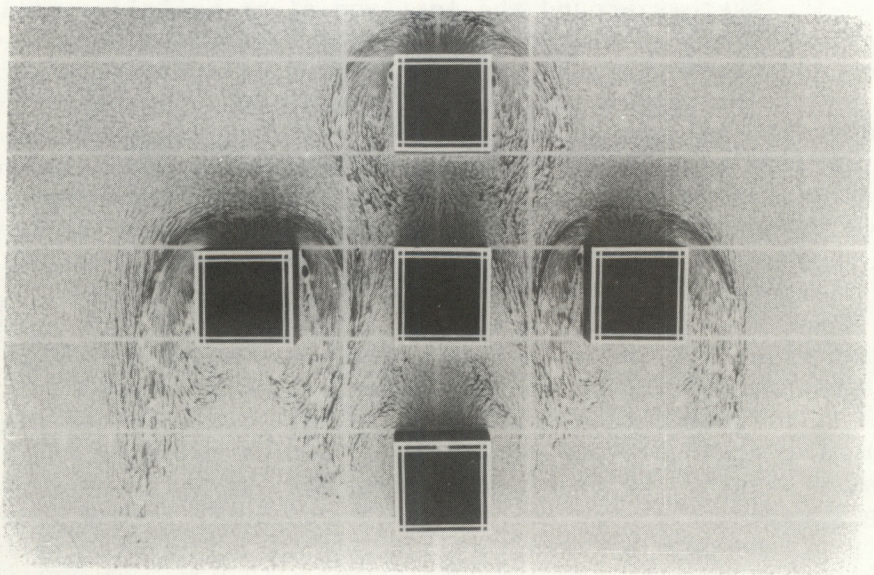

Figure 22. Surface flow patterns for five buildings (W/H = 1, L/H = 1) in a cruciform array, with inter-building along-wind spacing s_x and cross-wind spacing s_y. (a) $s_x = 1.0\ H = s_y$. (b) $s_x = 0.67\ H = s_y$. (c) $s_x = 0.33\ H = s_y$.

(b) $s_x = 0.67\ H = s_y$.

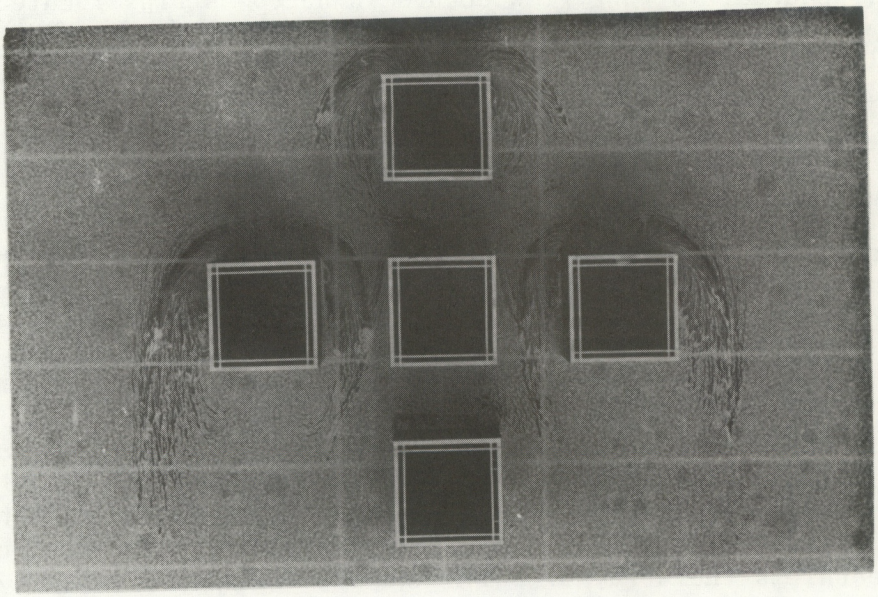

(c) $s_x = 0.33\ H = s_y$.

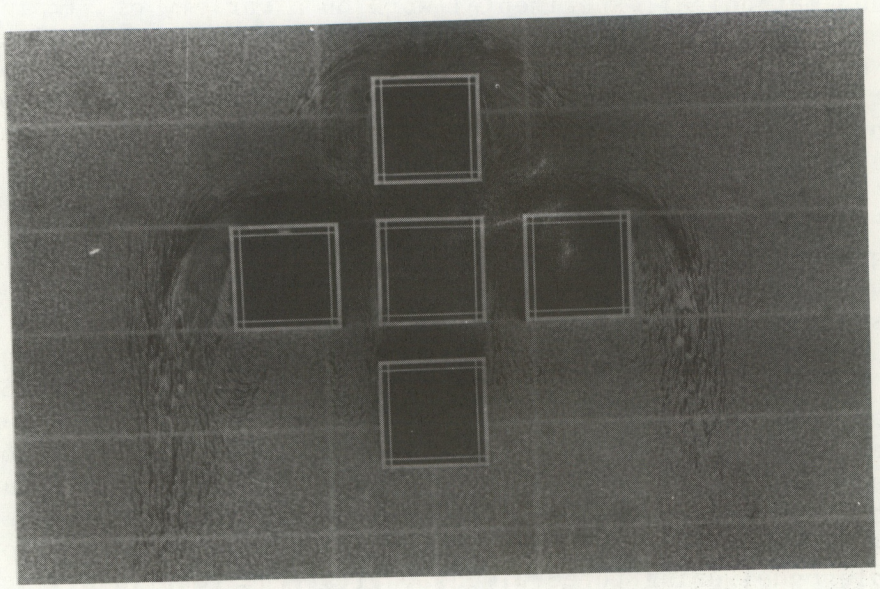

Figure 22 (continued)

separation/recirculation zones on the left and right buildings are smaller and less well defined, but the region near the inboard windward corner is still well-scoured. Strong flow occurs in narrow strips located about 1/3 of the gap width from either side of the central building. The downwind building is nearly completely sheltered.

3. CONCENTRATION CALCULATIONS

The preceding discussion of the complicated flow patterns that can be expected near a building complex suggests that attempts to estimate effluent concentration patterns should be separated into at least two stages, depending on the distance from the buildings.

3.1 Concentrations Within and Very Close to a Building Complex

Within and very close to a building complex, the flow patterns and the resulting concentration field are site-specific. Generalizations are impossible unless the array of buildings is unusually simple. Jetting of flow between the buildings, vortex production and interactions, shear layer impingement, and other phenomena seem to preclude simple models for concentration. At these short distances -- i.e., within about three to five average building heights of the downwind edge of the complex -- experiments are nearly always necessary. In fact, until a better understanding of the flow patterns generated around even very simple building arrays is attained, it is pointless to think of realistic descriptions of effluent dispersion on these scales. It is safe to say that our predictive capability just for effluent transport is virtually nil except in the simplest of cases; predictions of diffusion and the resultant pollutant concentrations are presently almost impossible. A great deal of careful and methodical experimental work on a variety of simple building arrangements is needed to improve the situation. Flow visualizations and velocity measurements are probably the most-needed data, but concentration distributions should be determined concurrently whenever possible. On the other hand, concentration distributions without flow data are not especially helpful.

Some mathematical modeling of the near-field flow patterns and resulting concentration is increasingly feasible as more experimental data become available to test the modeled results, and as larger, faster digital computers permit calculations at reasonable cost. A good deal of effort has already been expended; some relevant references can be found in Hosker (1984). Articles by Hirt and Cook (1972), Hirt, Ramshaw, and Stein (1978), and Puttock and Hunt (1979) are particularly interesting. Kotake and Sano (1981) recently reported on a kind of nested model to study flow over and within an urban area; the flow within the urban area on the scale of a few city blocks was driven by the flow over the urban region as a whole. Solutions were obtained for the large-scale domain, and then for the local-scale model using three-dimensional stream functions. Kotake and Sano's solutions show some of the expected behavior, but important features such as vortices and wake regions and their associated concentration

patterns were not predicted because their model could not deal with flow separation and related phenomena. It may be possible to combine numerical techniques with empirical parameterizations and flow "modules" (e.g., to insert wakes or lee-edge vortices where they are known to occur) to generate more realistic flow fields and concentration patterns, but this must still be demonstrated. In the meantime, recourse to field and/or laboratory studies remains essential for these near-field problems, with only a few exceptions.

3.1.1 Concentrations Near a Dominant Building

As noted earlier, when one building in a cluster is much larger than its neighbors, the flow and concentration patterns will be rather similar to those expected if the large building had no neighbors, although there will naturally be differences near ground level. In such cases it may be possible to use techniques originally developed for estimating concentrations on or near isolated structures. This has been done as a practical matter fairly routinely; for example, the dilution estimation procedures suggested by Halitsky (1963 a,b), ASHRAE (1974), and Wilson (1976 a,b;1977a) have often been applied to building complexes to estimate pollutant concentrations on building surfaces due to effluent vents on those same buildings. The equations used have been summarized by Hosker (1982), who included numerous graphs to facilitate use of the various forms of the expressions.

One of the simplest equations was suggested by Wilson (1976 a,b, and 1977a; see also Wilson and Britter, 1982) as an upper bound on the concentration of an effluent traveling from a flush-mounted roof vent to some receptor point on the same building:

$$K_{max} \cong 9\ A_p/s^2 \qquad (13)$$

where K_{max} is the nondimensional concentration $\chi_{max}UA_p/Q$ (Halitsky, 1961), A_p is the projected frontal area of the building, and s is the "stretched string" distance from the effluent vent to the receptor. Li, Meroney, and Peterka (1982), Meroney (1982), and Wilson and Britter (1982) have tested this relation against wind tunnel and field data, and found it to be an excellent upper bound for all cases where (a) the flow was normal to the building, and (b) the source was not on the upwind building face.

When the wind approaches a structure at an angle, a vortex pair is generated at the upwind corner of the roof; these counter-rotating vortices divert elevated effluent downward in the lee of the building, and produce higher concentrations than Equation (13) would indicate. Li, Meroney, and Peterka (1982) suggested that Wilson's upper bound could be modified slightly to account for winds at an angle to the building:

$$K_{max}(\theta) \cong 9.1\ (1 + 4\theta/\pi)\ A_p/s^2 \qquad (14)$$

where $0 \leq \theta \leq \pi/4$. The effect is to increase K_{max} with θ by up to a factor of two at $\theta = \pi/4$. This modification has been tested only for cubical structures; additional verification is needed for other building shapes. In particular, the data of Dean and Robins discussed by Fackrell (1984) suggest that a dependence on the building geometric ratios W/H and L/H is likely. An expression involving W/H is suggested in Section 3.2.2.

Wilson and Britter (1982) found that Equation (13) could be extended to the case of exhaust vents on the windward building face by increasing the constant from 9 to 30; whether this holds true when the wind is at an angle to the building is unknown at this time.

Given the substantial uncertainties about the influence of neighboring small buildings on the flow and concentration patterns near a large structure, especially close to ground level, it seems wise not to attempt to estimate concentrations on the surface of such a dominant building any more accurately than is permitted by Equations (13) or (14). Even if only an upper bound is needed, it should be remembered that those relations have been tested for a quite limited range of building shapes. If the building of interest is geometrically unusual (i.e., not a box-like structure), caution is warranted. In any case, if the upper bound calculations made with Equations (13) or (14) are unsatisfactory, or if more detailed results are needed, an experimental study will be necessary.

3.1.2 Concentrations in a Street Canyon

The street canyon is probably the best known and most widely modeled example of flow in a built-up area. As noted in Section 2.2, when the face-to-face spacing of a regular array of flow obstacles is less than about 1.4 H, the general character of the flow changes from the so-called "wake interference" regime to the "skimming" regime; the main flow skims across the tops of the obstacles, and secondary flows such as stable vortices are established in the gaps between the obstacles. In a densely built-up area, building separations less than 1.4 H (where H is the average building height) are rather common; a secondary flow more or less decoupled from the wind aloft can be expected in many cases. Street canyons obviously are generally associated with urban areas, but can also occur in large industrial facilities where buildings are tightly packed together in a more or less regular array.

Figure 23a (Hoydysh, Griffiths, and Ogawa, 1974) illustrates the simplest case of a very long street canyon with the wind aloft normal to the canyon axis. A well-developed vortex occurs. The first observations of this phenomenon are generally attributed to Albrecht (1933). Other investigators (e.g., Georgii, Busch, and Weber, 1967; Johnson et al., 1973) reported similar findings, with a helical circulation occurring when the roof-level wind is within about ± 60° of the normal to the street canyon axis. Figure 23b indicates the much more complex flow likely near an intersection, where the street canyon flow and the wind along a cross-street interact, with vertically-oriented vortices being generated at the lee corners of the upwind buildings.

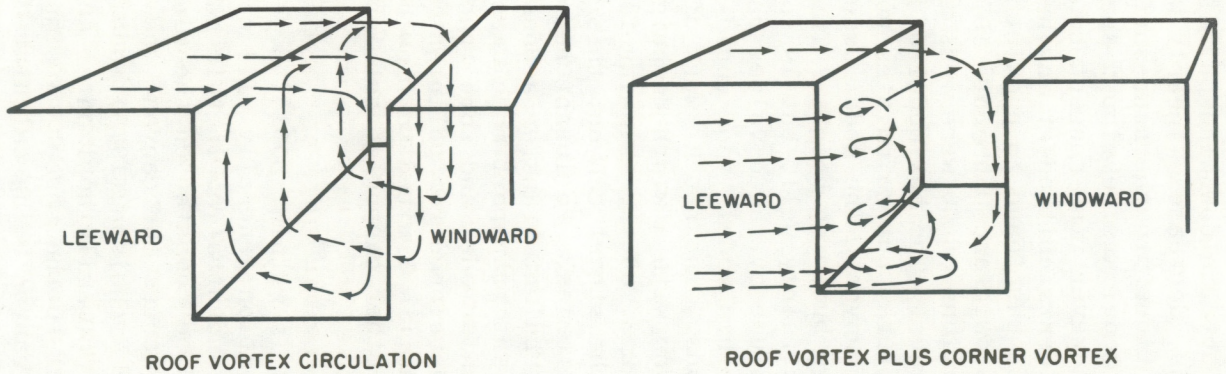

Figure 23. Street canyon flow (after Hoydysh, Griffiths, and Ogawa, 1974). (a) Very long street canyon, with wind aloft normal to the canyon axis. (b) Street canyon flow near an intersection.

Dispersion models for the simple case where the flows near intersections can be neglected and the emissions are near street level have been reported by Johnson et al., (1973; see also Dabberdt, Ludwig, and Johnson, 1973), by Nicholson (1975), and by DePaul and Sheih (1984). Figure 24 shows the physical picture postulated by Johnson et al. The concentration at a receptor is due to the sum of the background value at roof level plus the concentration due to the local emissions. Along the lee face of the upwind building, the increment in concentration directly depends on the source strength and is inversely proportional to the near-surface wind speed and to the distance between the source and the receptor. On the windward face of the downwind building, the concentration is proportional to the emissions, decreases linearly with height above the street, and is inversely proportional to the near-surface wind speed and to the width of the street. This model was developed specifically to deal with urban traffic pollution; however, the concept could easily be modified to deal with non-vehicular effluents emitted at any height into the street canyon. The model, when tested, was found to predict carbon monoxide observations moderately well (Ludwig and Dabberdt, 1972); it tended to underpredict when the concentrations of CO were less than 7 or 8 ppm, but somewhat overestimated high values. The box model of Nicholson (1975) is based on a similar physical picture, but calculates volume-averaged concentrations within a street canyon. The model assumes log-law velocity profiles apply above the average building height. This model also was found to predict concentrations fairly well, but is somewhat less useful since it inherently deals in volume-averaged values rather than those at a particular receptor location. This model, too, could easily be adjusted to deal with non-vehicular emissions. The recent work of DePaul and Sheih (1984) dealt with a street canyon with a width-to height ratio $s/H = 0.67$. From the discussion in Section 2.2, above, skimming flow would be expected, with a vortex confined within the street canyon; this was in fact observed by photographing balloon trajectories. Pollutant removal from the canyon must therefore be largely by turbulent transfer across the shear layer at the top of the canyon. A gradient transport model was developed to estimate this transfer. From this model and some tracer tests, a semi-empirical expression was developed for pollutant concentrations near street level. However, the model is limited to flow normal to the street canyon, and must be tested for other canyon geometries and receptor locations.

When the rooftop-level wind is within $\pm 30°$ of being parallel to the street canyon, a helical circulation generally will not occur. The Johnson et al. (1973) model estimates concentration in this case by simply averaging the values that would be computed on the windward and lee sides of the street if the wind were across the canyon; the justification for this treatment is unclear. The Nicholson (1975) model, on the other hand, assumes that mass flow must be primarily horizontal and along the street canyon when the wind is parallel to the street; a simple box model is used, with the average wind down the canyon being calculated from an assumed exponential wind speed profile below the average building height. In terms of its physics, at least, this model seems preferable to that of Johnson et al. (1973) for winds parallel to the street. The DePaul and Sheih (1984) model does not deal with the case of wind along the canyon.

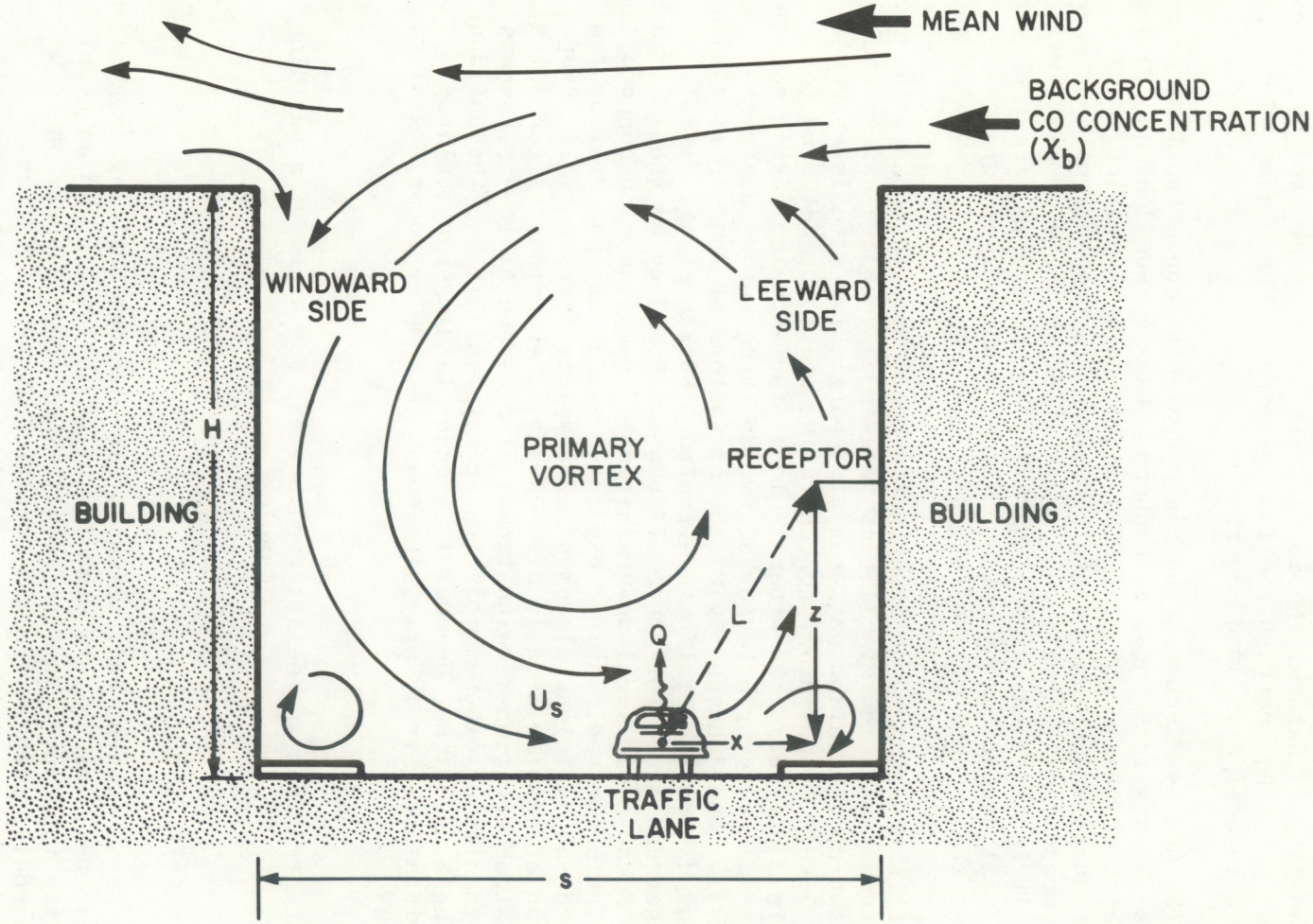

Figure 24. Street canyon circulation model of Johnson et al. (1973), for flow within about ±60° of the normal to the canyon axis.

It should be noted that none of the above models incorporates any thermal convective effects that might be significant during periods of light wind, when the mechanically driven circulations are weak. In industrial facilities, natural thermal effects may be augmented by process heat releases to further perturb the flow patterns. More advanced models will be needed to deal with such cases.

None of the models discussed above can deal with concentrations near cross streets. Tests in St. Louis (Dabberdt, Ludwig, and Johnson, 1973) indicated that the Johnson et al. (1973) model could be applied to within about 10 m of an intersection, but this estimate is probably site-dependent For example, broad cross streets running parallel to the wind aloft will probably result in a strong interaction with the transverse street canyon vortex; this will depend on the height, shape, and placement of the buildings near the corners of the intersection.

The street canyon can be an important problem both in urban areas and within industrial or nuclear facilities because an adequate understanding of the flow and concentration patterns at a particular site is essential if locally high levels of pollutant concentration are to be detected (or missed) by fixed samplers. In urban regions, for example, carbon monoxide concentrations can vary by a factor of two or three across a street (e.g., Dabberdt, Ludwig, and Johnson, 1973), or by factors of four or five when a sampler is moved from streetside to a rooftop (Bauman et al., 1982). Similar changes can occur for other effluents, depending on the location of the source. Because the legal determination of compliance or noncompliance with air pollution or radiological exposure regulations may rest on sampler data, informed and judicious placement of samplers is essential. Proper interpretation of sampler data is also essential when testing concentration models against observations. Wind tunnel studies and field experiments using smoke candles or other simple tracer materials (e.g., the balloons of DePaul and Sheih, 1984) may be useful in understanding particularly troublesome locations, or in selecting adequate sampler locations within built-up areas.

3.2 Concentrations in the Intermediate and Far Wakes of a Building Complex

3.2.1 Available Models

For distances between, say, three to five average building heights and ten to fifteen building heights downwind of an isolated building complex, one expects the turbulence and the resulting effluent dispersion to be dominated by eddies shed within the complex. Consequently the concentration patterns in this range should depend upon the physical dimensions of the structures generating those eddies. Beyond this range, the ambient atmospheric turbulence should be the dominant diffusive mechanism, and common atmospheric diffusion models should be applicable with only slight modification.

Many models have been suggested for estimating concentrations in these intermediate and far wake zones (see, for example, the summaries by Fackrell, 1984; Hosker, 1980, 1982, 1984; Huber, 1984; Meroney, 1982).

None of the models distinguishes between a single building and a building complex; the complicated patterns of jetting and flow deflection that occur in the immediate lee of a building cluster are presumed to have largely disappeared. In view of discussions in the literature based on both field and laboratory work, this presumption is probably true in most, but not all, cases. Instances which produce strong vortex wakes, and building clusters which contain one or two very large structures (e.g., natural draft cooling towers) among the other buildings are likely to exhibit highly individualized wake and dispersion characteristics out to greater distances than the approximate division above would recognize.

Nearly all of the models are based on some modification of the Gaussian plume model, "corrected" for the presence of the buildings. Two exceptions are Halitsky's (1977) work on the EBR-II building complex, and Kothari, Peterka, and Meroney's (1981) analytical perturbation solution based on the wake theory of Hunt and Smith (1969). These are discussed separately below.

The Gaussian-related models have been described in many places, and there is little point in repeating this material at length. The reader may consult the reviews cited just above for the details; the discussion by Fackrell (1984) is especially lucid and brief. The concepts underlying the model formulations can be broken into several categories as follow.

(a) An initial dilution (Gifford, 1960, attributed to Fuquay) proportional to the product of the windspeed and the projected building area. The ground-level centerline concentration χ_{CL} is the familiar expression

$$\chi_{CL} = \frac{Q}{(\pi\sigma_y\sigma_z + cA_p)U} \quad , \tag{15a}$$

often referred to as "Gifford's model"; where c is a constant whose value is somewhere between 1/2 and 2, and σ_y and σ_z are the usual (Pasquill-Gifford-Turner) forms of the dispersion parameters. In terms of the nondimensional concentration coefficient, this is

$$K_{CL}^{-1} = (\pi\sigma_y\sigma_z/A_p) + c \quad . \tag{15b}$$

(b) A looping plume (Gifford, 1968, attributed to Davidson), where the total mean-square diffusion is due to the spreading induced by ambient atmospheric turbulence plus a contribution attributed to the "looping" or meandering of the plume because of the eddies generated by the building;

$$\chi_{CL} = \frac{Q}{\pi\Sigma_y\Sigma_z U} \quad , \tag{16a}$$

or

$$K_{CL} = A_p/\pi\Sigma_y\Sigma_z \quad , \tag{16b}$$

with $\Sigma_{y,z}^2 = \sigma_{y,z}^2$ + a term dependent on the building dimensions. Gifford took this term to be cA_p/π, but forms dependent on the square of the building width (for Σ_y) and height (for Σ_z) have also been suggested (e.g., Huber, 1984).

(c) Linear dependence of dispersion parameters on the building dimensions; in the intermediate wake range, these parameters may or may not depend on the ambient turbulence. For example, Ferrara and Cagnetti (1980) suggested

$$\sigma'_y \cong \sigma_y + W/\sqrt{2\pi} \tag{17a}$$

$$\sigma'_z \cong \sigma_z + H/\sqrt{2\pi} \tag{17b}$$

For $x < 10$ H, Huber and Snyder (1976, 1982) recommended

$$\sigma'_y = 0.067\ (x - 3\ H) + 0.7\ (W/2) \tag{18a}$$

$$\sigma'_z = 0.067\ (x - 3\ H) + 0.7\ H \tag{18b}$$

In both these models, the ground-level centerline concentration is

$$\chi_{CL} = \frac{Q}{\pi\sigma'_y\sigma'_z\ U}\ , \tag{19a}$$

or

$$K_{CL} = A_p/\pi\sigma'_y\sigma'_z \tag{19b}$$

(d) A virtual source (e.g., Turner, 1969; Barker, 1982; Meroney, 1982), where the extra dispersion introduced by the buildings is accounted for by an effective upwind displacement of the effluent source. No modifications to the ambient diffusion rates are made:

$$\begin{aligned} \sigma'_y(x) &= \sigma_y(x + x_{yo}) \\ \sigma'_z(x) &= \sigma_z(x + x_{zo}) \end{aligned} \tag{20}$$

The concentration expression for a virtual source is also given by Equation (19). Huber and Snyder (1976,1982) restricted their virtual source model to the far wake ($x/H > 10$), subject to matching the parameters to those of the intermediate wake at $x/H = 10$. A computational procedure

to evaluvte x_{yo} and x_{zo} by matching Huber's (1977, 1979) expressions for σ_y and σ_z to Turner's (1969) curves at x = 10 H was given by Hosker (1982). The procedure can easily be amended to accommodate the other virtual source models cited above.

All of the above models assume normal (Gaussian) distributions of effluent in the crosswind and vertical directions. The source is assumed to be located close to the buildings, so that material is effectively mixed into the building wakes. If the source is elevated, various assumptions concerning enhancement of vertical mixing only, or partial entrainment of the plume into the wake, or effective stack heights, or combinations of these are possible; see the discussion by Hosker (1982).

Halitsky's (1977) wake dispersion model was developed specifically for the EBR-II site studied by Dickson, Start, and Markee (1969). Laboratory data on flow past a flat plate normal to the wind were used to predict a wake boundary that grows horizontally and vertically as $x^{1/3}$, and a $x^{-2/3}$ decay of mean velocity defect and turbulence intensity excess. Although these estimates do not agree with, for example, the wake theory of Counihan, Hunt, and Jackson (1974), Halitsky's predictions do agree well with Dickson, Start, and Markee's (1969) field data. One might reasonably speculate, however, that the field data do not really have sufficient accuracy, resolution, and spatial density to verify or reject competing theories of wake behavior. An interesting aspect of Halitsky's model is the parabolic (rather than Gaussian) crosswind distribution of concentration:

$$\chi \cong \frac{Q}{2.64\ \sigma_y \sigma_z} \left[1 - \frac{y}{\sqrt{10}\ \sigma_y}\right]^2 \exp\left[\frac{-z^2}{2\sigma_z^2}\right] \qquad (21)$$

However, Thuillier and Mancuso (1980) found that unimodal crosswind concentration distributions at a different facility were fitted fairly well by the more commonly used Gaussian curve. Further study at other sites is needed to resolve this question, but the shape is probably influenced by the distribution of buildings within the cluster and the distance at which the data are observed.

Kothari, Peterka, and Meroney's (1981) analytical model assumes the building's (or building cluster's) influence on effluent concentration can be treated as a small perturbation to the concentration pattern that would result from the same source if no buildings were present. The solution is mathematically complicated. The crosswind distribution is bell-shaped at any given distance and height above the ground, but the distribution width is a complex function of height and distance. The alongwind distribution is given in terms of modified Bessel functions, and depends on distance and height above the ground, the curvature of the wind profile, the effective source height, and the mean building height. Agreement with wind tunnel data for the EOCR building complex is quite good; further testing seems warranted, despite the present difficulty of use. Simplification of the functional forms would be especially helpful.

3.2.2 Agreement With Data

The most extensive testing of the simple models for intermediate and far wake concentrations has been carried out by Fackrell (1984), who compared predictions of the Gifford (1960) model, two virtual source models (Turner, 1969, and Barker, 1982), Ferrara and Cagnetti's (1980) enhanced dispersion parameter model, and Huber and Snyder's (1976; see also their 1982 paper) empirically-based enhanced dispersion parameters and virtual source model to wind tunnel and field data behind simple isolated buildings and various building complexes.

Fackrell's (1984) comparisons bring out several notable features. Firstly, when compared to the wind tunnel data of Dean and Robins (unpublished; cited by Fackrell, 1984) on isolated simple structures, no single model is the best for either ground level or rooftop effluent releases; the wake concentrations are apparently more dependent upon the building geometry than the simple physics incorporated in the various models would predict.

For example, consider a source at ground level at the center of the lee face of a building normal to the wind. For narrow buildings ($W/H \leq 1$), Barker's (1982) model is the best conservative* choice, although the Ferrara-Cagnetti (1980) model fits the data somewhat better. For a slightly wider building ($W/H = 2$), the Ferrara-Cagnetti model (1980) is the best; for a wider ($W/H = 3$), long ($L/H = 3$) building, the Barker (1982) model provides the best fit to the data, and the Turner (1969) model is the best conservative choice. For a very wide structure ($W/H = 5$), all of the models tested overpredict; the closest is the Ferrara-Cagnetti (1980) method.

For a centrally located rooftop vent (effective release height $h_e = H$), the results are again mixed. For a very narrow building ($W/H = 0.33 = L/H$), there is no good model; the closest agreement is obtained using the Huber-Snyder (1976, 1982) model for a stack release ($h_e = 1.4\ H$), and the Turner (1969) model for a rooftop release ($h_e = H$) is the best conservative model. For a slightly wider ($W/H = 0.5$) and longer ($L/H = 1$) building, the situation is quite similar; the Huber-Snyder (1976, 1982) stack release ($h_e = 1.5\ H$) prediction is closest to the data, but the Turner (1969) rooftop model is the best conservative choice. For a wider structure ($W/H = 1$), the Turner (1969) rooftop model actually fits the data best, but the best conservative model is the rooftop ($h_e = H$) Huber-Snyder (1976, 1982) approach. At $W/H = 2$, the Huber-Snyder rooftop model is the best. At $W/H = 3$, there is little to choose between the (ground level) Ferrara-Cagnetti (1980) and the Huber-Snyder (1976, 1982) ground level ($h_e = 0$) models; both, however, strongly overpredict near-building concentrations. For the widest structure tested ($W/H = 5$), the (ground level) Ferrara-Cagnetti (1980) model fits the data best, with some underprediction near the building; the Huber-Snyder (1976, 1982) ground level model is the best conservative choice. It is clear, as Fackrell (1984) points out, that rooftop (and stack) effluent releases on a narrow building lead to much

---

* "Conservative" here means that estimated concentrations are never less than the observed values.

lower concentrations than do corresponding ground level releases, but the elevated releases produce concentrations progressively closer to those from ground level releases as the building becomes wider. That is, wider buildings lead to more wake entrainment than narrower buildings, and so taller stacks will be needed on wider buildings to avoid excessive effluent ground level concentrations.

The situation is more clear cut for roof-center stack releases (h_e = 1.4 to 1.5 H). For narrow buildings (W/H $\leq$ 0.5), none of the models work very well, but the Huber-Snyder (1976, 1982) stack model overpredicts the least badly. For wider structures (W/H = 1 or 2), the Huber-Snyder (1976, 1982) stack model performs fairly well. For W/H = 3, the Huber-Snyder (1976, 1982) stack model again is closest to the data, but tends to slightly underpredict everywhere except close to the building. The Barker (1982) approach is the best conservative model, but it overpredicts rather strongly near the building. For a wide building (W/H = 5), the Huber-Snyder (1976,1982) stack model does fairly well, but overpredicts everywhere except close to the building; in this case the (ground level) Ferrara-Cagnetti (1980) model actually is the best fit to the data, although it is not conservative. An important consideration is that the Huber-Snyder (1976, 1982) model correctly predicts that a centrally located rooftop stack will produce higher ground level concentrations behind a wide building than would a roof level (vent) release at the same location.

It seems likely that some modification to the existing models is necessary to account for the effect of increasing building width, with its apparently more effective wake downwash and entrainment. Two possibilities come to mind.

(a) A "split-h" model akin to that of Johnson et al. (1975), which assumes that over the course of, say, one hour, a plume from a stack or roof vent will be downwashed into the building wake for some fraction of that hour, f, and that the plume will remain aloft for a time fraction (1 - f). The concentrations due to a wake-entrained plume and an elevated plume are then weighted by their respective time fractions and summed, to find the average ground level concentration for that hour (see, however, the discussion of problem areas by Hosker, 1982). To apply this procedure, the dependence of f on the building geometric ratios W/H and L/H must be quantified.

(b) An effective stack height, calculated by including the effect of a very wide building. The commonly used method suggested by Briggs (1973) is unfortunately independent of the building width for W/H > 1, perhaps because of a limited range of data at the time of the study.

Regardless of the model improvements that might be made in these ways, it must also be recognized that the exact location of the stack or vent on the building roof can strongly influence the amount of plume downwash present (see, for example, the work of Koga and Way, 1979a,b), and hence the wake concentrations. None of the presently available models attempt to deal with this factor and many additional experiments will be needed to provide the data for solidly based empirical expressions.

A second important finding of Fackrell's (1984) model comparisons for isolated simple buildings is that a model that accurately predicts wake concentrations for an elevated plume when the wind approaches at right angles to the building will strongly underpredict concentrations when the wind approaches at an angle to the structure. That is, the wake concentrations due to an elevated source on a building will be much higher when the building is not normal to the wind; this is due to the upwind roof-corner vortex pair and the resulting enhanced downwash (see the summary in Hosker, 1984).

One technique to compensate normal incidence models for the effect of wind approach angle is that of Li, Meroney, and Peterka (1982), discussed earlier.

$$\chi(\theta) \cong \chi(\theta=0) \cdot f(\theta) \qquad (22)$$

where $f(\theta) \cong 1 + 4\theta/\pi$ and $0 \leq \theta \leq \pi/4$, for cubical structures. However, the data of Dean and Robins (cited by Fackrell, 1984) suggest a dependence of $f(\theta)$ on both the alongwind distance x (i.e., the effect of wind approach angle is less noticable far downwind) and the building aspect ratio W/H (i.e., the effect of approach angle is more important for narrow buildings). The empirical expression

$$f(\theta) \cong 1 + a\,(W/H)^{-1}(x/H)^{-p}(4\theta/\pi) \qquad (23)$$

with $a \cong 16$ and $p \cong 1.6$ seems to fit Dean and Robins' data reasonably well, but this result should not be regarded as more than a first, crude attempt to estimate the wind angle compensation factor. Comprehensive testing is still needed.

The remaining points suggested by Fackrell's (1984) work are concerned with the building cluster problem per se: (a) there is a strong directional dependence of the wake concentrations, just as for individual buildings, and (b) there is a great deal of scatter in the field data (up to two orders of magnitude), even for the same wind direction and stability conditions. Such scatter is also apparent in the many data sets used by Huber (1977, 1979, 1984) in his tests of the Huber-Snyder model. The reasons for this scatter are not clear, but may be related to phenomena such as slight shifts in plume transport relative to discrete sampler locations, as well as the normal variability of other atmospheric conditions within a given classification.

Fackrell's (1984) comparisons may be summarized as follows: for ground level effluent releases, with the wind normally incident on the building, the Ferrara-Cagnetti (1980) model performed fairly well, but it slightly underpredicted wake concentrations if the building was narrow. For $x/H > 5$ or 10, all the models gave rather similar results, with concentrations within a factor of five, and generally within a factor of two or three. The Barker (1982) model provided the lowest predictions that remained conservative. This model is easy to apply; it is a virtual source model with the origin selected such that

$$\sigma_y(x_{yo}) = W/3$$
$$\sigma_z(x_{zo}) = H/3 \qquad (24)$$

with the effective source height h_e assumed to be H/3. If W/H > 3, $\sigma_y(x_{yo})$ is set equal to H. Equations (19) and (20) are then employed to estimate centerline concentrations. Concentrations off the centerline and/or above the ground are calculated by assuming Gaussian distributions in both the crosswind and vertical directions. This model has recently been recommended by the Working Group for the British National Radiological Protection Board (Jones, 1983) for use in routine estimates.

For elevated (roof vent or roof stack) releases, the models (Huber and Snyder, 1976, 1982; Turner, 1969) which can be adjusted for effective source height showed the correct trends with building dimensions, but slightly underpredicted concentrations behind wide buildings, and overpredicted behind narrow ones.

None of the models that deal well with winds at right angles to the buildings can cope with winds that approach at an angle; the vortex-induced downwash which then occurs increases ground-level concentrations considerably. The problem is worse when the source is elevated, rather than at ground level. Adjustment of the predictions for wind incidence angle might be achieved by introducing a compensation factor $f(\theta)$, as in Equation (23), or by assuming an effective stack height of zero, with no angular dependence of the model.

4.0 SUMMARY AND RECOMMENDATIONS

4.1 Caveats

This report is intended as a survey of and introduction to the literature dealing with flow and effluent dispersion in and near building complexes. In some limited instances it may be useful as an interim guide for users in the architectural, industrial, nuclear, and regulatory fields who must deal with air quality-related problems in non-ideal situations. It should be recognized from the start, however, that present understanding of these problems is still very incomplete, even for relatively simple cases, especially if quantitative predictions are needed. It may be possible for an experienced practitioner to make informed guesses as to the likely flow patterns that will occur in a particular cluster of buildings, and one may also be able to place approximate upper bounds on the concentrations that will be observed in such a cluster. However, detailed flow and concentration patterns cannot generally be predicted with any degree of accuracy without resorting to a specialized program of field or laboratory measurements. It seems unlikely that this situation will improve very much in the next few years without a considerable expansion of the present research effort in this field.

4.2 Flow Field Estimation

Before attempting to deal with flow near building clusters, one should have a good working understanding of the flow near isolated structures, because many of the same phenomena will be observed near or within clusters, although they may be greatly modified by flow interactions. Recent reports (e.g., Hosker, 1982, 1984) have summarized this topic, at least for very simple isolated buildings, and should be consulted for details. Conceptual flow models and empirical expressions are available for the extent of the perturbation zone upwind of a building, to determine whether or not roof reattachment occurs, and for the lateral and downwind extent of the wake cavity region. Nevertheless, a program to methodically test isolated simple buildings of a wide variety of architecturally common shapes is still needed; a kind of "cookbook" suitable for quick evaluations of likely near-building flow patterns would be a useful product of such research.

Understanding the flow near isolated single structures can also be important when dealing with building clusters or even large arrays, because when the structures are placed well apart there will be only limited interactions among their individual flow fields. Hussain and Lee (1980) suggest that the cluster problem can be dealt with in terms of three distinct flow regimes: the "isolated roughness" regime, the "wake interference" regime, and the "skimming flow" regime. The face-to-face spacing between the buildings and their geometry determine the regime that occurs. For small clusters of buildings, Beranek's (1979; 1984) concept of a circle of influence is useful in determining the inter-element spacing for transition from isolated roughness flow to mutual wake interference, at least in the range of building width to height ratios $0.8 < W/H < 3$. This seems to be true for both small clusters of obstacles (observed in the present study) and for uniform arrays of structures (Hussain and Lee's 198(work). The critical transition spacing-to-height ratio s_* seems to be in the range 2.0 to 2.8 for these moderate building geometries; such values are very likely to be found in any moderately built-up area. Less information is available on the important transition from the wake interference regime to situations where the above-building flow largely skims over the inter-building gaps, which are then dominated by recirculating flows. Hussain and Lee's (1980) data on uniform grid-like arrays suggest a critical value s_{**}/H in the range 1.25 to 1.55, depending on the building aspect ratio W/H, but these values will be different for different array configurations. Systematic, detailed study is needed to provide further data. It seems likely that skimming flow will be encountered frequently in heavily built-up areas or in densely packed industrial facilities. This may be an advantage, because the necessary models for flow and dispersion can probably be based on those already developed for street canyon applications.

The most complicated flow problem is probably that of the true building cluster -- a group of buildings of roughly comparable size, surrounded by insignificant or no neighbors. These clusters will usually give rise locally to a wake interference flow regime, so that individual flow fields are strongly perturbed. Generally speaking, experiments remain essential for understanding local flow and concentration patterns near even quite simple building arrays. Unfortunately the available data set is still

quite limited, especially for trustworthy quantitative measurements. However, recent instrumentation advances now permit more reliable determinations of flow and turbulence characteristics, particularly in the laboratory. Once a clear physical picture of these characteristics is obtained for a given building cluster configuration, a mathematical model can be developed with some confidence. A good deal of additional research is needed to reach this level, although a few generalizations are possible now.

For example, somewhat limited evidence suggests that the flow field around a very large building surrounded by small structures will be quite similar to the flow expected if the large building had no neighbors. The smaller structures seem to act mainly as a kind of enhanced surface roughness, although there are differences in the flow details near the ground. This suggests in turn that rough estimates of flow and diffusion near a dominant structure might be made using available models for an isolated building; in particular, one might be able to use the information on hand for isolated buildings as a first-order approximation to the flow for numerical modeling purposes. Additional testing of this possibility is needed.

In densely built-up areas or within large industrial facilities, flow channeling, flow acceleration through gaps, downwash near tall buildings, and standing wake vortices are common phenomena. Careful study of a particular building array's geometry will often suggest zones where these phenomena can be expected. From this inspection, it may be possible to estimate a crude mean flow field and hence determine the approximate trajectory of an air pollutant. These estimates must be refined by testing in nearly all cases, but the initial analysis may be useful in determining critical locations for observations or sites of unusual behavior. The literature available for guidance in this task is still very limited. A systematic study of a wide range of simple building clusters is also needed, so that a second "cookbook" can be established for flow assessment in these situations. Flow visualizations and wind vector data are particularly necessary, but concentration patterns produced by carefully located tracer sources should be collected*. Wind tunnel studies can be particularly helpful in this regard. A large, fast computer is necessary.

Numerical modeling in any detail of flow (and dispersion) over short distances in built-up areas is still in its infancy. Present models seem unable to predict significant phenomena such as separated wakes and vortices, let alone zones of interference. However, it might be possible to incorporate empirical insight into the models by inserting flow submodules associated with particular locations and building types, so that a more realistic flow field can be calculated. Again, a better understanding of the flows associated with simple building clusters is essential to the work.

---

* Concentration data alone should not be collected, since the patterns will generally be extremely difficult to interpret and understand without flow field information.

In a large, densely packed array of buildings subjected to skimming flow, the recirculation vortex of the idealized urban street canyon model is probably a good approximation to the flow, although direct tests using a tracer material might be helpful in modifying the model for more general use. However, an assessment of flow patterns and pollutant transport at the junctions of street canyons is badly needed to understand pollutant sampler data, to design better sampler placement procedures, and to improve modeling capabilities near these intersections. The cases of very light ambient wind, when thermal effects and motions induced by vehicle movements may be significant, and of wind parallel to the street canyon need further study.

4.3 Concentration Estimation Procedures

Within and very close to a building complex, effluent concentration patterns are determined by highly localized, site-specific flows, vortices, and turbulence. Predictions for even very simple building arrays are nearly impossible at this time, with only a few exceptions. In general, experimental studies are needed for each new example, although recent advances in computer technology may eventually permit realistic numerical simulations at reasonable costs.

If one building in a cluster is significantly larger than its companions, the flow and concentration patterns around it will be rather similar to those expected if there were no neighboring structures. In this case, one can use techniques developed for isolated buildings to at least place upper bounds on the expected concentrations near the building. However, it must be borne in mind that most of these estimation procedures have been developed and tested for a limited range of building shapes; extrapolation to unusual geometries may be risky.

If there are a large number of buildings of similar size, placed in a fairly regular array with a gap spacing ("street width") less than about 1.4 H, then a "skimming flow" pattern may occur. In this case, dispersion within the complex may be calculated in terms of a street canyon model. If the wind above the building array is approximately at right angles to the street of interest, then the model of Johnson et al., (1973) or the recent work of DePaul and Sheih (1984) are applicable. If the wind is roughly parallel to the street, Nicholson's (1975) model is more appropriate. None of these models can deal with concentrations near intersections. Furthermore, the models implicitly assume windy, neutrally stable conditions; in particular, they cannot deal with near-calm conditions, when local thermally-driven circulations may become a significant factor in pollutant dispersal.

Although many models have been suggested for estimating concentrations in the intermediate and far wake zones ($x/H > 5$, say) of both individual buildings and isolated building clusters, none of the models actually distinguishes between a single building and a building complex. In particular, jetting effects and organized vorticity are presumed to have dissipated at distances beyond a few building heights downwind. This presumption may be adequate in many cases, but building arrays that produce very strong jetting, or vortex wakes, or that contain a few very large

structures may have highly individualized wake and dispersion characteristics. The models must be applied cautiously when such problems are suspected.

Most of the intermediate and far wake concentration models are modifications of the simple Gaussian plume concept. The modifications may specify an initial plume dilution, or a looping plume, or a simple depen-dence of the in-wake dispersion parameters on building dimensions, or a virtual source, or even some combination of these that may vary with distance downwind. Exceptions to the Gaussian approach are the models proposed by Halitsky (1977), which is based on laboratory studies of flow around a simple building analog, and the mathematically complicated analytical solution of Kothari, Peterka, and Meroney (1981).

Extensive tests (Fackrell, 1984) of the Gaussian-based models against laboratory and field data reveal no "best" model. The wake concentrations seem to depend somewhat more strongly on building geometry than these simple models would predict. One important result is that wider buildings lead to more downwash of initially elevated plumes than do narrow buildings; hence taller stacks will be required on wide buildings to achieve concentrations comparable to those produced by a more modest stack on a narrower structure. It may be possible to adjust the concentration models for changes in building width by means of a "split-h" model (Johnson et al., 1975), which assumes that an elevated plume will be drawn into the building wake for an increasing time fraction as the building width is increased, or else by introducing an effective stack height that explicitly depends on building width. Both of these modifications will require additional experimental studies to deduce the needed formulations.

Fackrell's (1984) study of existing models suggests that the Ferrara-Cagnetti (1980) model fits the data fairly well for ground level effluent releases when the wind approaches at right angles to the building or cluster, although any of the ground level models may be acceptable in the far wake. If a slightly conservative model is required, the Barker (1982) virtual source model is attractive; this model has recently been recommended by experts of the British National Radiological Protection Board (Jones, 1983).

For elevated releases, whether from central roof vents or centrally located short stacks, Fackrell's (1984) work indicates that the models that can be adjusted for effective source height (Huber and Snyder, 1976, 1982; Turner, 1969) show the proper trends in concentration with changes in building geometry, although the predictions may be somewhat in error for very wide or very narrow buildings. In view of the very large scatter in the experimental data, additional model "tuning" may be unnecessary at this stage.

None of the models attempt to predict the dependency of wake concentration patterns on incident wind direction, even though significant increases in concentration due to elevated plumes will occur because of enhanced downwash. These increases will be less obvious with increasing distance downwind. The simplest way to account for the effect of winds at an angle to a building is to assume that a rooftop or stack source is actually at ground level behind the building, regardless of the actual wind

angle or the height of the stack relative to the building. A more elaborate approach would postulate a wind angle compensation factor as an explicit function of angle, distance downwind, and building aspect ratio. A rough estimate of such a factor has been suggested here, but additional testing is needed before it can be used with confidence.

ACKNOWLEDGEMENTS

This report was prepared for the Office of Nuclear Regulatory Research, U.S. Nuclear Regulatory Commission, under interagency agreement RES-76-106, and includes some preliminary work accomplished under interagency agreements among the National Oceanic and Atmospheric Administration, the Department of Energy, and the NRC. The authors are grateful to Leta Brown and Robert Kornasiewicz of the NRC for their support and patience. Thanks are due to Leonard Dickens, Brian Templeman, and Jess Wynn of Oak Ridge Associated Universities for their assistance in the laboratory and darkroom, and to Mary Rogers and Carol Sue Thompson of Oak Ridge Associated Universities for their expert typing and patient revisions. The helpful comments of several reviewers are gratefully acknowledged.

5.0 REFERENCES

Albrecht, F., 1933: Untersuchungen der vertikalen Luftzirkulation in der Grossstadt. Meteorol. Z. 50:93-98.

ASHRAE, 1974: Laboratories. Chapter 15 in Handbook and Product Directory, 1974, Applications. American Society Heating, Refrigeration, and Air-Conditioning Engineers, New York, 15.9 ff.

Barker, C. D., 1982: A virtual source model for building wake dispersion in nuclear safety calculations. Central Electrical Generating Board Report TPRD/B/0072/N82, 41 pp.

Bauman, S. E., E. T. Williams, H. L. Finston, E. F. Ferrond, and J. Sontowskie, 1982: Street level versus rooftop sampling: carbon monoxide and aerosol in New York City. Atmos. Environ. 16(10): 2489-2496.

Beranek, W. J., 1979: General rules for the determination of wind environment. Proceedings of Fifth International Conference on Wind Engineering, July, 1979, Fort Collins, CO, vol. 1. J. E. Cermak, (Ed.) Pergamon Press, Oxford, U.K., 225-234.

Beranek, W. J., 1984: Wind environment around single buildings of rectangular shape, and wind environment around building configurations. Heron 29(1):2-70.

Briggs, G. A., 1973: Diffusion estimation for small emissions. (unpublished mansuscript). ATDL Contribution File No. 79, 59 pp.

Britter, R. E., and J. C. R. Hunt, 1979: Velocity measurements and order of magnitude estimates of the flow between two buildings in a simulated atmospheric boundary layer. J. Indust. Aerody. 4(2):165-182.

Castro, I. P., and A. G. Robins, 1977: The flow around a surface-mounted cube in uniform and turbulent streams. J. Fluid Mech. 79(2):307-335.

Counihan, J., 1969: An improved method of simulating an atmospheric boundary layer in a wind tunnel, Atmos. Environ. 3(2):197-214.

Counihan, J., 1971: Wind tunnel determination of the roughness length as a function of the fetch and the roughness density of three-dimensional roughness elements. Atmos. Environ. 5(8):637-642.

Counihan, J., 1975: Adiabatic atmospheric boundary layers: a review and analysis of data from the period 1880-1972, Atmos. Environ. 9(10): 871-905.

Counihan, J., J. C. R. Hunt, and P. S. Jackson, 1974: Wakes behind two-dimensional surface obstacles in turbulent boundary layers. J. Fluid Mech. 64(3):529-563.

Dabberdt, W. F., F. L. Ludwig, and W. B. Johnson, Jr., 1973: Validation and applications of an urban diffusion model for vehicular pollutants. Atmos. Environ. 7(6):603-618.

Davenport, A. G., 1963: The relationship of wind structure to wind loading. In Wind Effects on Buildings and Structures, Proceedings of Conference at National Physical Laboratorial, 1963, Teddington, Middlesex, U.K., vol. I, 54-101.

DePaul, F. T., and C. M. Sheih, 1984: A study of pollutant dispersion in an urban street canyon. Argonne National Laboratory Report ANL/ER-84-1, 84 pp.

Dickson, C. R., G. E. Start, and E. H. Markee, Jr., 1969: Aerodynamic effects of the EBR-II reactor complex on effluent concentration. Nucl. Saf. 10(3):228-242.

Fackrell, J. E., 1982: Flow behavior near isolated rectangular buildings. Central Electrical Generating Board Report TPRD/M/1254/N82, 27 pp.

Fackrell, J. E., 1984: An examination of simple models for building influenced dispersion. Atmos. Environ. 18(1):89-98.

Fackrell, J. E., and J. E. Pearce, 1981: Parameters affecting dispersion in the near wake of buildings. Central Electrical Generating Board Report RD/M/1179 N81, 31 pp.

Ferrara, V., and P. Cagnetti, 1980: A simple formula for estimating airborne concentrations downwind of buildings for discharges near ground level. Proceedings of Commission of European Communities' Seminar on Radioactive Releases and Their Dispersion in the Atmosphere Following a Hypothetical Reactor Accident, 1980, Riso, Denmark, 993-1005.

Fox, J., 1964: Surface pressure and turbulent airflow in transverse rectangular notches. NASA Tech. Note TN D-2501, 18 pp.

Gandemer, J., 1976: Inconfort du au vent aux abords des batiments: concepts aerodynamiques. Cahiers du Centre Scientifique et Technique du Batiment, no. 170, Cahier 1384. C.S.T.B., Nantes, France, 27 pp. Also avail. in translation as N.B.S technical note 710-9, March, 1978, 48 pp.

Georgii, H. W., E. Busch, and E. Weber, 1967: Untersuchung uber die zeitliche und raumliche verteilung der immissions-konzentration des kohlenmonoxid in Frankfurt am Main. Berichte des Institutes fur Meteorol. und Geophys. der Universitat Frankfurt/Main #11, 60 pp. Also avail. as NAPCA translation 0477.

Gifford, F. A., 1960: Atmospheric dispersion calculations using the generalized Gaussian plume model. Nucl. Saf. 2(2):56-59.

Gifford, F. A., 1968: An outline of theories of diffusion in the lower layers of the atmosphere. In Meteorology and Atomic Energy-1968. D. Slade (Ed.), U.S. AEC No. TID-24190, 65-116.

Goldstein, S., 1965: Wakes. In Modern Developments in Fluid Dynamics, vol. II. Dover Publications, New York, 548-600.

Halitsky, J., 1961: Diffusion of vented gas around buildings. Presented at 54th Annual Meeting of Air Pollution Control Association, June 11-15, 1961, New York, paper #61-35, 26 pp.

Halitsky, J., 1963a: Gas diffusion near buildings. New York University Meteorology and Oceanography Geophysics Sciences Laboratory Report 63-3. New York University College of Engineering, New York, 163 pp.

Halitsky, J., 1963b: Gas diffusion near buildings, ASHRAE Trans. 69, Paper No. 1855, 464-485.

Halitsky, J., 1977: Wake and dispersion models for the EBR-II building complex. Atmos. Environ. 11(7):577-596.

Hatcher, R. V., R. N. Meroney, J. A. Peterka, and K. Kothari, 1978: Dispersion in the wake of a model industrial complex. U.S. National Regulatory Commission Report NUREG-0373, 231 pp.

Hirt, C. W., and J. L. Cook, 1972: Calculating three-dimensional flows around structures and over rough terrain. J. Comput. Phys. 10(2): 324-340.

Hirt, C. W., J. D. Ramshaw, and L. R. Stein, 1978: Numerical simulation of three-dimensional flow past bluff bodies. Comput. Meth. Appl. Mech. and Eng. 14:93-124.

Hosker, R. P., Jr., 1979: Empirical estimation of wake cavity size behind block-type structures. Preprints of Fourth Symposium on Turbulence Diffusion, and Air Pollution, Jan. 15-18, 1979, Reno, NV. American Meteorological Society, Boston, 603-609.

Hosker, R. P., Jr., 1980: Dispersion in the vicinity of buildings. Proceedings of Second Joint Conference on Applications of Air Pollution Meteorology Second Conference on Industrial Meteorology, March 24-28, 1980 New Orleans. American Meteorological Society, Boston, 92-107.

Hosker, R. P., Jr., 1982: Methods for estimating wake flow and effluent dispersion near simple block-like buildings. U.S. Nuclear Regulatory Commission Report NUREG/CR-2521 and NOAA Tech Memo. ERL-ARL-108, NOAA Atmospheric Turbulence and Diffusion Division, Oak Ridge, TN, 138 pp.

Hosker, R. P., Jr. 1984: Flow and dispersion near obstacles. In Atmospheric Science and Power Production. D. Randerson, (Ed.), U.S. Department of Energy/Technical Information Center DOE/TIC-27601, DE84005177, Oak Ridge, TN, 241-326.

Hoydysh, W. G., R. A. Griffiths, and Y. Ogawa, 1974: A scale model study of the dispersion of pollution in street canyons. Presented at 67th Annual Meeting of Air Pollution Control Association, June 9-13, 1974, Denver, CO. APCA paper #74-157, 25 pp.

Huber, A. H., 1977: Incorporating building/terrain wake effects on stack effluents. Preprints, Joint Conference on Application of Air Pollution Meteorology, Nov. 29-Dec. 2, 1977, Salt Lake City, American Meteorological Society, Boston, 353-356.

Huber, A. H., 1979: An evaluation of obstacle wake effects on plume dispersion. Presented at Fourth Symposium on Turbulence, Diffusion, and Air Pollution, Jan. 15-18, 1979, Reno, NV, American Meteorological Society, Boston, 8 pp.

Huber, A. H., 1984: Evaluation of a method for estimating pollution concentrations downwind of influencing buildings. Atmos. Environ. 18 (11):2313-2338.

Huber, A. H., and W. H. Snyder, 1976: Building wake effects on short stack effluents. Preprints, Third Symposium on Atmospheric Turbulence, Diffusion, and Air Quality, Oct. 19-22, 1976, Raleigh, NC. American Meteorological Society, Boston, 235-242.

Huber, A. H., and W. H. Snyder, 1982: Wind tunnel investigation of the effects of a rectangular-shaped building on dispersion of effluents from short adjacent stacks. Atmos. Environ. 16(12):2837-2848.

Hunt, J. C. R., C. J. Abell, J. A. Peterka, and H. Woo, 1978: Kinematical studies of the flows around free or surface mounted obstacles: applying topology to flow visualization. J. Fluid Mech. 86(1):179-200.

Hunt, J. C. R., and G. P. Smith, 1969: A theory of wakes behind buildings and some provisional experimental results. Central Electrical Generating Board Report RD/L/N31/69, 66 pp.

Hussain, M. and B. E. Lee, 1980: An investigation of wind forces on three-dimensional roughness elements in a simulated atmospheric boundary layer flow: II; flow over large arrays of identical roughness elements and the effect of frontal and side aspect ratio variations. University of Sheffield Report BS 56, 81 pp.

Isyumov, N., and A. G. Davenport, 1975: The ground level wind environment in built-up areas. Proceedings, Fourth International Conference on Wind Effects on Buildings and Structures, Sept. 8-12, 1975, Heathrow. Cambridge University Press, London, U.K., 1977, 403-422.

Johnson, W. B., F. L. Ludwig, W. F. Dabberdt, and R. J. Allen, 1973: An urban diffusion simulation model for carbon monoxide. J. Air Poll. Control Assoc. 23(6):490-498.

Johnson, W. B., E. Shelar, R. E. Ruff, H. B. Singh, and L. Salas, 1975: Gas tracer study of roof-vent effluent diffusion at Millstone Nuclear Power Station. Atomic Industrial Forum Report AID/NESP-007b, 295 pp.

Jones, J. A., 1983: Models to allow for the effects of coastal sites, plume rise and buildings on dispersion of radionuclides and guidance on the value of deposition velocity and washout coefficients. Fifth Report of Working Group on Atmospheric Dispersion. National Radiological Protection Board report NRPB-R157, 50 pp.

Koga, D. J., and J. L. Way, 1979a: Effects of stack height and position on pollutant dispersion in building wakes. Proceedings, Fifth International Wind Engineering Conference, Vol. 2, July, 1979, Fort Collins, CO. July, J. E. Cermak (Ed.), Pergamon Press, New York, 1003-1017.

Koga, D. J., and J. L. Way, 1979b: Effects of stack height and position on the dispersion of pollutants in building wakes. Illinois Institute of Technology Fluids and Heat Transfer Report No. R79-2, 238 pp.

Kotake, S., and T. Sano, 1981: Simulation model of air pollution in complex terrains including streets and buildings. Atmos. Environ. 15(6):1001-1009.

Kothari, K. M., J. A. Peterka, and R. N. Meroney, 1981: The wake and diffusion structure behind a model industrial complex. U.S. Nuclear Regulatory Commisson Report NUREG/CR-1473, 53 pp.

Li, W. W., R. N. Meroney, and J. A. Peterka, 1982: Wind tunnel study of gas dispersion near a cubical model building. U.S. Nuclear Regulatory Commission Report NUREG/CR-2395, 97 pp.

Logan, E., and D. S. Barber, 1980: Effect of lateral spacing on wake characteristics of buildings. NASA Contractor Report CR-3337, 74 pp.

Ludwig, F. L., and W. F. Dabberdt, 1972: Evaluation of the APRAC-1A urban diffusion model for carbon monoxide. Stanford Research Institute (now SRI International) Project 8563, Final Report to Coordinator Research Council and U. S. EPA, 148 pp.

Meroney, R. N., 1982: Turbulent diffusion near buildings. In Engineering Meteorology. E. J. Plate (Ed.), Elsevier Scientific Publishing Co., Amsterdam, 481-525.

Mulhearn, P. J., and J. J. Finnigan, 1978: Turbulent flow over a very rough, random surface. Boundary-Layer Meteorol. 15(1):109-132.

Nicholson, S. E., 1975: A pollution model for street-level air. Atmos. Environ. 9(1):19-31.

Penwarden, A. D., and A. F. E. Wise, 1975: Wind environment around buildings. Building Research Establishment Report, 52 pp.

Puttock, J. S., and J. C. R. Hunt, 1979: Turbulent diffusion from sources near obstacles with separated wakes -- part I, an eddy diffusivity model. Atmos. Environ. 13(1):1-13.

Raupach, M. R., A. S. Thom, and I. Edwards, 1980: A wind-tunnel study of turbulent flow close to regularly arrayed rough surfaces. Boundary-Layer Meteorol. 18(4):373-397.

Robins, A. H., and J. E. Fackrell, 1983: Mean concentration levels around buildings due to nearby low level emissions. Central Electrical Generating Board Report TPRD/M/1261/N82, 49 pp.

Roshko, A., 1955: Some measurements of flow in a rectangular cutout. National Advisory Committee for Aeronautics (now NASA) Tech. Note 3488, NACA, Washington, DC, 21 pp.

Schlichting, H., 1960: Boundary Layer Theory, 4th edition. McGraw-Hill, New York, 647 pp.

Tani, I., M. Iuchi, and H. Komoda, 1961: Experimental investigation of flow separation associated with a step or a groove. Aeronautical Research Institute Report No. 364, 27(4), University of Tokyo, Komaba, Meguroku, Tokyo, Japan, 119-137.

Thuillier, R. H., and R. L. Mancuso, 1980: Building effects on effluent dispersion from roof vents at nuclear power plants. EPRI Report No. NP-1380, project no. 1073-1, 218 pp.

Turner, D. B., 1969: Workbook of atmospheric dispersion estimates. U.S. Department of HEW, Public Health Service, Publication no. 999-AP-26, 84 pp.

Wilson, D. J., 1976a: Contamination of building air intakes from nearby vents. University of Alberta Department of Mechanical Engineering Report No. 1, 126 pp.

Wilson, D. J., 1976b: Contamination of air intakes from roof exhaust vents. ASHRAE Trans. 82(1):1028-1038.

Wilson, D. J., 1977: Dilution of exhaust gases from building surface vents. ASHRAE Trans. 83(1):168-176.

Wilson, D. J., 1979a: Height and location of exhaust stacks to reduce recirculation to air intakes. ASHRAE final report RP204, University of Alberta Department of Mechanical Engineering Report 15, 93 pp.

Wilson, D. J., 1979b: Flow patterns over flat-roofed buildings and application to exhaust stack design. ASHRAE Trans. 82(2):284-295.

Wilson, D. J., and R. E. Britter, 1982: Estimates of building surface concentrations from nearby point sources. Atmos. Environ. 16(11):2631-2646.

Woo, H. G. C., J. A. Peterka, and J. E. Cermak, 1977: Wind-tunnel measurements in the wakes of structures. NASA Contractor Report NASA CR-2806, 226 pp.

APPENDIX A

INTRODUCTION

From the literature, it is abundantly clear that many variables influence flow and dispersion around and within a building complex. These factors include meteorological variables such as the approach flow's vertical velocity profile and turbulence characteristics, the depth of the incident atmospheric boundary layer relative to the buildings, and the geometry and spacing of the buildings themselves.

A series of experiments was performed to explore some of these influences and to test recommendations such as Beranek's (1979, 1984) estimate for the radius of influence of a building and the point at which mutual flow interferences appear in building clusters. For simplicity, the approach flow characteristics and the basic building dimensions were held constant; the spacing between buildings and the array configurations were methodically varied. About 75 different cases were tested.

THE EXPERIMENTAL FACILITY

All measurements were conducted in the NOAA/ATDD'S meteorological wind tunnel. A sketch of the tunnel is shown in Figure A-1. It is an open-return facility with a 1m x 1m x 9m test section, using a 30 hp variable-speed DC motor with tachometer feedback. The speed can be varied continuously from about 0.2 m/s to about 20 m/s.

A simulated atmospheric boundary layer was produced using the vortex generator technique pioneered by Counihan (1969). The generating system is sketched in Figure A-2. The surface roughness consisted of nominal 1 cm diameter gravel epoxy cemented to plywood boards. The trip fence was 10 cm in height and the vortex generators were 79.5 cm tall.

The boundary layer structure was measured using a Thermo-Systems, Inc. model 1050 heated sensor anemometer system with a model 1051 hot film probe. Figure A-3 shows the normalized mean vertical velocity profile (for U_{ref} = 4.15 m/s) at 6 m downwind of the trip fence. Figure A-4 shows vertical profiles of both the longitudinal (u'_{rms}/U) and vertical (w'_{rms}/U) turbulence intensities at the same location. Evaluation of the mean velocity profile suggested a boundary layer depth of about 80 cm, a displacement height $d \cong 0.2$ cm, an aerodynamic roughness length $z_o \cong 0.06$ cm, and a friction velocity $u_* \cong 0.184$ m/s. The directly measured shear stress $(u'w')^{1/2}$ was 0.182 m/s, in excellent agreement with the value calculated from the log-law fit to the profile data. A power law

$$\frac{U}{U_{ref}} = \left(\frac{z-d}{\delta}\right)^n \qquad \text{(A-1)}$$

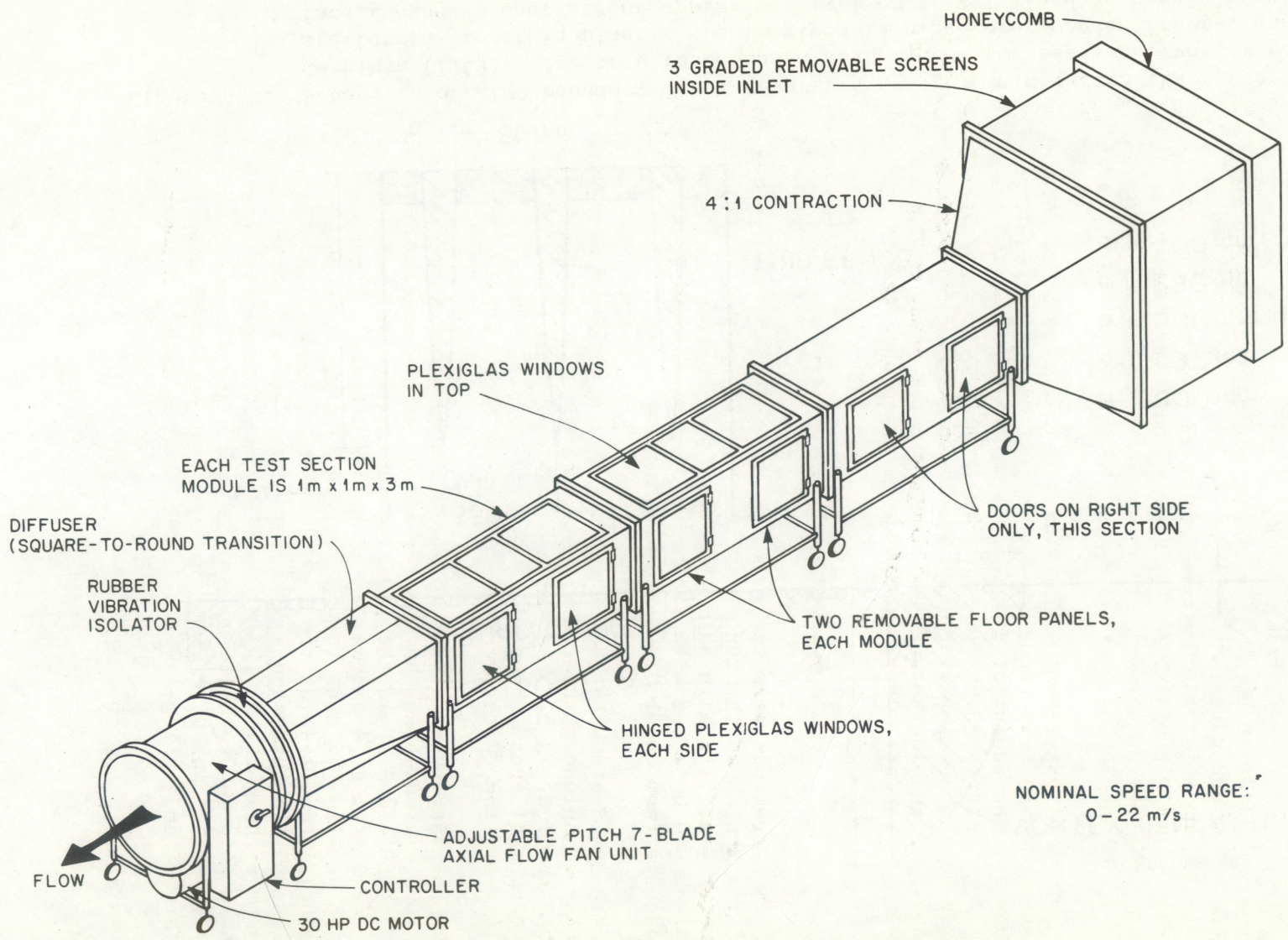

Figure A-1. NOAA/ATDD meteorological wind tunnel. The two front test section are used to develop a simulated atmospheric boundary layer, and model tests are performed in the last test section.

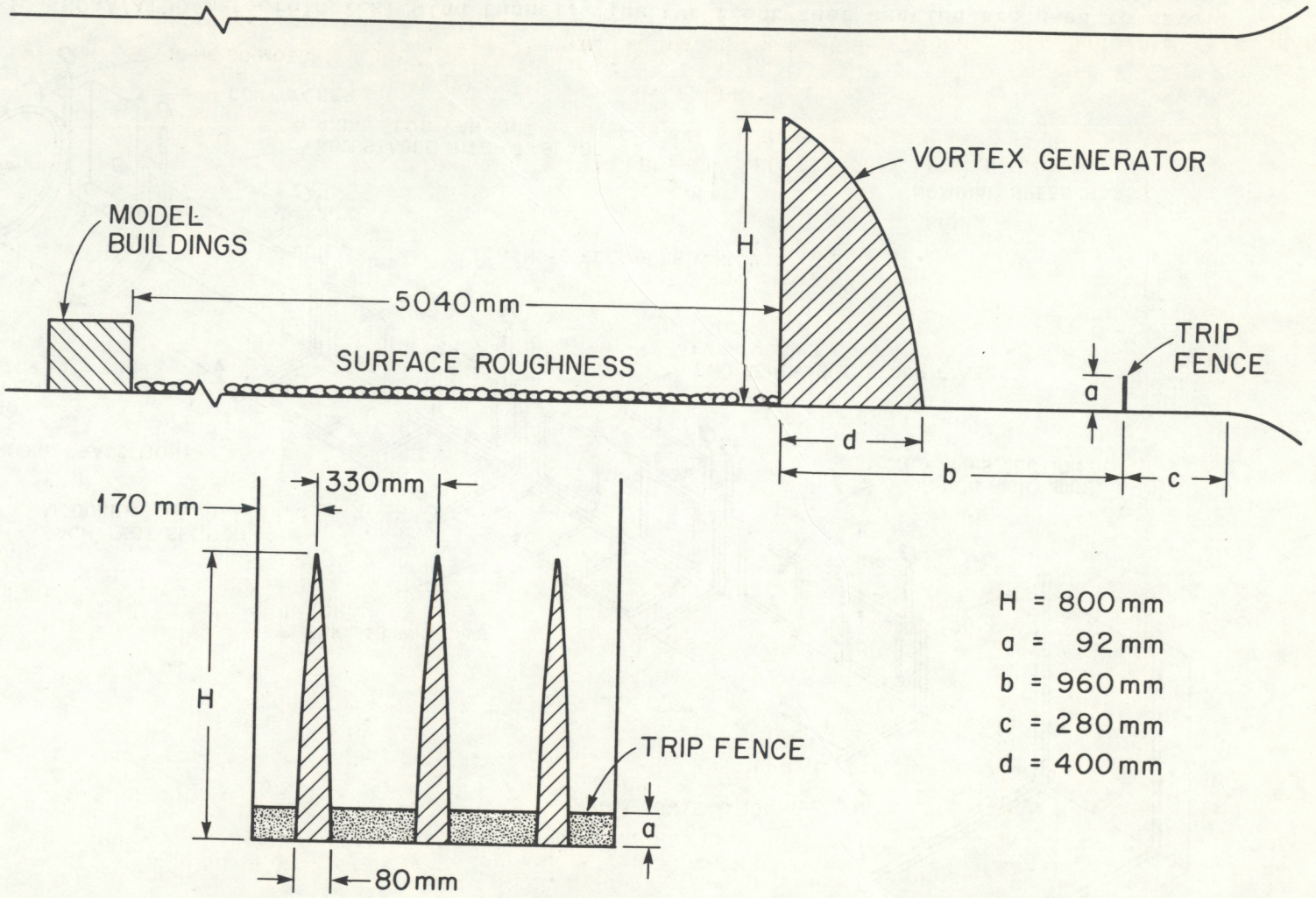

Figure A.2. Schematic of ATDD boundary layer generating system, similar to that suggested by Counihan (1969). The trip fence has a sharp metal top edge; the vortex generators are formed from thin plastic sheets glued in place over wooden frames, and the surface roughness consists of approximately 1 cm gravel glued to special inserts for the tunnel floor.

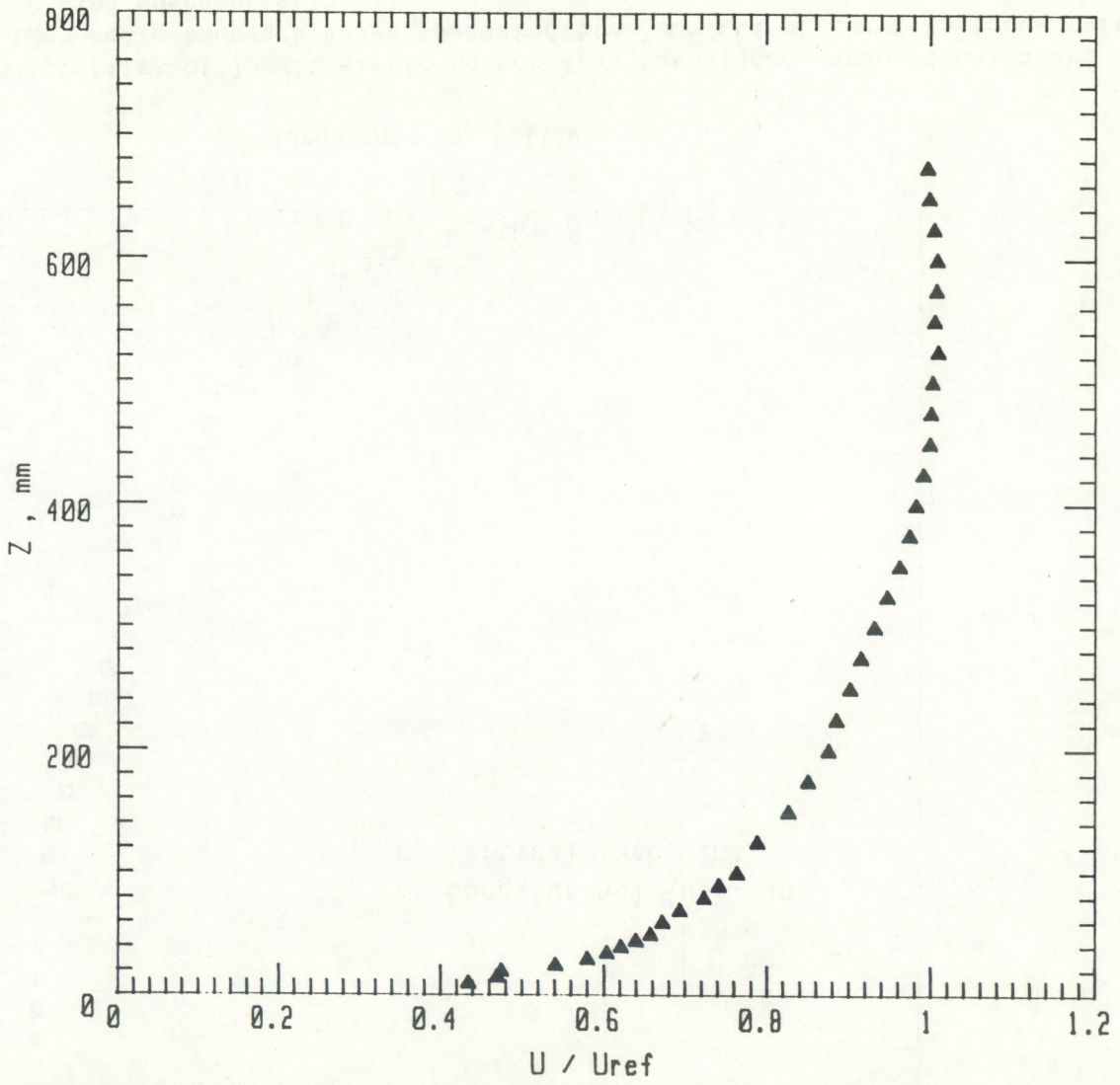

Figure A-3. Normalized mean velocity profile in the simulated atmospheric boundary reference wind speed of 4.15 m/s.

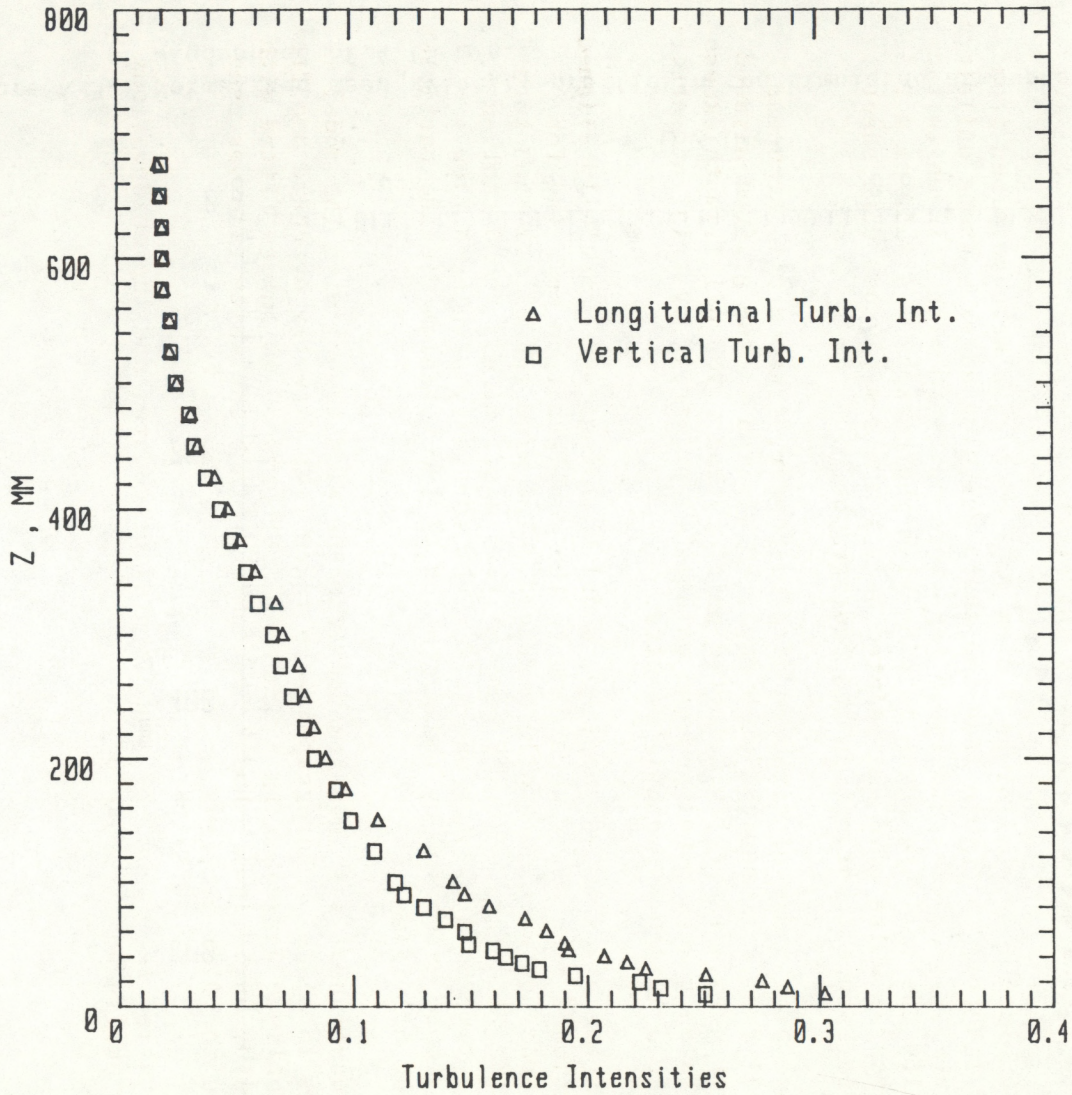

Figure A-4. Vertical profiles of longitudinal and vertical turbulence intensities in the simulated atmospheric boundary layer, measured 6 m downwind of the trip fence, with a reference wind speed of 4.15 m/s.

velocity profile was fitted to the data; the exponent $n \cong 0.21$. This is in good agreement with profiles generally observed over rural to suburban terrain (e.g., Davenport, 1963; Counihan, 1975), and should be appropriate for somewhat isolated industrial facilities such as a nuclear plant.

PROCEDURE

Time and financial constraints precluded a detailed investigation of the flow fields in modeled building complexes. Instead, flow visualization techniques were applied to evaluate regions of influence and the points at which flow fields began to mutually interfere.

Six cubical model buildings 7.6 cm (3") on a side were machined from hardwood (cherry) to ensure true and sharp building edges. These buildings were painted flat black, and their tops were outlined with thin white tape to identify the building edges in plan-view photographs. A 2.54 cm x 2.54 cm (1" square) white grid was painted on a 1 m x 2 m plywood base sheet to provide reference locations in the photographs.

A special mixture of titanium dioxide powder, linseed oil, kerosene, and diesel fuel was prepared each day, and applied to the gridded plywood base sheet with a carefully selected paint roller. The oil film thickness and consistency were developed and maintained primarily by trial and error; experience provided repeatable results.

After the oil film was applied, model buildings were carefully aligned on the gridded base sheet according to the configuration selected for study. Spacings were carefully measured. The wind tunnel was then turned on, and the reference velocity was set to 4 m/s. It was found that an operating time of 5 minutes was sufficient for fully developed flow patterns to be generated by the migration of the titanium dioxide particles within the oil film.

The base sheet was then removed from the wind tunnel with the model buildings in place. Photographs were taken from directly overhead and from various oblique angles using a Canon AE-1 Program 35 mm camera fitted with a 28 mm wide angle lens. Kodak Panatomic-X black and white film was used to record the flow patterns.

A detailed report on the experimental procedures and the observations is being published separately.